보건학박사 학위논문

Estimation of population exposure to particulate matter in Seoul

서울 인구의 미세먼지 노출 예측에 관한 연구

2021 년 8 월

서울대학교 대학원

환경보건학과 환경보건학 전공

곽 수 영

서울 인구의 미세먼지 노출 예측에 관한 연구

지도교수 이 기 영

이 논문을 보건학박사 학위논문으로 제출함
2021년 8월

서울대학교 보건대학원
환경보건학과 환경보건학 전공
곽 수 영

곽수영의 박사학위논문을 인준함
2021년 8월

위 원 장	이 승 묵
부위원장	윤 충 식
위　　원	원 성 호
위　　원	양 원 호
위　　원	이 기 영

Estimation of population exposure to particulate matter in Seoul

A dissertation submitted in partial fulfillment of
the requirements for the degree of
Doctor of Philosophy in Public Health

To the Faculty of the Graduate School of Public Health at
Seoul National University
by
Sooyoung Guak

Supervised by Professor Kiyoung Lee

August, 2021

Data approved by:

Chair	**Seung-Muk Yi**
Vice Chair	**Chung Sik Yoon**
Examiner	**Sungho Won**
Examiner	**Wonho Yang**
Examiner	**Kiyoung Lee**

Abstract

Estimation of population exposure to particulate matter in Seoul

Sooyoung Guak
Department of Environmental Health Sciences
Graduate School of Public Health
Seoul National University

Outdoor concentrations of particulate matter with an aerodynamic diameter of < 2.5 μm ($PM_{2.5}$) often used as a surrogate for population exposure to $PM_{2.5}$ in epidemiological studies. However, people spend the majority of their time indoors; therefore, the relationship between indoor and outdoor $PM_{2.5}$ concentrations should be considered in the estimation of population exposure to $PM_{2.5}$. The overall objective of this study was to estimate population exposure to $PM_{2.5}$ using time-location patterns and outdoor $PM_{2.5}$ concentrations which was applied by the relationship between indoor and outdoor $PM_{2.5}$ concentration. Additionally, direction of refining estimation of population exposure to $PM_{2.5}$ was explored to provide useful insights for further study for the estimates of population exposure to particulate matter.

Study 1 (chapter 2) aimed to develop a population exposure model to $PM_{2.5}$ and identify the determinants associated with the high-exposure group. The input data for the population exposure model were 3984 time-location patterns from Korea Time Use Survey data, outdoor $PM_{2.5}$ concentrations from ambient air quality monitoring station (AQMS), and the microenvironment-to-outdoor concentration (M/O ratio) of $PM_{2.5}$ at seven microenvironments in Seoul, Korea. A probabilistic approach was used to develop the simulation exposure model. The determinants for the population exposure group were identified using a multinomial logistic regression analysis. Population exposure to $PM_{2.5}$ varied significantly among the three seasons. The mean ± standard deviation of population exposures to $PM_{2.5}$ was 21.3 ± 4.0 μg/m^3 in summer, 9.8 ± 2.7 μg/m^3 in autumn, and 29.9 ± 10.6 μg/m^3 in winter. Exposure to $PM_{2.5}$ higher than 35 μg/m^3 mainly occurred in winter. Gender, age, working hours, and health condition were identified as significant determinants in the exposure groups. The high $PM_{2.5}$ exposure group was characterized as a higher proportion of males of a lower age with fewer working hours.

Study 2 (chapter 3) aimed to predict real-time indoor PM_{10} concentration in the daycare centers, kindergartens, and elementary schools using outdoor environmental data. Indoor PM_{10} concentrations were measured in 54 daycare centers, 12 kindergartens, and 21 elementary schools in Seoul, Korea, using a real-time monitor (AirGuard K) over a period of one year. Multiple linear regression models were used to predict real-time indoor PM_{10} concentration in these educational facilities using outdoor PM_{10} and meteorological data as inputs. Four formations (original, ratio of indoor-to-outdoor, root-transformation, and log-transformation) for dependent variable were compared to determine the best performance of the model. A 10-fold cross-validation method was used to evaluate the accuracy of the prediction models. Daycare centers showed the highest indoor PM_{10} concentration. Root-transformed models with high accuracy were developed to predict the real-time indoor PM_{10} concentration in educational facilities every 10 min. The R^2 of the prediction models were 0.64 in the daycare centers, 0.45 in the kindergartens, and 0.43 in the elementary schools. The 24 h profile of the predicted indoor PM_{10} was similar to the measured PM_{10} concentration.

Study 3 (chapter 4) aimed to determine the spatial variations of five air pollutants ($PM_{2.5}$, PM_{10}, NO_2, CO, and O_3) at city-scale and small-scale areas in Seoul, Korea in four seasons. Hourly concentrations of the five air pollutants at 25 AQMSs in Seoul from December 2017–December 2018 were obtained from a Korean government website (AirKorea). In-situ measurements in small-scale (1 km^2) areas were conducted to obtain the hourly concentrations of five air pollutants at eight monitoring sites surrounding the AQMS in Guro-gu, Seoul. Spatial autocorrelations were determined using Moran's index analyses. High $PM_{2.5}$ and PM_{10} concentrations were observed in winter, whereas high O_3 concentrations occurred in spring and summer. The hourly mean concentrations of air pollutants at in-situ monitoring sites (IMSs) were generally higher than those at the nearby AQMS, whereas the O_3 concentrations at IMSs were lower in spring and summer. Seasonal spatial autocorrelation patterns of air pollutants in the city-scale area did not reflect the variation in the small-scale area.

Through these studies, population exposure to $PM_{2.5}$ in Seoul was predicted by season using a population exposure model. The methodology could provide useful insights to conduct more accurate PM exposure assessment with less resources rather than without direct measurements. The population exposure model for $PM_{2.5}$ could be used to implement effective interventions and evaluate the effectiveness of control policies to reduce exposure.

Keywords: air pollutant, microenvironment, M/O ratio, spatial autocorrelation, particulate matter, $PM_{2.5}$, personal exposure, population exposure model

Student Number: 2017-35801

Contents

List of Tables

List of Figures

List of Supplements

Chapter I.

Introduction

1.1. Background

Particulate matter

Particulate matter (PM) is a complex mixture which has various size, chemical compositions, and origin. PMs originates from primary particles emitted directly into the air and secondary particles as a results of chemical reactions with PM precursor (SO_2, NO_x, NH_3, and non-methane volatile organic compounds) in specific atmospheric conditions (Popoola et al., 2018). Particles with an aerodynamic diameter of < 10 μm (PM_{10}) and of < 2.5 μm ($PM_{2.5}$) are well known in public.

On 17 October 2013, PM in outdoor air pollution was classified as carcinogenic to humans (Group 1) by International Agency for Research on Cancer (WHO, 2017). Exposure to PM has been associated with increased respiratory symptoms, pulmonary and cardiovascular diseases, and premature mortality (Du and Li., 2016; Shang et al., 2013). Especially, $PM_{2.5}$ can carry a lot of toxic and harmful substances through the nasal cavity and deep into the lungs, causing cardiovascular and respiratory disease due to its small particle size and large surface area (Yunesian et al., 2019).

The public's interest and concern about the relationship between adverse health effect and PM exposure have recently increased in Korea due to high PM concentration in winter and spring. On March 2019, the Korean national assembly enacted a misfortune and the safety supervision basic law which designated PM as a social disaster. High-level PM episodes (PM advisory and warning) were issued by Korea government. A PM advisory was defined when the hourly average of the ambient concentration at ambient air quality monitoring station (AQMS) exceeded

75 μg/m^3 for $PM_{2.5}$ and 150 μg/m^3 for PM_{10} with lasting for ≥ 2 h. A PM warning was defined when the hourly average of the ambient concentration at AQMS exceeded 150 μg/m^3 for $PM_{2.5}$ and 300 μg/m^3 for PM_{10} with lasting for ≥ 2 h. The PM advisories in Seoul, Korea were issued 61 times for $PM_{2.5}$ and 41 times for PM_{10} in 5 years (2015–2019) (http://www.airkorea.or.kr/autoStatistic). The PM warnings in Seoul, Korea were issued 4 times for $PM_{2.5}$ and 1 times for PM_{10} in 5 years (2015–2019).

Other air pollutants

Exposure to air pollutants was associated with increased morbidity and mortality in numerous epidemiologic studies (Du and Li, 2016; Loomis et al., 2013; Shang et al., 2013). Air quality in Korea has been monitored at AQMSs and determined by criteria air pollutants including PM_{10}, $PM_{2.5}$, nitrogen dioxide (NO_2), carbon monoxide (CO), sulfur dioxide (SO_2), ozone (O_3), lead, and benzene. PM_{10} and $PM_{2.5}$ are particles and others are gaseous pollutants. NO_2 is an irritant gas which is a gaseous pollutant with motor vehicle emissions as a main source. CO is a colorless, nonirritating, odorless, and tasteless gas caused by incomplete combustion. O_3 is a secondary air pollutants generated by photochemical reactions of oxides of nitrogen (NO_x) and volatile organic compounds (VOC). Korean government established Korean ambient air quality standard (KAAQS) of these pollutants with one, eight or 24-h mean (Table 1-1).

Table 1-1. KAAQSs by criteria air pollutants.

Unit	$\mu g/m^3$				ppm			
	$PM_{2.5}$	PM_{10}	Pb	Benzene	NO_2	CO	O_3	SO_2
1-h mean	-	-	-	-	0.10	25	0.1	0.15
24-h mean	35	100	-	-	0.06	-	-	0.05
8-h mean	-	-	-	-	-	9	0.06	-
Annual mean	15	50	0.5	5	0.03	-	-	0.02

Indoor air quality

Indoor environment plays crucial role on daily exposure to environmental pollutants because people generally spent more than 85% of their times in indoors (Klepeis et al. 2001, Yang et al., 2010). Indoor air pollution as well as ambient air pollution should be considered to estimate the actual exposure to air pollutants. Indoor air pollution could be caused by occupant's activity such as cleaning, cooking, smoking, and other activities (O'Leary et al., 2019).

The indoor air quality (IAQ) standards and guidelines managed by the Korea Ministry of Environment are shown in Table 1-2 ($PM_{2.5}$, PM_{10}, CO_2, CO, and NO_2), Table S-1 (Formaldehyde, Total airborne bacteria, Radon, Total volatile organic compounds, and Mold), and Table S-2 (https://www.law.go.kr/법령/실내공기질관리법시행규칙). In addition, IAQ standards and guidelines in school managed by Korea Ministry of Education are shown in Table S-3 (https://www.law.go.kr/법령/학교보건법시행규칙). IAQ guidelines in workplace managed by Korea Ministry of Employment and Labor are shown in Table S-4 (http://www.moel.go.kr/info/lawinfo/instruction/view.do?bbs_ seq=20200100692).

Table 1-2. IAQ standards and guideline ($PM_{2.5}$, PM_{10}, CO_2, CO, and NO_2) in indoor multi-use facilities managed by the Korea Ministry of Environment.

<table>
<tr><th rowspan="2">Facility</th><th colspan="4">Standard[a]</th><th>Guideline[b]</th></tr>
<tr><th>$PM_{2.5}$ (μg/m^3)</th><th>PM_{10} (μg/m^3)</th><th>CO_2 (ppm)</th><th>CO (ppm)</th><th>NO_2 (ppm)</th></tr>
<tr><td>1</td><td>50</td><td>100</td><td rowspan="3">1000</td><td rowspan="2">10</td><td>0.1</td></tr>
<tr><td>2</td><td>35</td><td>75</td><td>0.05</td></tr>
<tr><td>3</td><td>-</td><td>200</td><td>25</td><td>0.30</td></tr>
<tr><td>4</td><td>-</td><td>200</td><td>-</td><td>-</td><td>-</td></tr>
</table>

It was partially included in pollutants based on partial amendment by Ministry of Environment Decree No. 858, April 3, 2020. Locations (1-4) were classified in supplements.
a : annual measurement (once a year)
b : a biennial measurement

- **PM concentration in microenvironment**

Concentration is defined as the amount of air pollutant in microenvironment, but not to whether a person is exposed to pollutants. It was generally represented by an average over all measurements within a time spent in microenvironment. Microenvironment was defined as “a chunk of air space with homogeneous pollutant concentration” (Duan, 1982). Such microenvironments can include either outdoors (e.g. in front of the home) or indoor locations where personal exposure take places.

There was a variety of wide range in the measured $PM_{2.5}$ concentrations in various microenvironments from direct indoors monitoring. In Korea, microenvironmental $PM_{2.5}$ concentrations ranged from 0.7 to 106.4 μg/m^3 in residential indoor, from 2.1 to 191.5 μg/m^3 in office, from 8.1 to 1989.4 μg/m^{3}in restaurant, from 29.8 to 970.2 μg/m^3 in bar, from 10.5 to 84.0 μg/m^3 in elderly welfare facility, from 0.7 to 54.3 μg/m^3 in educational establishment, from 1.1 to 67.2 μg/m^3 in other indoor, and from 1.4 to 115.5 μg/m^3 in transportation (Lim et al., 2012). In another Korea study, median microenvironmental $PM_{2.5}$ concentrations in summer and winter were 21.1 and 20.5 μg/m^3 in supermarket, 30.6 and 30.6 μg/m^3 in store, 16.3 and 32.2 μg/m^3 in school, 28.2 and 35.0 μg/m^3 during walking, 13.8 and 33.7 μg/m^3 in bus, 19.4 and 37.8 μg/m^3 in subway, and 25.5 and 47.0 μg/m^3 in other indoors, respectively (Hwang and Lee, 2018).

- **I/O ratio**

Indoor air pollutants concentrations could be estimated by applying additional consideration of the relationship between the indoor and the outdoor air pollutant concentration (I/O ratio). The I/O ratio was used as an indicator for providing information of pollution in indoor microenvironments (Chen and Zhao, 2011). The I/O ratio might be different by many factors such as the existence of indoor pollutant sources, infiltration, and penetration to indoors (Moon, 2001). When microenvironments had the I/O ratio > 1, this indicated that there may be significant pollutant sources in indoor microenvironments. When microenvironments had the I/O ratio < 1, there was often lack of a significant source and limited infiltration from ambient air to indoors.

There was a variety of wide range in the I/O ratio of $PM_{2.5}$ depending on different microenvironments. In Korea studies, the I/O ratio of $PM_{2.5}$ ranged from 0.68 to 0.81 in residential homes (Park et al., 2020), from 0.47 to 1.02 in elementary school (Kim et al., 2020), from 0.34 to 0.72 in public transportation (Jeon et al., 2008). In other country studies, I/O ratio of $PM_{2.5}$ ranged from 0.20 to 0.88 in recent residential apartments (Wang et al., 2016), from 0.36 to 4.76 in old apartment buildings (Shao et al., 2017), from 0.44 to 0.62 in business offices (Zhu et al., 2015), from 0.82 to 0.94 in elementary schools (Braniš et al. 2009; Tofful and Perrino 2015; Blaszczyk et al., 2017), from 0.71 to 1.10 in kindergartens (Blaszczyk et al., 2017), from 0.90 to 1.28 in restaurants (Liu et al., 2004), and from 0.85 to 2.61 in public transportation (Wu et al., 2013).

Time spent in microenvironment

People move from one location to another and are exposed to air pollutants concentration in various location. The time spent in microenvironment as well as concentration in microenvironment should be also considered to estimate the actual exposure to air pollutants. The time spent in microenvironment was obtained from national Time Use Survey.

In Korea, Time Use Survey by Statistics Korea was conducted every 5 year from 1999. The 1999 and 2004 surveys were conducted in September once a year. Survey in 2009 was conducted twice a year (March and September). Surveys in 2014 and 2019 were conducted three times a year (July, September and December). The number of researched subjects in Korea Time Use Survey was 43000 in 1999, 31634 in 2004, 20263 in 2009 and 26988 in 2014. These survey researched demographic, socioeconomic, family information, and time-location-activity pattern data in microenvironments where people visited every 10 min.

Time-location patterns in 2004 Time Use Survey were analyzed for Seoul population in weekday and weekend (Hwang et al., 2016). Microenvironments in 2004 Time Use Survey were classified into 3 categories including home, other, and transit. Averages of times spent in a residence and transit for Seoul population were 14.0 ± 4.8 h and 2.0 ± 1.7 h, respectively. Times spent in a residence were 14.2 h during weekdays and 16.1 h during weekends. Times spent in transit were 1.8 h during weekdays and 1.7 h during weekends. In the study, the Seoul population was classified into 9 groups with distinctive time-activity patterns. The determinants associated with time spent in a residence were employment status, age, marriage status, education, and gender. Gender, education, employment status, and monthly income were significant factors affecting time spent in transit.

Seasonal time-location patterns in 2014 Time Use Survey were analyzed for Seoul population in weekday (Lee and Lee, 2017). Microenvironments in 2014 Time Use Survey were classified into 9 categories including home, other home, workplace/school, restaurant, other locations, walking, car, public transportation, and other transportation. Times spent in homes, workplaces/schools, other indoor locations, and walking for Seoul population were significantly different by season. The Seoul population spent approximately 60% of their time at home in all seasons (Table 1-3). Season was determinants affected on the times spent at the workplace/school and other locations in the Seoul participants.

Table 1-3. Seasonal times spent for Seoul population in 2014 (Lee and Lee., 2017).

Microenvironment	AM ± SD (min)		
	Summer	Autumn	Winter
Own home	867.7 ± 9.1	843.7 ± 6.2	890.0 ± 8.3
Other home	136.3 ± 22.5	178.9 ± 19.0	207.0 ± 26.3
Workplace/school	465.0 ± 7.7	479.5 ± 5.3	460.2 ± 6.9
Restaurant	85.6 ± 3.2	80.5 ± 2.2	83.5 ± 3.0
Other locations	176.2 ± 6.3	184.8 ± 4.6	169.6 ± 5.9
Walking	52.4 ± 1.2	47.8 ± 0.9	45.3 ± 1.1
Car	105.9 ± 5.0	110.7 ± 3.5	102.1 ± 4.2
Public transportation	101.2 ± 2.9	99.4 ± 1.9	101.9 ± 2.7
Other transportation	61.0 ± 4.9	73.3 ± 4.3	88.8 ± 10.3

Personal exposure assessment

Human exposure is defined as "an event that occurs when a person comes in contact with a pollutant" (Ott, 1982). Exposure to air pollutants is calculated by the sum of the time spent and concentration in microenvironments (Hertel et al., 2001), as below:

$$E_i = \sum_{m}^{n} C_m T_m / T$$

where E_i is the total exposure of person i in various microenvironments, C_m is the averaged air pollutant concentration in microenvironment m, T_m is the time spent in microenvironment m, and n is the number of microenvironments, T is the sum of total T_m.

Exposure can be estimated by direct (exposure monitoring) or indirect approaches (exposure modelling). Direct approach is to measure the exposure to pollutants by monitoring the air pollutants concentrations exposed to human. Indirect approach is to measure the pollutants concentration within microenvironments rather than the concentrations directly exposed to human. Exposure modelling is a more cost-effective and time-saving tool to assess personal exposure for individuals whose direct personal monitoring has not been conducted. There were two modelling approach; deterministic and probabilistic model. A deterministic approach provided one predicted value to model relationships. In contrast, a probabilistic approach provides a probability distribution of resulting values.

In numerous epidemiologic studies, the outdoor air pollutants concentrations at

AQMSs were used as a surrogate of exposure to air pollutants but it was insufficient to assess exposure (Dons et al. 2011). However, personal exposure to air pollutants depends on levels of both indoor and outdoor sources. Thus, I/O ratios in different microenvironments should be applied to the outdoor air pollutants concentration for exposure modeling (Borrego et al., 2009). In addition, spatial-temporal variation of air pollutants in the ambient air should considered to mitigate the error of estimation of outdoor air pollutants concentrations.

Population exposure

A population-based exposure model to air pollutants simulated distributions of exposure for a large group of individuals rather than for specific a single person. Exposure of an entire population could be determined by time-activity pattern at individual scale based on national census data and real-time air pollutants concentration in various microenvironments. A population exposure model could be useful to find the association between exposure to air pollutants and adverse health effects from epidemiologic studies. There were numerous population exposure studies as below and shown in Table 1-4.

- *SHEDS model*

The stochastic human exposure dose simulation–particulate matter (SHEDS-PM) model developed by U.S. Environmental Protection Agency's (EPA) simulated the distribution of daily $PM_{2.5}$ exposure for the Philadelphia population using a probabilistic approach (Burke et al., 2001). Inputs in SHEDS-PM model consisted of demographic, human time-location-activity data, PM concentrations. Demographic data during 1992-1993 were obtained from 1990 the United States (US) census and population time-location-activity data was based on 22000 diary days data from EPA's Consolidated Human Activity Database (CHAD). The outdoor $PM_{2.5}$ concentrations for Philadelphia population were taken from spatial interpolation of either ambient $PM_{2.5}$ measurements at AQMS or predicted values from atmospheric dispersion model. PM concentrations in residential microenvironment were calculated using a steady-state mass balance model from outdoor PM concentration, physical factors (e.g., air exchange, penetration, and deposition), and emission factors for PM sources in indoors (e.g., smoking and cooking). The PM concentrations in nonresidential microenvironments (offices, schools, stores, restaurants, bars, and vehicle) were calculated by a linear regression analysis of existing PM measurement data in indoor and outdoor.

Daily total $PM_{2.5}$ exposures were median with 20 μg/m^3 for the Philadelphia population. The distributions of daily $PM_{2.5}$ exposures with median of 13 μg/m^3 in residential indoors were the greatest influence on total $PM_{2.5}$ exposure compared to the other microenvironments. The distribution of daily exposure to ambient $PM_{2.5}$ with median of 7 μg/m^3 was similar to the distribution of ambient $PM_{2.5}$ concentrations.

- *APEX model*

Air pollutants exposure (APEX) model multipollutant (PM, O_3, and CO) developed by EPA could simulated a probability distribution of population exposure in indoor, outdoor, and in-vehicle microenvironments at the local, urban, or regional level for the US population using a probabilistic approach (EPA, 2017; Johnson et al., 2018). Inputs in APEX model were population demographic data (age, gender, race, etc.), physiological attributes (height, weight, etc.), meteorological data, human activities (22000 diaries compiled in EPA's CHAD), and hourly air quality data. Outdoor air pollutants concentrations were obtained from either monitored ambient data or predicted values from dispersion or other modelling runs. The indoor and/or in-vehicle concentrations were calculated using either a mass balance model or an empirical ratio-based factor.

- *HAPEM*

Hazardous Air Pollutant Exposure Model (HAPEM) was used to examine the relationship between modeled personal exposure levels and outdoor concentrations of 30 gaseous and particulate hazardous air pollutants (HAPs) in US (Ö zkaynak et al. 2008). Four inputs in HAPEM were population data from the US 2000 Census with 2500-8000 residents, population activity data from CHAD, air quality data, and microenvironmental data. The 37 microenvironments used in the national-scale assessment and included indoors at home, school, work, inside an automobile or bus, outdoors, etc. HAPEM predicted chronic exposures for outdoor HAPs were lower than modeled ambient concentrations by about 20 % for gaseous HAPs and by about 60% for particulate HAPs.

- *DEARS*

Detroit exposure and aerosol research study (DEARS) was conducted to measure in the central community monitoring site, residential indoors, and personal exposure of PM ($PM_{2.5}$ and $PM_{10-2.5}$) and various gaseous pollutants targeting 1200 participant-days (120 participants each monitored for 10 days) at six neighborhoods in Wayne County, MI, USA from 2004 to 2008 (Williams et al., 2009; Meng et al, 2012). Participants were monitored for 5 consecutive (24-h) days in each of two consecutive seasons (summer, winter). Data from the 2000 census was used to estimate potential populations in each EMA, their demographics and their housing stock.

- *EXPOLIS simulation model*

Air pollution exposure distributions within adult urban population in Europe (EXPOLIS) study was conducted in six cities (Athens, Basel, Grenoble, Helsinki, Milan and Prague) between 1996 and 2000 during working weeks (H€anninen et al., 2003; Kousa et al., 2002). Personal exposures to $PM_{2.5}$, CO, 30 volatile organic compounds (VOCs), and NO_2 (only Helsinki, Basel, Prague) were measured to provide the frequency distribution of exposure for European adult urban populations. Microenvironments were defined as home indoors, work indoor, and other places. The participants kept a time–microenvironment–activity diary every 15 min for 48 consecutive hours.

EXPOLIS simulation model was developed using a probabilistic approach and simulated frequency distribution of population $PM_{2.5}$ exposures (H€anninen et al., 2003; Kruize et al., 2003). Inputs in the EXPOLIS simulation model were data on the spatial location of the population, time-microenvironment activity data, and calculated spatial pollutant concentration distributions. In Helsinki, hourly ambient $PM_{2.5}$ concentrations at a traffic-oriented fixed monitoring station were randomly sampled for the other places microenvironment. In Athens, Basel, and Prague, there were no hourly $PM_{2.5}$ data in outdoor and the approximately 32-h average ambient concentrations were used. Comparison between simulated and measured values in EXPOLIS study was conducted.

- *EXPAND*

Based on EXPOLIS project, exposure model for particulate matter and nitrogen oxides (EXPAND) was developed to determine the spatial and temporal variation of average exposure to NO_2 (Kousa et al., 2002; Loh et al., 2009) and $PM_{2.5}$ (Soares et al., 2014; Kukkonen et al., 2016) for the whole urban adult (25-65 years) population in the Helsinki using a deterministic approach. Inputs in EXPAND were urban emissions, location of population, time-microenvironment-activity data (EXPOLIS data), infiltration rates, predicted traffic flow, and ambient air concentration from dispersion models. The model used as input values data on the spatial location of the population, time-microenvironment activity data and computed spatial pollutant concentration distributions.

- *LHEM*

London hybrid exposure model (LHEM) estimated the daily $PM_{2.5}$ and NO_2 exposure to outdoor air pollution for the London population for > 5 years of age (Smith et al., 2016). Population time-location-activity data was based on data set (45079 people) from the London Travel Demand Survey (LTDS, 2011) provided by Transport for London during 2005-2010. Outdoor concentrations were evaluated by the community multiscale air quality (CMAQ)-urban model and space-time-activity data. Indoor exposures to $PM_{2.5}$ and NO_2 were calculated using the outdoor CMAQ-urban applied to I/O ratios. In-vehicle exposure was derived from mass balance equation. Walking and cycling exposures were obtained from time and location CMAQ-urban modeled concentration. The means NO_2 and $PM_{2.5}$ exposures using LHEM were 13.0 (range: 4.3–55.3) μg/m^3 and 8.5 (6.0–32.2) μg/m^3, respectively. The means LHEM exposures to outdoor pollution were estimated to be 63% lower for NO_2 and 37% lower for $PM_{2.5}$ than at the residential address.

- *EXPLUME*

Exposure to atmospheric pollution modeling (EXPULME) simulated personal exposure to O_3 and $PM_{2.5}$ over the greater Paris region (over the Île-de-France region) at 2 km × 2 km resolution for the entire year of 2017 (Valari et al., 2020). Population time-location-activity data was based on data set (43000 people) from Enquête globale de transport survey provided by the Direction Régional et Interdépartemental de l'Equipement et de l'Aménagement d'Île-de-France (EGT, 2010). Outdoor pollutant concentrations were simulated with chemistry-transport model 2 km × 2 km resolution. Indoor pollutant concentrations were calculated from outdoor concentrations applied by I/O ratio. I/O ratios in buildings were calculated by a ventilation model called the Simulation of air RENewal (SIREN). I/O ratio in other indoors were taken from values in previous studies or obtained from previous concentration data in indoor and outdoor. The mobility of the population was simulated by matching the journeys of 2010 EGT. The results showed the spatial distribution of $PM_{2.5}$ and O_3 exposure which was similar to the concentration maps over the region, but the exposure scale is very different when accounting for indoor exposure.

Table 1-4. Summary of population exposure models to air pollutants in previous studies.

Reference	Model	Air pollutant	Location	Microenvironment	Inputs	Modelling method
Kruize et al., 2003; H€anninen et al., 2003	EXPOLIS simulation model	$PM_{2.5}$, PM_{10}	Athens, Basel, Helsinki, Prague	Home, work indoors, other places	EXPOLIS data, spatial location of the population, time-location data, PM conc.	Probabilistic model
Kousa et al., 2002; Loh et al., 2009; Soares et al., 2014 Kukkonen et al., 2016	EXPAND	$PM_{2.5}$, NO_2	Helsinki, Finland	home, workplace, in traffic, other place	EXPOLIS data, time activity, emission data, infiltration rates, predicted traffic flow, ambient air conc.	Deterministic model
Burke et al., 2001	SHEDS-PM model	$PM_{2.5}$	Philadelphia, PA, USA	Outdoors, residence, office, school, store, restaurant, bar, in vehicles	CHAD, 2010 census, AQMS data, mass balance modelled data	Probabilistic model

Table 1-4. Summary of population exposure models to air pollutants in previous studies (continued).

Reference	Model	Air pollutant	Location	Microenvironment	Inputs	Modelling method
EPA, 2017; Johnson et al., 2018	APEX model	PM, O_3, CO	12 metropolitan area, USA	Outdoors, indoors residence, in-vehicle	CHAD, 2010 census, physiological attributes, meteorological data, hourly air quality data	Probabilistic model
Ö zkaynak et al. 2008	HAPEM	30 HAPs	USA	Outdoor, Home, school, work, inside an automobile or bus, etc. (37)	CHAD, 2010 census, air quality data, microenvironmental data	Probabilistic model
Smith et al., 2016	LHEM	$PM_{2.5}$, NO_2	London, UK	Outdoor, indoor, in-vehicle, walking and cycling	LTDS, CMAX-urban modelled conc., I/O ratio	Deterministic model
Valari et al., 2020	EXPLUME	$PM_{2.5}$, O_3	Paris, France	Outdoors, home, other indoors, work/school, public transportation, car	EGT, I/O ratio, outdoor conc., geometry model, mobility data	Probabilistic model

KoSEM-$PM_{2.5}$

The Korea Simulation Exposure Model for $PM_{2.5}$ (KoSEM-$PM_{2.5}$) was base on measurements in the limited locations (home, other, and transportation) and times using time-activity pattern in one season (Hwang et al. 2018). In addition, the microenvironmental $PM_{2.5}$ measurements were used to develop the model only when outdoor concentrations were lower than 100 μg/m^3 of PM_{10}. Therefore, this study reduced uncertainty and further refined the model structure by adding inputs for initial version of KoSEM-$PM_{2.5}$ as shown in Table 1-5.

Unlike other population exposure models, this study developed a population exposure to $PM_{2.5}$ model using direct measurement of $PM_{2.5}$ in various microenvironment by season. We considered the relationship between indoor and outdoor concentration in the development of model. Inputs for Korea (e.g., Korea time-activity patterns and microenvironmental concentration in Korea) were applied in this population exposure model. KoSEM-$PM_{2.5}$ can identify characteristics of high-exposure group and determinant associated with high exposure to $PM_{2.5}$.

Table 1-5. A summary of refinement of KoSEM in this study.

	Previous study (2018)	This study (2021)
Time-activity data (Korean Time Use Survey)	2004 Autumn (Sep.)	2014 Summer (Jul.) Autumn (Sep.) Winter (Dec.)
Measurement	2013 Summer Winter	2017-2018 Summer Autumn Winter
Modelling season	Summer	Summer Autumn Winter
Microenvironment	Residential indoor Other locations Transportation	Residential indoor Workplace/school Other locations Restaurant Walking Car Public transportation
Microenvironmental concentration	Only indoor conc.	Outdoor conc. applied by I/O ratio
Outdoor PM level	< 100 μg/m^3 for PM_{10}	No limit

1.2. Objectives

The overall objective of this study was to estimate Seoul population exposure to $PM_{2.5}$ by season using time-location patterns from Korean Time Use Survey, outdoor $PM_{2.5}$ concentrations, and microenvironment-to-outdoor concentration (M/O ratio) of $PM_{2.5}$ from real-time microenvironment measurement. Additionally, direction of refining estimation of population exposure to $PM_{2.5}$ was explored to provide useful insights for further study. The specific objectives of three studies were as follows:

1) To develop a population exposure model to $PM_{2.5}$ for predicting distribution of population exposure to $PM_{2.5}$ by season and identify determinants associated with the high-exposure group in Seoul, Korea.

2) To predict real-time indoor PM_{10} concentrations using outdoor factors every 10 min over one year.

3) To identify spatial-temporal variation of air pollutants concentration in city-scale and small-scale areas.

Outline of the study is shown in Figure 1-1. Firstly, population exposure to $PM_{2.5}$ was estimated using KoSEM-$PM_{2.5}$ based on time spent and outdoor $PM_{2.5}$ concentration applied by M/O ratio in microenvironments. Secondly, real-time indoor PM concentrations in educational facilities were predicted using outdoor PM concentration and meteorological data over one year. Thirdly, seasonal spatial variations of air pollutants concentrations were identified in city-scale and small-scale areas in Seoul, Korea. Study 2 and study 3 will provide useful insights into refining a population exposure model in further study for the estimates of population exposure to PM.

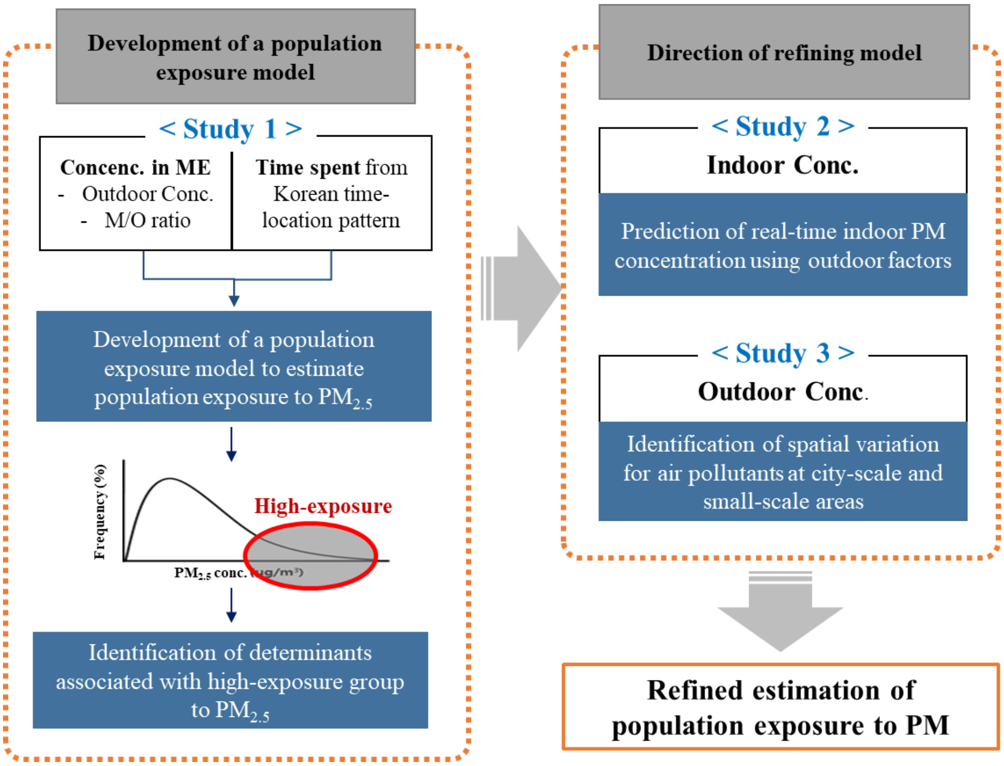

Figure 1-1. The overall outline of the study. Abbreviation; Conc. = concentration; ME = microenvironment.

References

Błaszczyk, E., Rogula-Kozłowska, W., Klejnowski, K., Kubiesa, P., Fulara, I., Mielżyńska-Švach, D., 2017. Indoor air quality in urban and rural kindergartens: short-term studies in Silesia, Poland. Air Quality, Atmosphere & Health 10, 1207-1220.

Borrego, C., Sá, E., Monteiro, A., Ferreira, J., Miranda, A.I., 2009. Forecasting human exposure to atmospheric pollutants in Portugal – A modelling approach. Atmospheric Environment 43, 5796-5806.

Braniš, M., Šafránek, J., Hytychová, A., 2009. Exposure of children to airborne particulate matter of different size fractions during indoor physical education at school. Building and Environment 44, 1246-1252.

Burke, J.M., Zufall, M.J., Özkaynak, H., 2001. A population exposure model for particulate matter: case study results for $PM_{2.5}$ in Philadelphia, PA. Journal of Exposure Science and Environmental Epidemiology 11, 470-489.

Chen, C., Zhao, B., 2011. Review of relationship between indoor and outdoor particles: I/O ratio, infiltration factor and penetration factor. Atmospheric Environment 45, 275-288.

Dionisio, K.L., Nolte, C.G., Spero, T.L., Graham, S., Caraway, N., Foley, K.M., Isaacs, K.K., 2017. Characterizing the impact of projected changes in climate and air quality on human exposures to ozone. Journal of Exposure Science and Environmental Epidemiology 27, 260-270.

Dons, E., Int Panis, L., Van Poppel, M., Theunis, J., Willems, H., Torfs, R., Wets, G., 2011. Impact of time–activity patterns on personal exposure to black carbon.

Atmospheric Environment 45, 3594-3602.

Du, Y., Li, T., 2016. Assessment of health-based economic costs linked to fine particulate ($PM_{2.5}$) pollution: a case study of haze during January 2013 in Beijing, China. Air Quality, Atmosphere & Health 9, 439-445.

Duan, N., 1982. Models for human exposure to air pollution. Environment International 8, 305-309.

EGT: Enquête Globale Transport 2010-STIF-OMNIL-DRIEA, 2010. Technical Report.

Hänninen, O., Kruize, H., Lebret, E., Jantunen, M., 2003. EXPOLIS simulation model: $PM_{2.5}$ application and comparison with measurements in Helsinki. Journal of Exposure Science and Environmental Epidemiology 13, 74-85.

Hänninen, O., Alm, S., Katsouyanni, K., Künzli, N., Maroni, M., Nieuwenhuijsen, M.J., Saarela, K., Srám, R.J., Zmirou, D., Jantunen, M.J., 2004. The EXPOLIS study: implications for exposure research and environmental policy in Europe. Journal of Exposure Science and Environmental Epidemiology 14, 440-456.

Hwang, Y., An, J., Lee, K., 2018. Characterization of a high $PM_{2.5}$ exposure group in Seoul using the Korea simulation exposure model for $PM_{2.5}$ (KoSEM-PM) based on time–activity patterns and microenvironmental measurements. International Journal of Environmental Research and Public Health 15, 2808.

Hwang, Y., Lee, K., 2018. Contribution of microenvironments to personal exposures to PM_{10} and $PM_{2.5}$ in summer and winter. Atmospheric Environment 175, 192-198.

Hwang, Y., Lee, K., Yoon, C.-S., Yang, W., Yu, S., Kim, G., 2016. Determination of similar exposure groups using weekday time activity patterns of urban populations. Journal of Environmental Health Sciences 42, 353-364.

Hertel, O., De Leeuw, F.A., Jensen, S.S., Gee, D., Herbarth, O., Pryor, S., Palmgren, F., Olsen, E., 2001. Human exposure to outdoor air pollution (IUPAC technical report). Pure and Applied Chemistry 73, 933-958.

Jeon, B.-H., Hwang, I.Y., 2015. Concentrations of total culturable microorganisms and its identification in public facilities. Journal of the Korea Academia-Industrial cooperation Society 16, 868-876.

Johnson, T.R., Langstaff, J.E., Graham, S., Fujita, E.M., Campbell, D.E., 2018. A multipollutant evaluation of APEX using microenvironmental ozone, carbon monoxide, and particulate matter ($PM_{2.5}$) concentrations measured in Los Angeles by the exposure classification project. Cogent Environmental Science 4, 1453022.

Kim, D.-h., Son, Y.-S., Lee, T.-J., Jo, Y.M., 2020. A Comparative Study on Concentrations of Indoor and Outdoor Particulate Matters in Elementary Schools. Korean Journal of Remote Sensing 36, 1721-1732.

Klepeis, N.E., Nelson, W.C., Ott, W.R., Robinson, J.P., Tsang, A.M., Switzer, P., Behar, J.V., Hern, S.C., Engelmann, W.H., 2001. The National Human Activity Pattern Survey (NHAPS): a resource for assessing exposure to environmental pollutants. Journal of Exposure Analysis and Environmental Epidemiology 11, 231-252.

Kousa, A., Kukkonen, J., Karppinen, A., Aarnio, P., Koskentalo, T., 2002. A model for evaluating the population exposure to ambient air pollution in an urban area. Atmospheric Environment 36, 2109-2119.

Kruize, H., Hänninen, O., Breugelmans, O., Lebret, E., Jantunen, M., 2003.

Description and demonstration of the EXPOLIS simulation model: Two examples of modeling population exposure to particulate matter. Journal of Exposure Science and Environmental Epidemiology 13, 87-99.

Kukkonen, J., Singh, V., Sokhi, R., Soares, J., Kousa, A., Matilainen, L., Kangas, L., Kauhaniemi, M., Riikonen, K., Jalkanen, J.-P., 2016. Assessment of Population Exposure to Particulate Matter for London and Helsinki, Air Pollution Modeling and its Application XXIV. Springer, 99-105.

Lee, S., Lee, K., 2017. Seasonal differences in determinants of time location patterns in an urban population: a large population-based study in Korea. International Journal of Environmental Research and Public Health 14, 672.

Lim, S., Kim, J., Kim, T., Lee, K., Yang, W., Jun, S., Yu, S., 2012. Personal exposures to $PM_{2.5}$ and their relationships with microenvironmental concentrations. Atmospheric Environment 47, 407-412.

Liu, Y., Chen, R., Shen, X., Mao, X., 2004. Wintertime indoor air levels of PM_{10}, $PM_{2.5}$ and PM_1 at public places and their contributions to TSP. Environment International 30, 189-197.

Loh, M.M., Soares, J., Karppinen, A., Kukkonen, J., Kangas, L., Riikonen, K., Kousa, A., Asikainen, A., Jantunen, M.J., 2009. Intake fraction distributions for benzene from vehicles in the Helsinki metropolitan area. Atmospheric Environment 43, 301-310.

Loomis, D., Grosse, Y., Lauby-Secretan, B., El Ghissassi, F., Bouvard, V., Benbrahim-Tallaa, L., Guha, N., Baan, R., Mattock, H., Straif, K., 2013. The carcinogenicity of outdoor air pollution. Lancet Oncology 14, 1262.

LTDS, 2011. Transport for London, 2011, travel in London. Supplementary Report.

London Travel Demand Survey (LTDS).

Meng, Q., Williams, R., Pinto, J.P., 2012. Determinants of the associations between ambient concentrations and personal exposures to ambient $PM_{2.5}$, NO_2, and O_3 during DEARS. Atmospheric Environment 63, 109-116.

Monn, C., 2001. Exposure assessment of air pollutants: a review on spatial heterogeneity and indoor/outdoor/personal exposure to suspended particulate matter, nitrogen dioxide and ozone. Atmospheric Environment 35, 1-32.

O'Leary, C., Jones, B., Dimitroulopoulou, S., Hall, I.P., 2019. Setting the standard: The acceptability of kitchen ventilation for the English housing stock. Building and Environment 166, 106417.

ONS, 2012. 2011 Census - Population and Household Estimates for England and Wales, March 2011. Statistical Bulletin, Office for National Statistics, UK. http://www.ons.gov.uk/ons/dcp171778_270487.pdf.

Ott WR. 1982. Concepts of human exposure to air pollution. Environment International 7, 79-96.

Özkaynak, H., Palma, T., Touma, J.S., Thurman, J., 2008. Modeling population exposures to outdoor sources of hazardous air pollutants. Journal of Exposure Science and Environmental Epidemiology 18, 45-58.

Park, J., Kim, E., Choe, Y., Ryu, H., Kim, S., 2020. Indoor to outdoor ratio of fine particulate matter by time of the day in house according to time-activity patterns. Journal of Environmental Health Sciences 46, 504–512.

Popoola, L., Adebanjo, S., Adeoye, B., 2018. Assessment of atmospheric particulate matter and heavy metals: a critical review. International Journal of Environmental Science and Technology 15, 935-948.

Shang, Y., Sun, Z., Cao, J., Wang, X., Zhong, L., Bi, X., Li, H., Liu, W., Zhu, T., Huang, W., 2013. Systematic review of Chinese studies of short-term exposure to air pollution and daily mortality. Environment International 54, 100-111.

Shao, Z., Bi, J., Ma, Z., Wang, J., 2017. Seasonal trends of indoor fine particulate matter and its determinants in urban residences in Nanjing, China. Building and Environment 125, 319-325.

Smith, J.D., Mitsakou, C., Kitwiroon, N., Barratt, B.M., Walton, H.A., Taylor, J.G., Anderson, H.R., Kelly, F.J., Beevers, S.D., 2016. London hybrid exposure model: improving human exposure estimates to NO_2 and $PM_{2.5}$ in an urban setting. Environmental Science & Technology 50, 11760-11768.

Soares, J., Kousa, A., Kukkonen, J., Matilainen, L., Kangas, L., Kauhaniemi, M., Riikonen, K., Jalkanen, J.-P., Rasila, T., Hänninen, O., 2014. Refinement of a model for evaluating the population exposure in an urban area. Geoscientific Model Development 7, 1855-1872.

Tofful, L., Perrino, C., 2015. Chemical composition of indoor and outdoor $PM_{2.5}$ in three schools in the city of Rome. Atmosphere 6, 1422-1443.

Valari, M., Markakis, K., Powaga, E., Collignan, B., Perrussel, O., 2020. EXPLUME v1. 0: a model for personal exposure to ambient O_3 and $PM_{2.5}$. Geoscientific Model Development 13, 1075-1094.

Wang, F., Meng, D., Li, X., Tan, J., 2016. Indoor-outdoor relationships of $PM_{2.5}$ in four residential dwellings in winter in the Yangtze River Delta, China. Environmental Pollution 215, 280-289.

WHO, 2017. https://www.iarc.who.int/wp-content/uploads/2018/07/pr221_E.pdf.

Williams, R., Rea, A., Vette, A., Croghan, C., Whitaker, D., Stevens, C., McDow, S., Fortmann, R., Sheldon, L., Wilson, H., 2009. The design and field implementation of the Detroit Exposure and Aerosol Research Study. Journal of Exposure Science and Environmental Epidemiology 19, 643-659.

Wu, D.-L., Lin, M., Chan, C.-Y., Li, W.-Z., Tao, J., Li, Y.-P., Sang, X.-F., Bu, C.-W., 2013. Influences of commuting mode, air conditioning mode and meteorological parameters on fine particle ($PM_{2.5}$) exposure levels in traffic microenvironments. Aerosol and Air Quality Research 13, 709-720.

Yang, W., Lee, K., Yoon, C., Yu, S., Park, K., Choi, W., 2011. Determinants of indoor activity pattern in Korean population. Journal of Exposure Science and Environmental Epidemiology 21, 310-316.

Yunesian, M., Rostami, R., Zarei, A., Fazlzadeh, M., Janjani, H., 2019. Exposure to high levels of $PM_{2.5}$ and PM_{10} in the metropolis of Tehran and the associated health risks during 2016–2017. Microchemical Journal 150, 104174.

U.S. Environmental Protection Agency. (2017). Air pollutants exposure model documentation (APEX, Version 5) volume I: User's guide, volume II: Technical support document. Office of Air Quality Planning and Standards, U.S. Environmental Protection Agency, Research Triangle Park, NC. EPA-452/R-17-001a,b.

Zhu, Y., Yang, L., Meng, C., Yuan, Q., Yan, C., Dong, C., Sui, X., Yao, L., Yang, F., Lu, Y., Wang, W., 2015. Indoor/outdoor relationships and diurnal/nocturnal variations in water-soluble ion and PAH concentrations in the atmospheric $PM_{2.5}$ of a business office area in Jinan, a heavily polluted city in China. Atmospheric Research 153, 276-285.

Chapter II.

A model for population exposure to $PM_{2.5}$: Identification of determinants for high population exposure in Seoul, Korea [1]

This chapter was partially published in *Environmental Pollution,* 2021, *285:117406.*

2.1. Introduction

Fine particulate matter (i.e., particulate matter with an aerodynamic diameter of < 2.5 µm; $PM_{2.5}$) exposure was linked with adverse health effects on respiratory and cardiovascular morbidity and mortality (Du and Li, 2016; Shang et al., 2013). Outdoor $PM_{2.5}$ concentrations at AQMSs have commonly been often used as a substitute for population exposure to $PM_{2.5}$ in epidemiological studies (Anderson et al., 2013; Atkinson et al., 2013). The approach is based on the assumption that outdoor $PM_{2.5}$ data represent the personal $PM_{2.5}$ exposure of individuals living in the vicinity of AQMS. However, people in developed countries such as US and Korea spend approximately 90% of their daily activities indoors (Klepeis et al., 2001; Yang et al., 2011) and pollutant concentrations may differ depending on the microenvironment (Hsu et al., 2020). Using outdoor $PM_{2.5}$ concentrations as a proxy for $PM_{2.5}$ exposure should be cautiously considered because the adverse effects of $PM_{2.5}$ might be underestimated in such evaluations. The mortality risk attributed to indoor and outdoor $PM_{2.5}$ exposure has been reported to be higher than the risk associated with only outdoor $PM_{2.5}$ exposure (Dong et al., 2020). Therefore, both indoor and outdoor air pollution should be considered to reduce the errors in the estimates of $PM_{2.5}$ exposure.

Population exposure to $PM_{2.5}$ could be determined by integrating partial exposure to $PM_{2.5}$ in each microenvironment. Modeling of population $PM_{2.5}$ exposure requires microenvironmental $PM_{2.5}$ concentrations and time-location patterns data for individuals. A few such population exposure models have been developed by the US Environmental Protection Agency (EPA), e.g., the stochastic human exposure dose simulation (SHEDS) (Burke et al., 2001) and Air pollution Exposure (APEX) models (Johnson et al., 2018). SHEDS and APEX are probabilistic models that predict the distribution of population exposure to $PM_{2.5}$ by randomly sampling from inputs. In these models, a mass balance equation using outdoor $PM_{2.5}$ concentrations, emission data, and microenvironment-specific characteristics was applied to calculate microenvironmental $PM_{2.5}$ concentrations. The microenvironmental $PM_{2.5}$ concentrations were combined with US time-location patterns from EPA's consolidated human activity database in order to simulate population exposure.

In previous study, a population exposure model, referred to as the Korea Simulation Exposure Model for $PM_{2.5}$ (KoSEM-$PM_{2.5}$), was developed to estimate population $PM_{2.5}$ exposure in Korea (Hwang et al., 2018). KoSEM-$PM_{2.5}$ used the time-activity patterns from the Korea Time Use Survey in 2004, and direct $PM_{2.5}$ measurements in microenvironments. However, the model was based on measurements from limited microenvironments (home, other, and transit) and time-activity pattern in one season. In addition, the microenvironmental $PM_{2.5}$ concentrations used in this model were measured only when outdoor concentrations were < 100 μg/m^3; however, high $PM_{2.5}$ concentration events do occur in Korea. A fine dust advisory in Korea is defined as when the hourly average of the ambient $PM_{2.5}$ concentration exceeds 150 μg/m^3 and continues for ≥ 2 h. The fine dust advisories in Seoul, Korea were issued 61 times in five years (2015-2019) (Air Korea, 2020). Therefore, the population exposure model developed in this study reflected various microenvironmental concentrations and seasons of $PM_{2.5}$ exposure.

A key aspect of an updated population exposure model should reflect the microenvironmental concentrations corresponding to the time-activity-location patterns by seasons and diverse outdoor levels. The microenvironmental $PM_{2.5}$ concentration could be determined using the outdoor $PM_{2.5}$ concentration by applying by the M/O ratio of $PM_{2.5}$. The M/O ratio has been used as an indicator for providing information of $PM_{2.5}$ pollution in indoor microenvironments because of many factors such as indoor pollutant sources, infiltration, and penetration to indoors (Chen and Zhao, 2011). The M/O ratio of $PM_{2.5}$ varies widely depending on the different microenvironments. The M/O ratio of $PM_{2.5}$ ranged from 0.68 to 0.81 in residential homes in Korea (Park et al., 2020b), from 0.44 to 0.62 in offices (Zhu et al., 2015), from 0.71 to 1.10 in kindergartens (Błaszczyk et al., 2017), from 0.90 to 1.28 in restaurants (Liu et al., 2004), and from 0.85 to 2.61 on public transportation (Wu et al., 2012).

The group with the highest exposure to $PM_{2.5}$ in the entire population would be of the greatest regulatory interest for assessing overall population exposure to $PM_{2.5}$. Even at the same $PM_{2.5}$ levels in ambient air, high $PM_{2.5}$ exposure may occur due to different time-activity patterns. Determining the characteristics of people who experience high exposures is important for health risk assessment and management (Chen et al., 2018). Exposure determinants should be identified in high $PM_{2.5}$ exposure group. For example, people's time-activity patterns in various microenvironments and demographic and socio-demographic factors, have been found to be significant determinants in estimation of $PM_{2.5}$ exposure (Matz et al., 2014).

The aims of this study were to predict population exposure to $PM_{2.5}$ by season and identify the determinants associated with the high-exposure group using KoSEM version 2 for $PM_{2.5}$ (KoSEM II-$PM_{2.5}$). This study upgraded an existing population exposure model (KoSEM) to predict the seasonal distribution of population exposure to $PM_{2.5}$ using time-location patterns from national population survey data, outdoor $PM_{2.5}$ concentrations, and M/O ratios of $PM_{2.5}$.

2.2. Methods

Input data

Inputs to the KoSEM II-$PM_{2.5}$ included three types of data: Times spent in each microenvironment, outdoor $PM_{2.5}$ concentrations, and M/O ratios of $PM_{2.5}$. An individual's total $PM_{2.5}$ exposure was calculated using the times spent in a microenvironment and the microenvironmental $PM_{2.5}$ concentrations. The times spent in the various microenvironments were obtained from the Time Use Survey for the Seoul population. Outdoor $PM_{2.5}$ concentrations were downloaded from a national website. M/O ratios of $PM_{2.5}$ were calculated using the microenvironment-specific $PM_{2.5}$ concentrations and the outdoor $PM_{2.5}$ concentrations.

- **Time spent dataset**

In Korea, Time Use Survey by Statistics Korea was conducted every 5 year from 1999. The time-location patterns of 3984 person-days in Seoul were obtained from the Time Use Survey data in 2014 provided by Statistics Korea (https://meta.narastat.kr/metasvc/index.do?confmNo=101052&inputYear=2014). The numbers of survey datapoints from summer, autumn, and winter were 960, 1898, and 1126, respectively. Subjects recorded the microenvironment in which they stayed every 10 min over 24 h, as well as their demographic and socio-economic information. Seven microenvironments were categorized; home, workplace/school, other indoor locations, restaurant, walking, car, and public transportation. "Walking" refers to surroundings during walking outdoors. Demographic and socio-economic information of the subjects are summarized in Table S-5.

- **Outdoor $PM_{2.5}$ concentration dataset**

The Korea Ministry of Environment measures outdoor $PM_{2.5}$ concentrations at national AQMSs using the standard monitoring method based on the β-ray absorption principle (Korea standard methods for the examination of air pollution, No. ES 01606.2a). Due to the maintenance of the monitor, the room conditions in AQMS were maintained at a temperature ranging 10–25 °C and a relative humidity ranging 30%–40%. The detection limit of the $PM_{2.5}$ monitor at AQMS was 5 μg/m^3 and the monitoring range was 0–1000 μg/m^3. Quality assurance/quality control (QA/QC) for measurements at AQMS was conducted weekly and valid data were selected based on the national QA/QC operational guidelines published by the Korea Ministry of Environment (https://www.airkorea.or.kr/web/board/3/267/?pMENUNO=145).

For 2015–2019, hourly $PM_{2.5}$ concentrations at 25 urban AQMSs in Seoul were downloaded from a website managed by the Korea Environment Corporation (http://www.airkorea.or.kr/autoStatistic). The obtained outdoor $PM_{2.5}$ concentrations at 25 AQMSs were averaged hourly by season for use in the model.

- **M/O ratio of $PM_{2.5}$ dataset**

The $PM_{2.5}$ concentrations in microenvironments were measured by MicroPEM v3.2 (RTI incorporated, Research Triangle Park, NC, USA) which is a portable $PM_{2.5}$ monitor with filter-based and real-time measurements. Previous study performed collocation test between MicroPEM data and AQMS data in Seoul, Korea (Guak and Lee, 2018); performance of MicroPEM data with AQMS data of $PM_{2.5}$ had good linearity with the R^2 of 0.93. Additionally, there were many studies evaluated the baseline drift of MicroPEM (Zhang et al., 2018; Wang et al., 2019; Cox et al., 2019; Shao et al., 2017); they also reported good performance of MicroPEM. In this study, the real-time $PM_{2.5}$ mass concentrations of MicroPEM were calibrated by the gravimetric mass concentration from each $PM_{2.5}$ sample on filter. Additional information on QA/QC for the MicroPEM data in this study is shown in Table S-6.

Field measurements of 24 h personal exposure to $PM_{2.5}$ were conducted by field technicians following the simulated time-location pattern scenarios by season for the Seoul population (Lee and Lee, 2017). A total of 140 24-h personal exposure samples (summer: 50, autumn: 40, and winter: 50) were collected in Seoul. The sampling periods were summer (July–August 2017), winter (December 2017–February 2018), and autumn (September–October 2018). The $PM_{2.5}$ concentrations in the seven microenvironments were categorized by season. The numbers of samples in each microenvironment by season are shown in Table S-7. Outdoor $PM_{2.5}$ concentrations at the nearest AQMS to the personal monitoring area were matched to calculate the M/O ratio in the same time period. Seasonal $PM_{2.5}$ M/O ratios in the seven microenvironments were calculated using the microenvironmental $PM_{2.5}$ concentrations and the corresponding outdoor $PM_{2.5}$ concentrations, as shown in Equation (1):

$$M/O\ ratio = \frac{C_{micro}}{C_{out}} \qquad (1)$$

where C_{micro} and C_{out} are the microenvironment and outdoor $PM_{2.5}$ concentrations, respectively.

Development of KoSEM II-$PM_{2.5}$

KoSEM II-$PM_{2.5}$ was developed to predict the seasonal distribution of population $PM_{2.5}$ exposures based on the time-location patterns in the seven microenvironments and the microenvironmental $PM_{2.5}$ concentrations in Seoul. The structure of the KoSEM II-$PM_{2.5}$ is shown in Figure 2-1. A probabilistic modeling approach, i.e., a Monte Carlo simulation, was used to simulate the daily population $PM_{2.5}$ exposure of 3984 Seoul residents. The 24-h personal exposure simulation for each person was based on Equation (2):

$$PE_n = \sum_{t=0}^{143} C_{mt} \times T_{mnt} \qquad (2)$$

where PE_n is the mean 24-h personal exposure to $PM_{2.5}$ of person n; C is the $PM_{2.5}$ concentration in the microenvironment m (home, workplace/school, other locations, restaurant, walking, car, and public transportation); and T is the fraction of time spent in microenvironment m by a person n at 10-min timecode t over 24 h.

The distribution of input variables for KoSEM II-$PM_{2.5}$ were classified into two categories for the outdoor $PM_{2.5}$ concentrations and $PM_{2.5}$ M/O ratios. The input distributions were fitted from each dataset using the *fitdist()* function in the package *"fitdistrplus"* (Delignette-Muller et al., 2010) for R software (version 4.0.3, R Core Team, Vienna, Austria). The best probability distributions were determined among candidate distributions (exponential, weibull, gamma, normal, and log-normal) using the lowest Bayesian information criterion. The input distributions of the outdoor $PM_{2.5}$ concentrations were created every 10-min timecodes for 24 hours depending on season. The three seasons were classified as summer (June–August), autumn

(September–November), and winter (December–February). The hourly outdoor $PM_{2.5}$ concentration in each month over 5 year was classified by the corresponding season, and then the distribution was created hourly over 24 h depending on season. Other input distributions of the $PM_{2.5}$ M/O ratio were created in the seven microenvironments by season.

The microenvironmental $PM_{2.5}$ concentrations were determined using the outdoor $PM_{2.5}$ concentrations and M/O ratios of $PM_{2.5}$. The outdoor $PM_{2.5}$ concentrations and $PM_{2.5}$ M/O ratios were randomly extracted from their distributions with 10,000 iterations of Monte Carlo sampling every 10 min. Two inputs were multiplied and were matched to time-location pattern with 144 10-min timecodes for a person. The 24-h personal exposure of 3984 individuals was repeatedly simulated through 10,000 iterations of Monte Carlo simulations. The probabilistic distributions of daily population exposure to $PM_{2.5}$ in summer, autumn, and winter were determined for 960, 1898, and 1126 individuals, respectively.

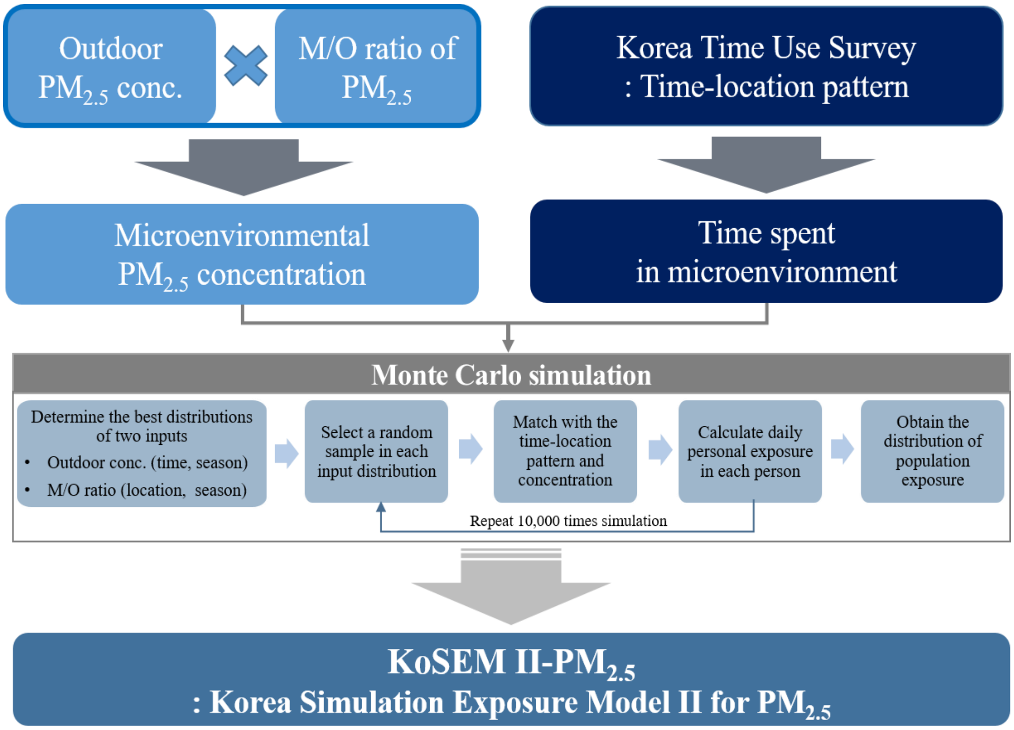

Figure 2-1. Structure of the KoSEM II-$PM_{2.5}$.

Determinants of exposure group

For exposure groups, the top 20% were assigned to the high-exposure group, the bottom 20% to the low-exposure group, and the reminder to the mid-exposure group for population exposure to $PM_{2.5}$ in winter. A stepwise approach involving allowing both backward elimination and forward addition of determinants was used through multinomial logistic regression analysis to identify the determinants that affected the levels of population exposure to $PM_{2.5}$. The nine covariates were housing type, housing ownership, age, gender, marital status, working status, education level, monthly income, and health condition. Continuous variables included housing size and working hours. Interactions with each variable were considered to explore the potential determinants. A stepwise regression analysis was conducted with $PM_{2.5}$ exposure of groups as dependent variable and other determinants as explanatory variables. In first stage, candidate variables with p-values < 0.1 in the likelihood ratio test (p-LRT) of the univariate analysis were selected. In the second stage, determinants having correlation coefficients > 0.75 with other variables were eliminated. Correlation coefficients (r) were calculated using Pearson correlation analysis between continuous variables, Cramér's V correlation (φ_c) between categorical variables, and polyserial correlation (ρ) between continuous and categorical variables. The combination of determinants with minimum Akaike information criterion (AIC)s were selected to determine the factors associated with the exposure group. Multinomial logistic regression model analysis was conducted to identify the final determinants for each exposure group using the *vglm()* function in the package *"VGAM"* (Yee and Hastie, 2003) of the R software version 4.0.3

Statistical analysis

Seasonal differences in times spent, outdoor $PM_{2.5}$ concentrations, and the $PM_{2.5}$ M/O ratios at microenvironments were evaluated using one-way analysis of variance (ANOVA) and Tukey's *post-hoc* test for comparison. A p-value < 0.05 indicated statistical significance for the two-sided statistical tests. All calculations and statistical analyses were conducted using R version 4.0.3.

2.3. Results

Model input variables

- **Time spent**

The times spent in the seven microenvironments are shown in Table 2-1. The times spent at homes ($p < 0.001$), workplaces/schools ($p < 0.05$), other indoor locations ($p < 0.05$), and walking ($p < 0.001$) were significantly different by season. In the three seasons, the Seoul population spent the majority of their time at home. The time spent in public transportation, restaurants, and cars was not significantly different by season. Microenvironments where people spent < 1 hour of the day were public transportation, restaurants, and cars.

Table 2-1. Times spent in different microenvironments by season.

Microenvironment	Time spent (hour)						
	Summer (n = 960)		Autumn (n = 1898)		Winter (n = 1126)		*p*-value
	Mean ± SD	Percent (%)	Mean ± SD	Percent (%)	Mean ± SD	Percent (%)	
Home	14.5 ± 4.8	60.5	14.2 ± 4.2	59.0	14.9 ± 4.8	62.2	< 0.001
Workplace/School	4.7 ± 4.5	19.4	5.0 ± 4.6	20.9	4.6 ± 4.4	19.2	< 0.001
Other indoor locations	2.2 ± 2.7	9.2	2.3 ± 2.8	9.5	2.0 ± 2.7	8.2	0.015
Restaurant	0.7 ± 1.1	2.8	0.6 ± 1.0	2.6	0.7 ± 1.1	2.8	0.416
Walking	0.7 ± 0.6	2.8	0.6 ± 0.6	2.4	0.5 ± 0.5	2.2	< 0.001
Car	0.4 ± 1.0	1.8	0.5 ± 1.0	1.9	0.5 ± 1.0	2.1	0.442
Public transportation	0.8 ± 1.1	3.3	0.9 ± 1.1	3.5	0.8 ± 1.2	3.3	0.296

SD : Standard deviation

- **Outdoor $PM_{2.5}$ concentration**

The outdoor $PM_{2.5}$ concentrations over 5 years (2015-2019) in Seoul are shown in Figure 2-2. The Daily means outdoor $PM_{2.5}$ concentrations differed significantly among the three seasons ($p < 0.001$), and the arithmetic mean (AM) ± standard deviation (SD) was 19.7 ± 9.6 (2.7–53.2) μg/m^3 in summer, 19.2 ± 11.4 (3.1–71.5) μg/m^3 in autumn, and 29.6 ± 15.4 (8.1–128.7) μg/m^3 in winter. In each year, outdoor $PM_{2.5}$ concentrations in winter were significantly higher than that in other seasons ($p < 0.001$), except in 2016 ($p = 0.07$). In 2015, daily AM ± SD of outdoor $PM_{2.5}$ concentrations was 20.0 ± 8.6 (3.9–46.8) μg/m^3 in summer, 20.5 ± 13.7 (3.6–70.2) μg/m^3 in autumn, and 27.6 ± 11.1 (10.8–65.6) μg/m^3 in winter. In 2016, daily AM ± SD of outdoor $PM_{2.5}$ concentrations was 23.7 ± 9.6 (4.5–47.4) μg/m^3 in summer, 23.8 ± 11.3 (5.2–54.8) μg/m^3 in autumn, and 26.8 ± 10.4 (10.2–57.8) μg/m^3 in winter. In 2017, daily AM ± SD of outdoor $PM_{2.5}$ concentrations was 19.1 ± 9.9 (3.9–44.5) μg/m^3 in summer, 18.6 ± 8.9 (4.6–46.3) μg/m^3 in autumn, and 31.0 ± 17.7 (10.4–94.8) μg/m^3 in winter. In 2018, daily AM ± SD of outdoor $PM_{2.5}$ concentrations was 17.8 ± 9.4 (2.7–38.3) μg/m^3 in summer, 17.5 ± 12.5 (3.6–71.5) μg/m^3 in autumn, and 28.8 ± 16.4 (8.1–87.8) μg/m^3 in winter. In 2019, daily AM ± SD of outdoor $PM_{2.5}$ concentrations was 18.1 ± 9.3 (3.3–53.2) μg/m^3 in summer, 15.6 ± 7.8 (3.1–39.7) μg/m^3 in autumn, and 33.6 ± 18.7 (10.9–128.7) μg/m^3 in winter. The hourly variation in outdoor $PM_{2.5}$ concentrations over 5 years is shown in Figure S-1.

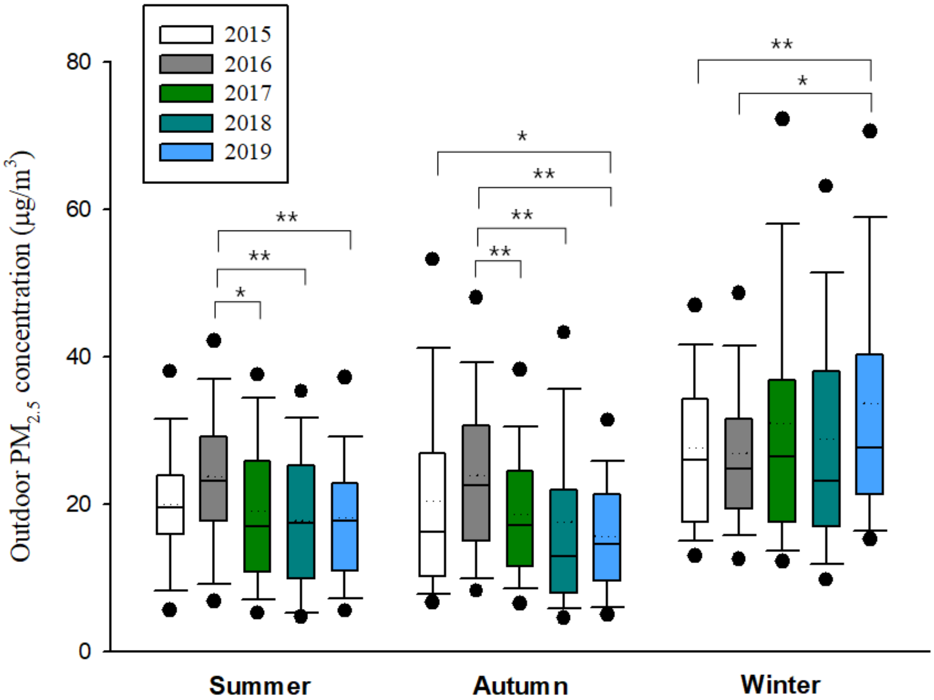

Figure 2-2. Daily average of outdoor $PM_{2.5}$ concentrations by season from 2015–2019. Mean and median are represented by the dotted line and plain line in the box. Box limits represent the 25th and 75th percentiles. The whiskers extend to the 10th and 90th percentiles. Circles above the 90th percentile represent the 95th percentile, and circles below the 10th percentile represent the 5th percentile. * : $p < 0.01$, ** : $p < 0.001$.

- **M/O ratio of $PM_{2.5}$**

Statistical descriptions of the $PM_{2.5}$ M/O ratio in microenvironments by season are shown in Table 2-2. $PM_{2.5}$ concentrations in each microenvironment are shown in Table S-8. Homes, workplaces/schools, and cars had $PM_{2.5}$ M/O ratios < 1. The lowest $PM_{2.5}$ M/O ratios in summer, autumn, and winter were in workplaces/schools, in homes, and in homes. Other indoor locations, restaurants, walking, and public transportation had $PM_{2.5}$ M/O ratios > 1. The highest M/O ratios of $PM_{2.5}$ in summer, autumn, and winter were in restaurants, respectively. All $PM_{2.5}$ M/O ratios in the microenvironments differed significantly by season ($p < 0.001$).

Table 2-2. Descriptive statistics of the $PM_{2.5}$ M/O ratio in various microenvironments by season.

Microenvironment	M/O ratio					
	Summer		Autumn		Winter	
	Mean ± SD	95% CI	Mean ± SD	95% CI	Mean ± SD	95% CI
Home	0.89 ± 0.79	(0.88, 0.90)	0.64 ± 0.78	(0.63, 0.64)	0.57 ± 0.51	(0.57, 0.58)
Workplace/School	0.78 ± 0.71	(0.77, 0.79)	0.75 ± 0.49	(0.74, 0.76)	0.95 ± 1.00	(0.93, 0.97)
Other indoor locations	1.34 ± 1.83	(1.30, 1.38)	1.23 ± 1.09	(1.09, 1.16)	1.72 ± 3.36	(1.63, 1.80)
Restaurant	2.46 ± 3.48	(2.31, 2.61)	2.92 ± 3.57	(2.72, 3.13)	3.84 ± 8.30	(3.50, 4.18)
Walking	1.75 ± 1.59	(1.68, 1.81)	0.99 ± 0.61	(0.96, 1.01)	1.25 ± 0.79	(1.21, 1.29)
Car	0.60 ± 0.93	(0.55, 0.64)	0.77 ± 0.40	(0.75, 0.80)	0.69 ± 0.46	(0.67, 0.71)
Public transportation	1.33 ± 1.26	(1.29, 1.38)	1.59 ± 1.29	(1.52, 1.66)	1.73 ± 1.42	(1.68, 1.79)

SD : Standard deviation. CI : Confidence interval (lower, upper)

Distribution of population $PM_{2.5}$ exposure by season

The probability distribution of population exposures to $PM_{2.5}$ by season are shown in Figure 2-3. Population exposures to $PM_{2.5}$ differed significantly by season ($p < 0.01$). The highest population exposure to $PM_{2.5}$ occurred in winter, while the lowest was in autumn. The AM ± SD of population exposures to $PM_{2.5}$ was 29.9 ± 10.6 (17.0–114.8; 20th percentile = 22.9, 80th percentile = 35.2) μg/m^3 in winter (n = 1126), 21.3 ± 4.0 (16.0–46.2; 20th percentile = 18.1, 80th percentile = 23.5) μg/m^3 in summer (n = 960), and 9.8 ± 2.7 (7.2–33.3; 20th percentile = 8.1, 80th percentile = 11.0) μg/m^3 in autumn (n = 1898), respectively. The 20% of daily mean population exposure to $PM_{2.5}$ in winter exceeded the Korean $PM_{2.5}$ ambient standard of 35 μg/m^3 with a 24-h mean.

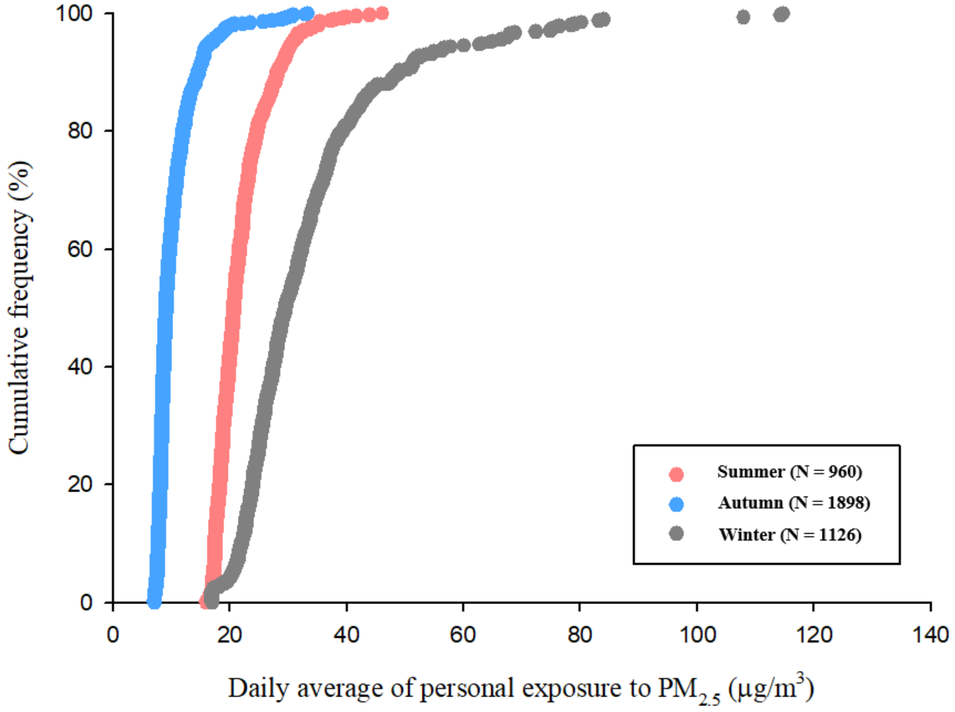

Figure 2-3. Cumulative frequency of population exposures to $PM_{2.5}$ by season using a probabilistic simulation.

Characteristics of $PM_{2.5}$ exposure groups

For the high-exposure group for the top 20% in winter, the AM ± SD of population exposures to $PM_{2.5}$ was 45.4 ± 13.1 (35.2–114.8) μg/m^3. The AM ± SD of the low- and mid-exposure groups was 20.4 ± 2.1 μg/m^3 and 27.9 ± 3.4 μg/m^3, respectively. The demographic and socio-economic characteristics and times spent in microenvironments by exposure groups are shown in Table 2-3. The high-exposure group was characterized by having more males, being of lower ages, and having a higher monthly income and longer working hours. In the high-exposure group, the age was significantly lower than that in the low-exposure group ($p < 0.05$). Working hours in the high-exposure group were significantly higher than those in the low-exposure group ($p < 0.001$). The high-exposure group spent 60% of their time at home, while the low-exposure group spent the majority of their time (81%) at home. Times spent in other indoor locations by the high-exposure group were five-fold higher than that in the low-exposure group.

Table 2-3. Demographic and socio-economic characteristics of the exposure groups for $PM_{2.5}$.

Variable	Characteristic	Exposure level					
		Low (n=226)		Mid (n=674)		High (n=226)	
		n	%	n	%	n	%
Gender							
	Male	83	36.7	339	50.3	135	59.7
	Female	143	63.3	335	49.7	91	40.3
Age	AV±SD (years)	44.6±20.8		40.8±17.7		41.3±20.2	
	<20	38	16.8	95	14.1	47	20.8
	20-39	62	27.4	228	33.8	59	26.1
	40-59	68	30.1	234	34.7	74	32.7
	≥60	58	25.7	117	17.4	46	20.4
Marital status							
	Single	64	28.3	237	35.2	84	37.2
	Married	162	71.7	437	64.8	142	62.8
Education level							
	Elementary school and below	27	11.9	63	9.3	21	9.3
	Middle/High school	86	38.1	220	32.6	85	37.6
	College/University	101	44.7	346	51.3	103	45.6
	Graduate school	12	5.3	45	6.7	17	7.5
Monthly income[a]							
	No income	87	38.5	214	31.8	88	38.9
	<200	86	38.1	217	32.2	69	30.5
	200-300	23	10.2	100	14.8	29	12.8
	>300	30	13.3	143	21.2	40	17.7
Housing type							
	Detached house	56	24.8	187	27.7	61	27.0
	Apartment	110	48.7	310	46.0	104	46.0
	Others	60	26.5	177	26.3	61	27.0
Housing ownership							
	Owner	116	51.3	373	55.3	127	56.2
	Tenant	110	48.7	301	44.7	99	43.8
Housing size	AV±SD (m^2)	77.3±32.5		81.5±32.6		79.8±33.0	
Working status							
	Unemployed	137	60.6	291	43.2	129	57.1

	Employed	89	39.4	383	56.8	97	42.9
	Working hours (AV±SD)	37.5±21.0		44.0±17.3		44.0±16.2	
Health condition							
	Healthy	69	30.5	290	43.0	106	46.9
	Normal	100	44.2	291	43.2	100	44.2
	Unhealthy	57	25.2	93	13.8	20	8.8
Time spent (min)							
	Home	1162	80.7	738	51.2	859	59.7
	Workplace/school	209	14.5	148	10.3	342	23.7
	Restaurant	8	0.6	60	4.2	45	3.2
	Other indoor locations	14	1.0	344	23.9	78	5.4
	Walking	21	1.4	38	2.7	32	2.3
	Car	18	1.2	38	2.6	31	2.1
	Public transportation	9	0.6	73	5.0	51	3.6

[a] : Korean Republic Won, KRW, one thousand won

Determinants associated with high population exposure

Among the demographic and socio-economic factors, gender, age, working status, working hours, monthly income, and health condition were significantly associated with the exposure group as determined by univariate regression analysis ($p < 0.05$). Gender, age, working hours, and health condition were determined as the fixed effect after a stepwise variable selection with the lowest AIC.

The final multinomial logistic regression results, with the mid-exposure groups as the reference, are shown in Table 2-4. An "unhealthy" health condition was the most significant determinant of exposure group, followed by gender in all exposure groups. People with an "unhealthy" health condition were approximately 40% less likely to report high exposure ($p < 0.05$). Meanwhile, people with an 'unhealthy' health condition were approximately 2.3 times more likely to report low exposure ($p < 0.001$). Females were approximately 40% less likely to report high exposure ($p < 0.01$), but were approximately 68% more likely to report low exposure. No significant difference was found in age in the high-exposure group ($p = 0.24$).

Table 2-4. Determinants associated with the $PM_{2.5}$ exposure group by a multinomial logistic regression model.

Exposure group		Estimate	SE[a]	z value	*p*-value	OR[b]
Low vs Mid.	Intercept	-1.561	0.234	-6.683	<0.001†	0.210
	Gender					
	Male	Reference				
	Female	0.277	0.166	1.670	0.095	1.319
	Age	0.008	0.004	1.961	0.049†	1.008
	Working hours	-0.017	0.004	-4.831	<0.001†	0.983
	Health condition					
	Healthy	Reference				
	Normal	0.324	0.183	1.768	0.077	1.382
	Unhealthy	0.822	0.223	3.684	<0.001†	2.274
High vs Mid.	Intercept	-0.704	0.207	-3.393	<0.001†	0.495
	Gender					
	Male	Reference				
	Female	-0.509	0.163	-3.123	0.002†	0.601
	Age	0.005	0.004	1.169	0.24	1.005
	Working hours	-0.013	0.003	-3.824	<0.001†	0.987
	Health condition					
	Healthy	Reference				
	Normal	-0.059	0.167	-0.353	0.724	0.943
	Unhealthy	-0.509	0.277	-1.838	0.046†	0.601

[a]: SE : Standard error. [b]: OR : Odds ratio. †: Estimates are statistically significant at $p < 0.05$.

2.4. Discussion

A model, KoSEM II-$PM_{2.5}$ was developed to estimate the seasonal distributions of population $PM_{2.5}$ exposures in Seoul. In the previous version of the model, the input data were measurements in three microenvironments when the outdoor $PM_{2.5}$ concentration was < 100 μg/m^3 and the time-activity pattern in only one season (Hwang et al., 2018). In this study, microenvironmental $PM_{2.5}$ concentrations, which were estimated by the outdoor $PM_{2.5}$ concentrations and the M/O ratios, were matched by the time spent in microenvironments in three seasons. In addition, the updated version of the model included more specific microenvironments, such as home, others (workplaces/schools, other indoor locations, and restaurants), and transit (walking, cars, and public transportation). Therefore, KoSEM II-$PM_{2.5}$ could reflect more realistic population exposure to $PM_{2.5}$.

KoSEM II-$PM_{2.5}$ is based on a probabilistic modeling using measurements in various microenvironments. Direct personal exposure measurements for large populations have often been difficult to conduct in epidemiological studies due to the high-cost and low practicality. A probabilistic approach could overcome the uncertainties of limited data by simulating the possible distributions of inputs. Microenvironmental $PM_{2.5}$ concentrations for the KoSEM II-$PM_{2.5}$ were calculated by multiplying the probability distributions of the outdoor $PM_{2.5}$ concentrations and the $PM_{2.5}$ M/O ratios corresponding to the time-location pattern by season. KoSEM II-$PM_{2.5}$ provided the frequency distribution of population exposure to $PM_{2.5}$, similar to other models such as SHEDS (Burke et al., 2001), APEX (Johnson et al., 2018), EXPOLIS simulation model (Hänninen et al., 2003), and EXPLUME (Valari et al., 2020).

Population exposure could be affected by seasonal differences in the microenvironmental $PM_{2.5}$ concentration and time-activity pattern. In this study, daily average outdoor $PM_{2.5}$ concentrations in winter were significantly higher than that in other seasons. The $PM_{2.5}$ M/O ratios in microenvironments were also significantly different by season. In homes, the $PM_{2.5}$ M/O ratio decreased from summer to winter. In several indoor microenvironments, the $PM_{2.5}$ M/O ratios in workplaces/schools, other indoor locations, restaurants, and public transportation increased from summer to winter. These seasonal differences in the $PM_{2.5}$ M/O ratio in these four microenvironments might indicate a lack of indoor ventilation in winter. The times spent in several microenvironments (including homes, workplaces/schools, other indoor locations, and walking) were significantly different by season. A previous study reported that season was the determinant that affected the time spent in microenvironments (Lee and Lee, 2017).

The $PM_{2.5}$ M/O ratio could indicate microenvironment characteristics. Microenvironments with a $PM_{2.5}$ M/O ratio > 1 (i.e., in other indoor locations, restaurants, and on public transportation) indicate that there may be significant pollutant sources in indoor microenvironments. In particular, the $PM_{2.5}$ M/O ratios in restaurants were twice as high as that in other microenvironments. Cooking was the major activity that generated indoor air pollutants and induced high indoor $PM_{2.5}$ concentrations (Sarigiannis et al., 2014; Shao et al., 2017). Although walking occurred outdoors, the $PM_{2.5}$ M/O ratio slightly exceeded 1 possibly due to resuspension activities and particles generated from vehicles when walking on the roadside. When the $PM_{2.5}$ M/O ratio was < 1 (i.e., in homes, workplaces/schools, and cars), there was often lack of a significant source and limited infiltration from ambient air to indoors.

Population exposure to $PM_{2.5}$ was higher in winter than in other seasons. High exposure in winter was affected by high outdoor $PM_{2.5}$ concentrations in winter. Personal exposure to $PM_{2.5}$ was closely associated with outdoor $PM_{2.5}$ concentrations when the time-activity pattern was fixed, as for an office worker (Guak and Lee, 2018). In China, population exposure to $PM_{2.5}$ was also the highest in winter at 102.1 $\mu g/m^3$ (Wang et al., 2019), which was consistent with the seasonal variation in outdoor $PM_{2.5}$ concentrations in the present study. High $PM_{2.5}$ concentrations were typically observed in Korea in winter. The air quality was affected by the long-range transport of air pollutants from East Asia, regional sources, and meteorological conditions on the Korean Peninsula (Kim et al., 2018). Policies for improving air quality will be necessary to mitigate personal exposure to air pollution during winter in Korea.

The high-exposure group had more males of a lower age and longer working hours. A previous study of time-activity pattern data in 2004 reported consistent results, showing that age and working hours were significantly associated with high $PM_{2.5}$ exposure (Hwang et al., 2018). In addition, an 'unhealthy' health condition was the most significant determinant for low- and high-exposure groups. Individuals with an 'unhealthy' health condition tended to be included in the low-exposure group more than the high-exposure group. The times spent at home in the low-exposure group (80.7%) were significantly higher compared with that of the high-exposure group (59.7%). This was consistent with other findings that showed that vulnerable groups such as patients, the elderly, and children spent > 90% of their day indoors in Korea (An et al., 2018). Vulnerable groups spent > 19 h indoors because they were less active than other groups (Buonanno et al., 2014).

The development of KoSEM II-$PM_{2.5}$ has some limitations. The model did not consider the spatial variation of outdoor $PM_{2.5}$ concentration in Seoul. The outdoor $PM_{2.5}$ concentration at 25 AQMSs was averaged hourly and used as inputs in KoSEM II-$PM_{2.5}$. The study was based on the assumption that the average $PM_{2.5}$ concentrations in 25 AQMSs could represent all locations in Seoul. However, the spatial variation should be considered to accurately estimate the population exposure (Hu et al., 2020; Valari et al., 2020). In this study, outdoor $PM_{2.5}$ concentrations could not be matched with participant's district information in Seoul because the Time Use Survey data did not provide specific address.

Korean Time Use Surveys were conducted every 5 year from 1999. There were data for 1999, 2004, 2009, 2014, and 2019, but data in 2019 were established to open the public in September 2020. We designed this study in 2017 when Time Use Survey data in 2019 were not available. Therefore, we used 2014 data to measure microenvironmental $PM_{2.5}$ concentrations.

A challenge in population exposure model is the validation of the model since personal measurement data for population needs significant time and resources. As KoSEM II-$PM_{2.5}$ was not validated by comparison with personal exposure to $PM_{2.5}$, this model did not estimate specific personal exposure. Personal measurement data in this study were used as inputs for the model. Our model could be useful in identifying the characteristics of high exposure group for prevention of health effects of public. For future studies, the validation of population model could be conducted through additional personal exposure measurements with statistical analysis. A Bayesian hierarchical framework that assimilates the distribution of actual individuals in a population was proposed to validate population exposure model (Rodriguez et al., 2016).

KoSEM II-$PM_{2.5}$ was unable to take into account population exposure to $PM_{2.5}$ in spring because there were no spring data for time-location patterns in the Korean Time Use Survey in 2014. In Korea, high PM concentrations mainly occurred in spring due to severe air pollution episodes such as Asian dust and fine dust advisory (Kim et al., 2020). Thus, it is important to identify personal exposure to $PM_{2.5}$ in spring when outdoor $PM_{2.5}$ levels are high. In addition, input measurements were only conducted in Seoul, and the population exposure to $PM_{2.5}$ in Seoul was simulated using KoSEM II-$PM_{2.5}$. If additional national time-activity pattern data in spring and measurements in other regions become available, additional input data could be included that would improve the model accuracy for estimating population exposure to $PM_{2.5}$ in spring and in other regions.

2.5. Conclusions

A population exposure model was developed in this study to estimate the distribution of population exposure to $PM_{2.5}$ in Seoul using time-location patterns, outdoor $PM_{2.5}$ concentrations, and M/O ratios of $PM_{2.5}$. The Seoul population spent approximately 60% of their time at home in all seasons. Population exposure to $PM_{2.5}$ in Seoul differed significantly by season, which was statistically verifies using ANOVA test. High Population exposure to $PM_{2.5}$ mainly occurred in winter. Significant determinants of high population exposure to $PM_{2.5}$ were identified in the model, including gender, age, working hours, and health condition. The high $PM_{2.5}$ exposure group was characterized as having a higher proportion of males of a lower age with longer working hours, and having fewer 'unhealthy' health condition. The identification of determinants for population exposure to $PM_{2.5}$ could be used to evaluate the effectiveness of control policies to reduce personal exposure to $PM_{2.5,}$ and to implement effective interventions.

References

Air KOREA. Available: http://www.airkorea.or.kr/web.

An, J., Oh, Y., Im, J., Ahn, M., Hong, E., Son, B., 2018. Concentration and risk assessment of indoor air quality in day care centers and postnatal care centers. Journal of Odor Indoor Environment 17, 337–345.

Anderson, H.R., Favarato, G., Atkinson, R.W., 2013. Long-term exposure to outdoor air pollution and the prevalence of asthma: meta-analysis of multi-community prevalence studies. Air Quality, Atmosphere & Health 6, 57-68.

Atkinson, R.W., Carey, I.M., Kent, A.J., van Staa, T.P., Anderson, H.R., Cook, D.G., 2013. Long-term exposure to outdoor air pollution and incidence of cardiovascular diseases. Epidemiology 24, 44-53.

Błaszczyk, E., Rogula-Kozłowska, W., Klejnowski, K., Kubiesa, P., Fulara, I., Mielżyńska-Švach, D., 2017. Indoor air quality in urban and rural kindergartens: short-term studies in Silesia, Poland. Air Quality, Atmosphere & Health 10, 1207-1220.

Buonanno, G., Stabile, L., Morawska, L., 2014. Personal exposure to ultrafine particles: The influence of time-activity patterns. Science of The Total Environment 468–469, 903-907.

Burke, J.M., Zufall, M.J., Özkaynak, H., 2001. A population exposure model for particulate matter: case study results for $PM_{2.5}$ in Philadelphia, PA. Journal of Exposure Science and Environmental Epidemiology 11, 470-489.

Chen, C., Zhao, B., 2011. Review of relationship between indoor and outdoor particles: I/O ratio, infiltration factor and penetration factor. Atmospheric Environment 45, 275-288.

Chen, X.-C., Ward, T.J., Cao, J.-J., Lee, S.-C., Chow, J.C., Lau, G.N.C., Yim, S.H.L., Ho, K.-F., 2018. Determinants of personal exposure to fine particulate matter ($PM_{2.5}$) in adult subjects in Hong Kong. Science of The Total Environment 628-629, 1165-1177.

Cohen, A.J., Brauer, M., Burnett, R., Anderson, H.R., Frostad, J., Estep, K., Balakrishnan, K., Brunekreef, B., Dandona, L., Dandona, R., Feigin, V., Freedman, G., Hubbell, B., Jobling, A., Kan, H., Knibbs, L., Liu, Y., Martin, R., Morawska, L., Pope, C.A., Shin, H., Straif, K., Shaddick, G., Thomas, M., van Dingenen, R., van Donkelaar, A., Vos, T., Murray, C.J.L., Forouzanfar, M.H., 2017. Estimates and 25-year trends of the global burden of disease attributable to ambient air pollution: an analysis of data from the Global Burden of Diseases Study 2015. The Lancet 389, 1907-1918.

Cox, J., Cho, S.-H., Ryan, P., Isiugo, K., Ross, J., Chillrud, S., Zhu, Z., Jandarov, R., Grinshpun, S.A., Reponen, T., 2019. Combining sensor-based measurement and modeling of $PM_{2.5}$ and black carbon in assessing exposure to indoor aerosols. Aerosol Science and Technology 53, 817-829.

Delignette-Muller, M.L., Pouillot, R., Denis, J.B., Dutang, C., 2010. fitdistrplus: help to fit of a parametric distribution to non-censored or censored data. R package version 0.1–3. https://cran.r-project.org/web/packages/fitdistrplus/index.html.

Du, Y., Li, T., 2016. Assessment of health-based economic costs linked to fine particulate ($PM_{2.5}$) pollution: a case study of haze during January 2013 in Beijing, China. Air Quality, Atmosphere & Health 9, 439-445.

Guak, S., Lee, K., 2018. Different relationships between personal exposure and ambient concentration by particle size. Environmental Science and Pollution Research 25, 16945-16950.

Hänninen, O., Kruize, H., Lebret, E., Jantunen, M., 2003. EXPOLIS simulation model: $PM_{2.5}$ application and comparison with measurements in Helsinki. Journal of Exposure Science and Environmental Epidemiology 13, 74-85.

Hsu, W.T., Chen, J.L., Candice Lung, S.C., Chen, Y.C., 2020. $PM_{2.5}$ exposure of various microenvironments in a community: Characteristics and applications. Environmental Pollution 263, 114522.

Hwang, Y., An, J., Lee, K., 2018. Characterization of a high $PM_{2.5}$ exposure group in Seoul using the Korea simulation exposure model for $PM_{2.5}$ (KoSEM-PM) based on time–activity patterns and microenvironmental measurements. International Journal of Environmental Research and Public Health 15, 2808.

Johnson, T.R., Langstaff, J.E., Graham, S., Fujita, E.M., Campbell, D.E., 2018. A multipollutant evaluation of APEX using microenvironmental ozone, carbon monoxide, and particulate matter ($PM_{2.5}$) concentrations measured in Los Angeles by the exposure classification project. Cogent Environmental Science 4, 1453022.

Kim, D., Choi, H.-E., Gal, W.-M., Seo, S., 2020. Five year trends of particulate matter concentrations in Korean regions (2015–2019): when to ventilate? International Journal of Environmental Research and Public Health 17, 5764.

Kim, Y., Seo, J., Kim, J.Y., Lee, J.Y., Kim, H., Kim, B.M., 2018. Characterization of $PM_{2.5}$ and identification of transported secondary and biomass burning contribution in Seoul, Korea. Environmental Science and Pollution Research 25, 4330-4343.

Klepeis, N.E., Nelson, W.C., Ott, W.R., Robinson, J.P., Tsang, A.M., Switzer, P., Behar, J.V., Hern, S.C., Engelmann, W.H., 2001. The National Human Activity Pattern Survey (NHAPS): a resource for assessing exposure to environmental pollutants. Journal of Exposure Science and Environmental Epidemiology 11, 231–252.

Lee, S., Lee, K., 2017. Seasonal differences in determinants of time location patterns in an urban population: a large population-based study in Korea. International Journal of Environmental Research and Public Health 14, 672.

Liu, Y., Chen, R., Shen, X., Mao, X., 2004. Wintertime indoor air levels of PM_{10}, $PM_{2.5}$ and PM_1 at public places and their contributions to TSP. Environment International 30, 189-197.

Loomis, D., Grosse, Y., Lauby-Secretan, B., El Ghissassi, F., Bouvard, V., Benbrahim-Tallaa, L., Guha, N., Baan, R., Mattock, H., Straif, K., 2013. The carcinogenicity of outdoor air pollution. Lancet Oncology 14, 1262.

Matz, C.J., Stieb, D.M., Davis, K., Egyed, M., Rose, A., Chou, B., Brion, O., 2014. Effects of age, season, gender and urban-rural status on time-activity: Canadian Human Activity Pattern Survey 2 (CHAPS 2). International Journal of Environmental Research and Public Health 11, 2108-2124.

Park, J., Jo, W., Cho, M., Lee, J., Lee, H., Seo, S., Lee, C., Yang, W., 2020a. Spatial and temporal exposure assessment to $PM_{2.5}$ in a community using sensor-based air monitoring instruments and dynamic population distributions. Atmosphere 11, 1284.

Park, J., Kim, E., Choe, Y., Ryu, H., Kim, S., 2020b. Indoor to outdoor ratio of fine particulate matter by time of the day in house according to time-activity patterns. Journal of Environmental Health Sciences 46, 504–512.

Sarigiannis, D.A., Karakitsios, S.P., Kermenidou, M., Nikolaki, S., Zikopoulos, D., Semelidis, S., Papagiannakis, A., Tzimou, R., 2014. Total exposure to airborne particulate matter in cities: the effect of biomass combustion. Science of The Total Environment 493, 795-805.

Shang, Y., Sun, Z., Cao, J., Wang, X., Zhong, L., Bi, X., Li, H., Liu, W., Zhu, T., Huang, W., 2013. Systematic review of Chinese studies of short-term exposure to air pollution and daily mortality. Environment International 54, 100-111.

Shao, Z., Bi, J., Ma, Z., Wang, J., 2017. Seasonal trends of indoor fine particulate matter and its determinants in urban residences in Nanjing, China. Building and Environment 125, 319-325.

Valari, M., Markakis, K., Powaga, E., Collignan, B., Perrussel, O., 2020. EXPLUME v1.0: a model for personal exposure to ambient O_3 and $PM_{2.5}$. Geoscientific Model Development 13, 1075-1094.

Wang, H., Li, J., Gao, Z., Yim, S.H., Shen, H., Ho, H.C., Li, Z., Zeng, Z., Liu, C., Li, Y., 2019. High-Spatial-Resolution population exposure to $PM_{2.5}$ pollution based on multi-satellite retrievals: a case study of seasonal variation in the Yangtze River Delta, China in 2013. Remote Sensing 11, 2724.

Wang, Y., Du, Y., Wang, J., Li, T., 2019. Calibration of a low-cost $PM_{2.5}$ monitor using a random forest model. Environment International 133, 105161.

Wu, D.-L., Lin, M., Chan, C.-Y., Li, W.-Z., Tao, J., Li, Y.-P., Sang, X.-F., Bu, C.-W., 2012. Influences of commuting mode, air conditioning mode and meteorological parameters on fine particle ($PM_{2.5}$) exposure levels in traffic microenvironments. Aerosol and Air Quality Research 13, 709-720.

Yang, W., Lee, K., Yoon, C., Yu, S., Park, K., Choi, W., 2011. Determinants of residential indoor and transportation activity times in Korea. Journal of Exposure Science and Environmental Epidemiology 21, 310-316.

Yee, T.W., Hastie, T.J., 2003. Reduced-rank vector generalized linear models. Stat. Modelling. 3, 15–41.

Zhu, Y., Yang, L., Meng, C., Yuan, Q., Yan, C., Dong, C., Sui, X., Yao, L., Yang, F., Lu, Y., Wang, W., 2015. Indoor/outdoor relationships and diurnal/nocturnal variations in water-soluble ion and PAH concentrations in the atmospheric $PM_{2.5}$ of a business office area in Jinan, a heavily polluted city in China. Atmospheric Research 153, 276-285.

Zhang, T., Chillrud, S.N., Pitiranggon, M., Ross, J., Ji, J., Yan, B., 2018. Development of an approach to correcting MicroPEM baseline drift. Environmental research 164, 39-44.

Chapter III.

Prediction models using outdoor environmental data for real-time PM_{10} concentrations in daycare centers, kindergartens, and elementary schools [2]

This chapter was partially published in *Building and Environment,* 2021, 187:107371

3.1. Introduction

Indoor environments play an important role in personal exposure to environmental pollutants because people generally spend more than 85% of their time indoors (Klepeis et al., 2001; Yang et al., 2011). Children are particularly affected as they spend long hours in educational facilities such as daycare centers, kindergartens, and elementary schools. Children are more susceptible to air pollutants than adults because of their physiological functions. These include a higher inhalation rate per unit of body weight (Quirós-Alcalá et al., 2016) and active cell growth in tissues and organs (Santamouris et al., 2008).

Indoor air pollution in educational facilities might be associated with the deterioration of children's health, attendance, and academic performance. Indoor air pollutants could cause immediate health effects including cough, headaches, eye irritation, dizziness, and fatigue (Santamouris et al., 2008). These symptoms have also been linked to decreased attendance of children in educational facilities. The poor indoor air quality (IAQ) in the educational facilities was associated with significant increase in yearly absence (Shendell et al., 2004). Significant rise in the mathematical scores of students was observed on improving the IAQ by managing ventilation in the educational facilities (Haverinen-Shaughnessy and Shaughnessy, 2015).

Particulate matter (PM) is a critical indoor air pollutant affecting human health and increasing the risk of lung and respiratory diseases (Sørensen et al., 2003). The Korea Ministry of Environment has tightened the indoor PM_{10} standard from 100 $\mu g/m^3$ to 75 $\mu g/m^3$ in classrooms at daycare centers. This was implemented in Korea since October 2018. The Korea Ministry of Education from October 2019 onwards has also tightened the indoor PM_{10} standard from 100 $\mu g/m^3$ to 75 $\mu g/m^3$ in classrooms at kindergartens and elementary schools under the School Health Act. The standards were evaluated using over 6 h time-integrated gravimetric concentration once in a year. The indoor PM_{10} standard in educational facilities has been controlled more tightly than the ambient PM_{10} standard which is a daily mean of 100 $\mu g/m^3$ regulated by the Korea Ministry of Environment.

The time weighted indoor PM_{10} standard could determine the general tendency of IAQ; however, it cannot be useful for immediate intervention. For effective control of the indoor PM_{10} levels in educational facilities, real-time data are needed to intervene for sudden high peaks. IAQ can be predicted without direct measurement which can produce real-time data. Prediction of real-time indoor PM_{10} concentrations can be determined by mechanistic or statistical methods. Mechanistic methods require information of pollutant sources, chemical composition of the emissions, and physical processes in the air (Hrust et al., 2009). On the other hands, statistical methods do not need to consider information of the physical behavior of pollutants and use of costly computer resources.

Statistical prediction models of real-time indoor PM_{10} concentration could be developed using real-time data for long measurement times. Real-time data for one year are needed for the models because of seasonal variation (Sun et al., 2019). IAQ statistical modelling commonly used input parameters such as indoor air pollutant concentration, indoor information, and outdoor environmental data (Du et al., 2018; Elbayoumi et al., 2014). However, direct indoor measurement and observation of indoor information requires a lot of labor time and money. In this study, the prediction models in educational facilities were developed using real-time outdoor environmental data.

This study aimed to develop and evaluate prediction models for the real-time indoor PM_{10} concentration in daycare centers, kindergartens, and elementary schools. To validate predicting the indoor PM_{10} concentration in each educational facility, a statistical model was adopted using real-time direct indoor measurements at minute scale over one year.

3.2. Methods

Data set

From July 2016 to June 2017, indoor PM_{10} concentrations were measured by real-time monitors with Wi-Fi or LTE (AirGuard K, K weather Inc., Korea) at 54 daycare centers (0–5 age), 12 kindergartens (6–7 age), and 21 elementary schools (8–13 age) in Seoul, Korea over a period of one year. The numbers of data-point for real-time measurements were 2,668,048 in daycare centers, 481,482 in kindergartens, and 957,902 in elementary schools every 10 minute. The specifications of AirGuard K are shown in Table S-9. Measurement PM_{10} data were downloaded from a web site (AirGuard K Manager) via wifi or LTE connection (K weather Inc., Korea). The performance of AirGuard K was validated in comparison with gravimetric PM_{10} monitor from 40 co-location tests (Figure S-3). The co-located gravimetric data were measured by 2 day time integrated PM_{10} samples collected onto Teflon filter (Zefon International, Ocala, FL, USA) placed in MicroPEM v3.2 (RTI incorporated, Research Triangle Park, NC, USA). They found agreement (R^2 = 83.1%, correction factor = 1.50) and used this relationship to convert from AirGuard K to filter-based PM_{10} concentrations. In our study, all indoor PM_{10} concentrations were also adjusted by 1.50 (Kim et al., 2017).

For the period between July 2016 and June 2017, outdoor PM_{10} concentrations were obtained from the Korean Ministry of Environment and managed by the Korea Environment Corporation, which provide hourly PM_{10} concentration from the urban AQMSs in Seoul, Korea (http://www.airkorea.or.kr/autoStatistic). The PM_{10} concentrations from the closest AQMS to each educational facility's address were used to develop the indoor PM_{10} prediction model. AQMSs were within 3.3 km from the educational facilities. Location of the AQMSs and educational facilities in Seoul are shown in Figure S-4.

The minute meteorological data were obtained from the Korea Meteorological Administration to examine the influence of the weather conditions on the indoor PM_{10} concentration in Seoul, Korea during sampling periods (https://data.kma.go.kr/cmmn/main.do). Eight meteorological variables including outdoor temperature (°C), relative humidity (%), wind speed (m/s), wind direction (deg), solar radiation (MJ/m^2), sunshine (s), atmospheric pressure (hPa), and precipitation (mm) were measured by the sole and official station located in the center of Seoul and used for analysis.

Selection of variables

The outdoor PM_{10} concentration was matched to indoor PM_{10} concentration and meteorological data every 10 min. Spearman correlation analysis was used to find the relationship between indoor PM_{10} concentration and the input predictors including outdoor PM_{10} concentration and meteorological variables (temperature, humidity, precipitation, wind speed, wind direction, atmospheric pressure, solar radiation, and sunshine). An alpha value (α) value of 0.05 was defined to indicate statistical significance. Input variables for outdoor predictors were selected for the next step of the regression if *p*-values of the variable were less than 0.05. The temporal and weekday variables were included as the input variables. The temporal variables were hour of the day, day of the week, and month of the year. The weekday variable was coded as one for Saturday, Sunday, and public holidays, and otherwise coded as zero. In addition, the interaction effect between the day of the weekday and hours in a day (day-time predictor) was included as an input variable. The interaction effect was included because the indoor PM_{10} concentration in the educational facilities might have been affected by the class schedule with different days and hours in a day.

Four types of indoor PM_{10} concentration were tested as dependent variable in multiple linear regression (MLR) analysis; (1) original (untransformed indoor PM_{10} concentration), (2) I/O ratio (indoor-to-outdoor PM_{10} concentration), (3) root-transformed (square-root transformed indoor PM_{10} concentration), and (4) log-transformed (exponential-log transformed indoor PM_{10} concentration). For comparison of the better dependent variable, root mean squared errors (RMSE) of the prediction models with original, I/O ratio, root-transformed, and log-transformed indoor PM_{10} concentration were compared for three types of educational facilities. The dependent variable with the lowest RMSE was selected in the prediction model. The RMSE were calculated as below:

$$RMSE = \sqrt{\frac{1}{n}\sum_{k=1}^{n}(y_k - \hat{y}_k)^2}$$

where, y_k and $\hat{y}_k$ are the observed and predicted value of indoor PM_{10} concentration, respectively; n is the number of samples in the test data set.

Development of prediction model

The final MLR models were developed to predict the ten-minute indoor PM_{10} concentrations in the daycare centers, kindergartens, and elementary schools using selected input variables, as shown below:

$$Y_i = \beta_0 + \beta X_i + \gamma Z_i + \varepsilon_i$$

where i represents the ten-minute average of the measured value; Y_i denotes indoor PM_{10} concentration; β_0 is the intercept of Y; β is designated as the effect of X on Y; X_i represents outdoor PM_{10} concentration; γ is designated as the effect of Z on Y; Z_i represents the temporal and seasonal variable; and ε_i is the error term.

The prediction accuracy of the MLR model was assessed by a 10-fold cross-validation (CV) method (Bergmeir et al., 2018). The training group with 90% of the data were used to train the model, and 10% of the data were utilized for the testing and verification of the prediction accuracy. The determination coefficient (R^2) and the RMSE between the predicted and measured indoor PM_{10} concentrations were calculated to evaluate the performance of the model. The R^2 values assessed the correlation between measured and predicted value that could be explained by the model. The RMSE determined discrepancies between measured and predicted values. All statistical analyses in our study were conducted with R software (Version 3.5.2, R Core Team, Vienna, Austria).

3.3. Results

Descriptive statistic of indoor and outdoor variables

The statistics for all variables are described in Table 3-1. The annual mean indoor PM_{10} concentrations were 57.8 ± 26.2 μg/m^3 at 54 daycare centers, 26.1 ± 6.5 μg/m^3 at 12 kindergartens, and 32.3 ± 10.2 μg/m^3 at 21 elementary schools. The annual indoor PM_{10} concentrations ranged between 20.9–147.5 μg/m^3 in the daycare centers, 18.7–39.7 μg/m^3 in the kindergartens, and 21.0–60.9 μg/m^3 in the elementary schools. The indoor PM_{10} concentration in the daycare centers was significantly higher than that in the other facilities ($p < 0.001$). The daily mean PM_{10} concentrations over the 365 monitoring days exceeded the Korean PM_{10} IAQ standard of 75 μg/m^3 with a 24-h mean of 25.1% in the 54 daycare centers, 2.5% in the 12 kindergartens, and 4.8% in the 21 elementary schools. The daily mean PM_{10} concentrations over the 365 monitoring days exceeded by 47.6% in the 54 daycare centers, 9.1% in the 12 kindergartens, and 13.9% in the 21 elementary schools from the World Health Organization (WHO) PM_{10} IAQ guideline of 50 μg/m^3 with a 24-h mean. The annual outdoor PM_{10} concentration was 46.2 ± 23.7 μg/m^3 and ranged from 4.8–43.4 μg/m^3. The annual mean outdoor temperature, outdoor relative humidity, and precipitation were 13.7 ± 10.9 °C, 57.6 ± 13.7%, and 1.1 ± 5.3 mm, respectively.

Table 3-1. Descriptive statistics of the average indoor and outdoor variables during one year.

	Mean±SD[a]	Min	Max	Median
Indoor PM_{10} concentration (μg/m^3)				
Daycare center (n=54)	57.8±26.2	20.9	147.5	57.3
Kindergarten (n=12)	26.1±6.5	18.7	39.7	25.1
Elementary school (n=21)	32.3±10.2	21.0	60.9	30.3
Outdoor variables				
PM_{10} concentration (μg/m^3)	46.2±23.7	4.8	208.4	43.4
Temperature (°C)	13.7±10.9	-8.7	31.5	15.1
Relative humidity (%)	57.8±13.7	18.9	93.6	59.2
Precipitation (mm)	1.1±5.3	0.0	70.4	0.0
Wind direction (deg)	191.7±68.5	39.6	296.2	203.4
Wind speed (m/s)	2.3±0.7	0.8	4.3	2.2
Atmospheric pressure (hPa)	1006.0±7.9	980.4	1023.5	1005.9
Solar radiation (MJ/m^2)	6.2±3.4	0.0	19.5	6.0
Sunshine (min)	202.4±118.6	0.0	456.0	233.7

[a]: SD : Standard Deviation

Selection of variables

The correlation between the indoor PM_{10} concentration and other variables is shown in Table 3-2 using Spearman correlation coefficients (ρ). Of the 9 candidate outdoor predictor variables (outdoor PM_{10} concentration, temperature, humidity, precipitation, wind speed, wind direction, atmospheric pressure, solar radiation, and sunshine), all predictors were found to be significantly correlated to the indoor PM_{10} concentration ($p < 0.001$). The largest correlation coefficient was 0.51 between the indoor and outdoor PM_{10} concentrations. The indoor PM_{10} concentration showed a positive correlation coefficient with the atmospheric pressure ($\rho = 0.10$), wind speed ($\rho = 0.08$), solar radiation ($\rho = 0.07$), sunshine ($\rho = 0.07$), and wind direction ($\rho = 0.04$). However, a negative correlation coefficient was observed with the outdoor temperature ($\rho = -0.16$), relative humidity ($\rho = -0.14$), and precipitation ($\rho = -0.08$).

Table 3-2. Spearman correlation coefficients among indoor PM_{10} concentration, outdoor PM_{10} concentration, and meteorological variables.

	Variables	1	2	3	4	5	6	7	8	9	10
1	Indoor PM_{10}	1.00									
2	Outdoor PM_{10}	0.51	1.00								
3	Temperature	-0.16	-0.10	1.00							
4	Precipitation	-0.08	-0.17	0.05	1.00						
5	Relative humidity	-0.14	-0.01	0.05	0.33	1.00					
6	Wind direction	0.04	-0.02	-0.09	0.00	-0.22	1.00				
7	Wind speed	0.08	-0.08	0.05	0.13	-0.30	0.28	1.00			
8	Atmospheric pressure	0.10	0.13	-0.74	-0.21	-0.22	-0.01	-0.15	1.00		
9	Solar radiation	0.07	0.02	0.33	0.01	-0.46	0.25	0.36	-0.17	1.00	
10	Sunshine	0.07	0.03	0.20	-0.11	-0.53	0.27	0.32	-0.03	0.94	1.00

*All spearman correlation coefficients had p-values less than 0.01.

The outdoor PM_{10} concentration, all meteorological data, temporal, weekday, and day-time predictor were applied as input variables for the development of the prediction models of indoor PM_{10} concentration. For selection of the better dependent variable, RMSEs of the prediction models with original indoor PM_{10}, I/O ratio, root-transformed indoor PM_{10}, and log-transformed indoor PM_{10} were compared in each educational facility, as shown in Table 3-3. The lowest RMSE for the development of the best model was observed in root-transformed indoor PM_{10} concentration in all educational facilities. The RMSEs with root-transformed indoor PM_{10} concentration were 26.7 μg/m^3 in the daycare centers, 18.9 μg/m^3 in the kindergartens, and 19.9 μg/m^3 in the elementary schools.

To confirm day-time predictor as input variables, the models with and without the interaction effect were compared. The RMSEs without day-time predictor were 27.1 μg/m^3 in the daycare centers, 19.3 μg/m^3 in the kindergartens, and 20.1 μg/m^3 in the elementary schools in root-transformation. The RMSEs with day-time predictor were smaller than without day-time predictor.

Table 3-3. The comparison of the RMSE ($\mu g/m^3$) among the four types of transformed models with day-time predictor.

Facility	RMSE ($\mu g/m^3$)			
	Original	I/O ratio	Root-transformation	Log-transformation
Daycare center	27.27	29.09	26.66	27.99
Kindergarten	18.92	20.86	18.90	19.90
Elementary school	19.95	21.62	19.93	20.93

Development and validation of the prediction models

For real-time indoor PM_{10} prediction over one year, the prediction models in the three types of educational facilities were developed every 10 min. The outdoor PM_{10} concentration was the most important input variable of the indoor PM_{10} concentration in the final MLR models. The regression coefficients (β) of outdoor PM_{10} concentration were 0.517 in the daycare centers, 0.407 in the kindergartens, and 0.412 in the elementary schools (Table S-10). The R^2 values of the prediction models between the measured and predicted indoor PM_{10} concentration were 0.640 in the daycare centers, 0.453 in the kindergartens, and 0.426 in the elementary schools. The prediction model explained 64.0% in the daycare centers, 45.3% in the kindergartens, and 42.6% in the elementary schools of the variation in the measured PM_{10} concentration. The highest association between the measured and the predicted PM_{10} concentration was observed in the daycare centers. The slopes of prediction models were 0.611 in the daycare centers, 0.361 in the kindergartens, and 0.338 in the elementary schools, as shown in Figure S-2. The final models of the predicted indoor PM_{10} concentrations were validated in the daycare centers (CV $R^2 = 0.6391$), kindergartens (CV $R^2 = 0.4525$), and elementary schools (CV $R^2 = 0.4259$) using a 10-fold CV.

Application of the prediction model every 10 min in 24 hours

The indoor PM_{10} concentrations were predicted every 10 min in 24 h in the three types of educational facilities using the 365 days data. The 24 h profiles of the predicted indoor PM_{10} in these educational facilities were similar to those of the measured PM_{10} concentration, as shown in Figure 3-1. The means of the predicted PM_{10} concentrations were 54.1 μg/m^3 in the daycare centers, 26.9 μg/m^3 in the kindergartens, and 27.0 μg/m^3 in the elementary schools. The predicted PM_{10} concentrations were slightly lower than the measured PM_{10} concentrations. The differences between the predicted and measured values were 2.2 μg/m^3 in the daycare centers, 1.5 μg/m^3 in the kindergartens, and 1.5 μg/m^3 in the elementary schools.

The daily profiles of the indoor PM_{10} concentration differed for the educational facilities. The indoor PM_{10} concentrations increased from 8:00 a.m. at these educational facilities. The peak PM_{10} concentrations were observed around 11:00 a.m.–12:00 p.m. in the daycare centers and 1:00–2:00 p.m. in the kindergartens and elementary schools. The indoor PM_{10} concentrations decreased in late afternoon. The indoor PM_{10} concentration in elementary schools decreased earlier than in the daycare centers and kindergartens. The indoor PM_{10} concentrations in the operating hours were 1.5 times higher than the non-operating hours in these educational facilities.

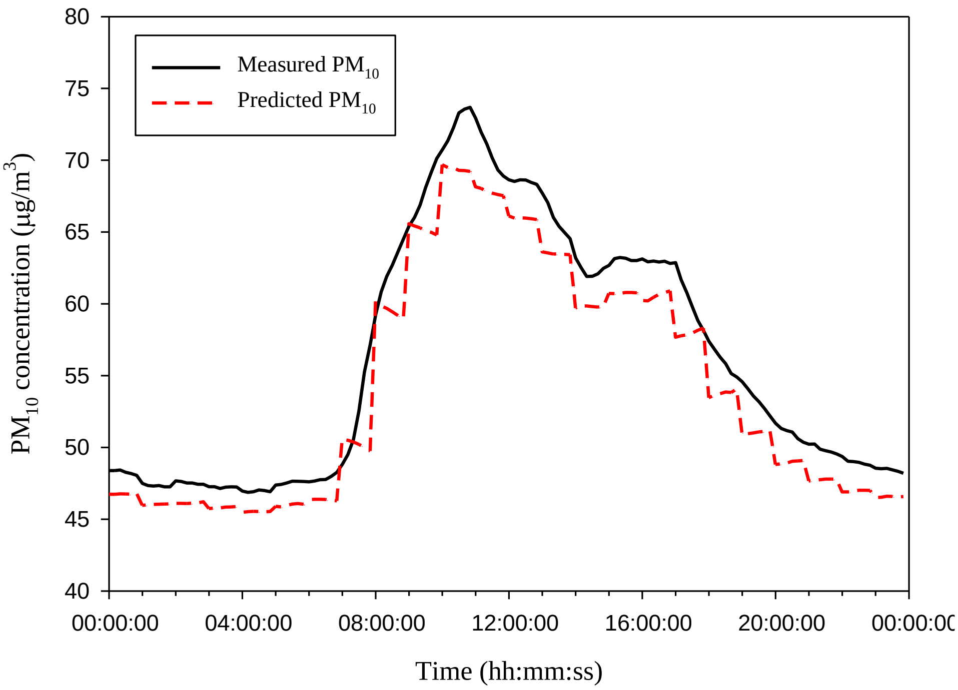

Measured PM10
Predicted PM10
80
75
70
65
60
55
50
45
40
PM10 concentration (µg/m3)
00:00:00
04:00:00
08:00:00
12:00:00
16:00:00
20:00:00
00:00:00
Time (hh:mm:ss)

(a)

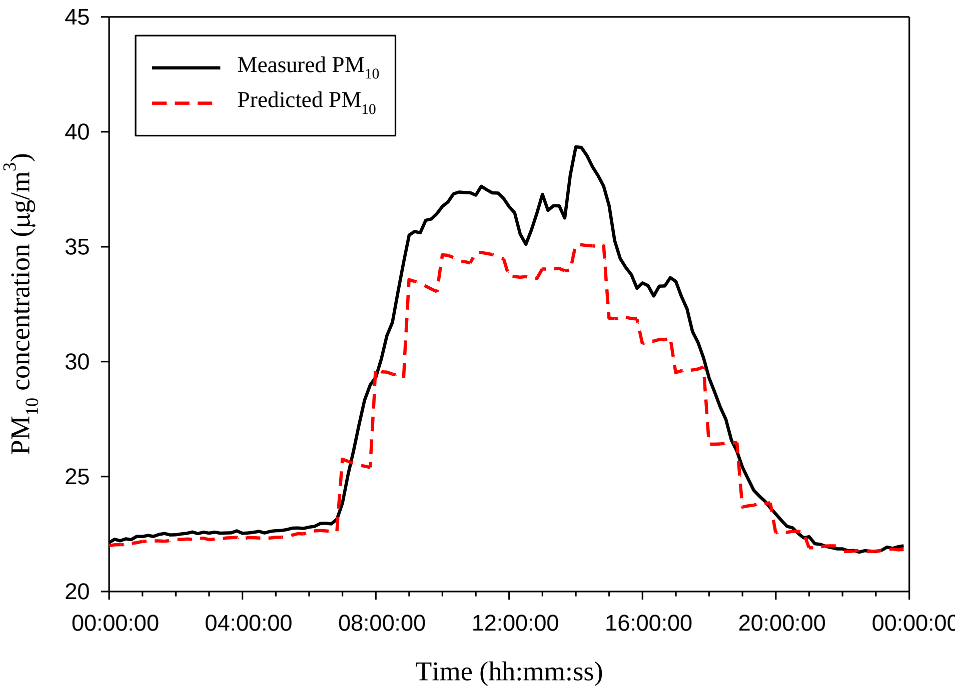

Measured PM10
Predicted PM10
45
40
35
30
25
20
PM10 concentration (µg/m3)
00:00:00
04:00:00
08:00:00
12:00:00
16:00:00
20:00:00
00:00:00
Time (hh:mm:ss)

(b)

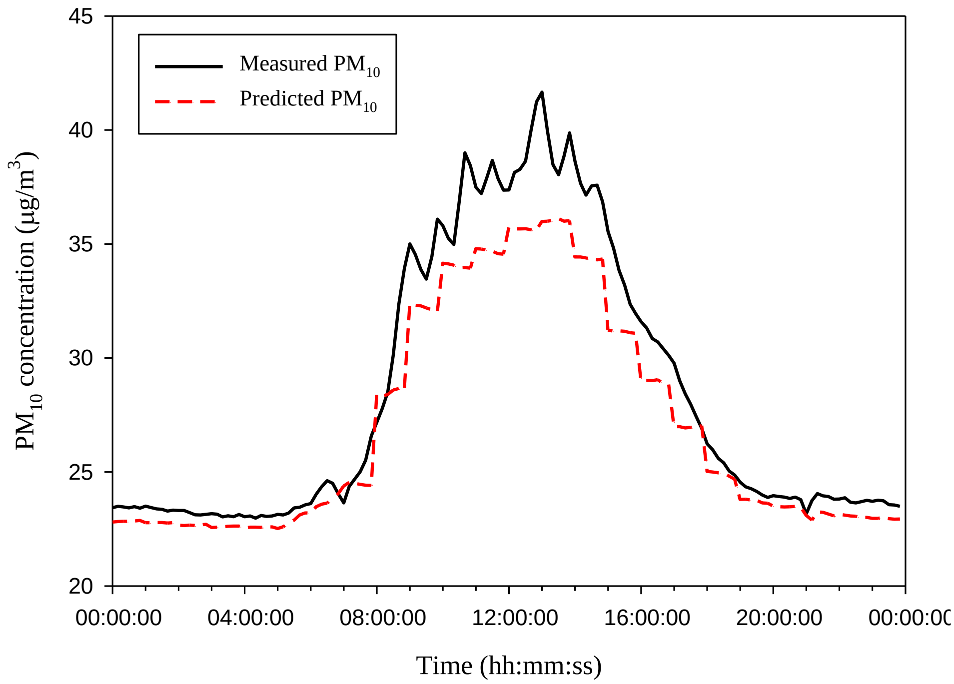

(c)

Figure 3-1. Comparison between the measured and predicted indoor PM_{10} concentration every 10 min during 24 h. (a) Daycare centers (b) Kindergartens (c) Elementary schools.

The predicted indoor PM_{10} concentrations were used to determine whether the measured level was exceeding the high concentration of 75 μg/m^3. The measured ten-minute PM_{10} levels over a year exceeded 75 μg/m^3 in 26.6% at the daycare centers, 4.9% at the kindergarten, and 5.6% at the elementary schools. The predicted PM_{10} levels exceeded 75 μg/m^3 in 22.8% at the daycare centers, 0.3% at the kindergarten, and 0.4% at the elementary schools (Table 3-4). The highest rate of exceeding the KAAQS of PM_{10} was observed in daycare center.

Table 3-4. The rate of exceeding the KAAQS of PM_{10} (75 μg/m^3).

Facility	The rate of exceeding the KAAQS of PM_{10} (%)	
	Measured PM_{10}	Predicted PM_{10}
Daycare center	26.6	22.8
Kindergarten	4.9	0.3
Elementary school	5.6	0.4

For above 75 μg/m^3, the prediction accuracy of the models was 69.2% in the daycare centers, 5.8% in the kindergartens, and 6.1% in the elementary schools, as shown in Table 3-5. The prediction accuracy of the models in the kindergartens and elementary schools were ten times lower than the daycare centers. When the predicted value of 50 μg/m^3 was applied as the classification criteria to the measured value above 75 μg/m^3, the predicted PM_{10} level was estimated to exceed 95.0% in the daycare centers, 61.8% in the kindergartens, and 53.9% in the elementary schools. As applied to the predicted value of 50 μg/m^3, the performance of the prediction models improved 1.4 times for the daycare centers, 10 times for the kindergartens, and 8.8 times for the elementary schools.

Table 3-5. Agreement of measured PM_{10} (standard of > 75 μg/m^3) and different levels of predicted 10 min PM_{10}.

	Facility	Predicted PM_{10}	
		> 75 μg/m^3	> 50 μg/m^3
Measured PM_{10} (> 75 μg/m^3)	Daycare center	69.2%	95.0%
	Kindergarten	5.8%	61.8%
	Elementary school	6.1%	53.9%

3.4. Discussion

The indoor PM_{10} concentrations in the daycare centers were similar to the previous studies in Seoul; these ranged from 15.5–106.8 μg/m^3 (Hwang et al., 2017). The indoor PM_{10} concentration could differ according to outdoor air pollution; these were 77.0 ± 29.9 μg/m^3 in the 43 daycare centers in the commercial city (Kabir et al., 2012) and 66.7 ± 4.8 μg/m^3 in the 6 daycare centers in areas adjacent to roads with heavy traffic (Oh et al., 2014). Children stayed longer in daycare centers with high indoor PM_{10} concentration than in other educational facilities. Such high PM_{10} exposure to younger children could cause more serious health effects because of their vulnerability and physiological functions.

Outdoor PM_{10} concentration was the largest contributor to indoor PM_{10} concentration (ρ = 0.51). The outdoor particles might infiltrate indoors and contribute to the increasing indoor particle concentration (Jung et al., 2018). The correlation coefficient between indoor and outdoor PM_{10} concentration in this study was similar to 0.41 in South Africa (Nkosi et al., 2017) and 0.44 in Turkey (Argunhan and Avci, 2018). In addition to outdoor PM_{10}, precipitation, outdoor temperature, and wind speed were important contributors to the indoor PM_{10} concentration. Precipitation, outdoor temperature, and wind speed were negatively correlated with outdoor PM_{10} concentration. These were indirectly affected by increasing indoor PM_{10} concentration. The relationship was also found in another study. Wind speed, air temperature, and rainfall were negatively correlated to outdoor PM_{10} concentration with correlation coefficients (r) between -0.21 and -0.30 (Gualtieri et al., 2018).

Prediction models using real-time outdoor environmental data can be useful to manage IAQ. Some studies directly measured IAQ in educational facilities (Hwang et al., 2018). However, direct real-time measurement and observation of occupants and indoor condition for a long period of time have the limitations of resources. Much of the outdoor data are already being continuously generated by local monitoring stations and can be easy to access for indoor predictions. The models with outdoor data were time-saving and cost-effective. In other study, prediction models for indoor PM levels in educational facilities was developed using outdoor PM concentration, meteorological parameters (humidity and temperature), and classroom characteristic (size, occupancy level, and ventilation rate) as input variables; the R^2 in weekdays and weekend was 0.0270 and 0.4728, respectively (Goyal and Khare, 2011).

The prediction models in this study included additional predictors of the interaction effect between the day of the weekday and hours in a day. The prediction models with day-time predictor showed the best performance with the lowest RMSE compared to models without day-time predictor. The day-time predictor can be explained, because the indoor PM_{10} concentration in educational facilities might be different by the class schedule for the day of the weekday and hours in a day. Hence, our prediction models with day-time predictor can predict real-time indoor PM_{10} concentration in the educational facilities with regards to the class schedule. In another study, the effect of interaction between the time and day has also been considered in prediction model for the best performance (de Hoogh et al., 2018).

In this study, four formations (original, I/O ratio, root-transformation, and log-transformation) for the dependent variable were compared to find the best performance of the model. The selection of the appropriate formation for the dependent variable was important to reflect the characteristics of the data for the best fitting model. The best formation of the prediction model in this study was root-transformation with the lowest RMSE. Square-root transformation can stabilize the variance in data (Bartlett et al., 1947). Other study developed prediction models with log-transformation for the normalization of data (Yuchi et al., 2019). Natural log-transformed for the MLR model was developed to predict indoor levels (Xu et al., 2020). An indoor-to-outdoor ratio model was developed to predict the indoor PM_{10} level for considering the relationship between the indoor and outdoor PM_{10} concentration (Lee et al., 2016). They also selected appropriate formation considering the characteristics of their data. In future, the prediction model with the most suitable transformation should be considered for the best fitting of own data.

The prediction models at educational facilities could predict the indoor PM_{10} concentration with a relatively high prediction accuracy and high time resolution of every 10 min. In other studies, models to predict PM concentration were developed using longer time intervals with the R^2 of 0.66 for daily concentration (Lee et al., 2016), 0.74 for monthly concentration (Huang et al., 2018), and 0.67 for annual concentration (Elbayoumi et al., 2014). Although they had a slightly higher R^2 than our results, the models with longer time interval were difficult to attain real-time intervention and control of indoor PM exposure. Real-time elevation of exposure to PM was important to find the association with effects on health (Krauskopf et al., 2018). The model with 10 min intervals can be useful to find real-time indoor PM_{10} levels and control of the poor IAQ for the sake of the health of the occupants.

RMSE in our models were relatively high, because the prediction models were developed using real-time big data with 10 min intervals for one year monitoring period. The models predicted 10 minutes indoor PM_{10} for one year. The RMSE determined discrepancies between measured and predicted values of 10 minutes. Therefore, the RMSE were based on over 41 million indoor data points. If long time interval (ex. 1 day, 1 month, or 1 year) is applied in the prediction model, performance of model could be better than the model with 10 min interval. Nevertheless, it is important to focus on the good real-time correlation between measured and predicted value with a relatively high the R^2 rather than predicting exact indoor PM_{10} concentrations. Actually, the 24 h profile of the predicted PM_{10} level was similar to the measured PM_{10} concentration, as shown in Figure 3-1. Although the prediction model could not predict the exact indoor PM_{10} concentration, our models could be useful to immediate intervention of the poor real-time PM_{10} levels for prevention of health effects of occupants.

In our model, the daily profiles of indoor PM_{10} concentration every 10 min differed for each facility. At the beginning of the operating schedule, the indoor PM_{10} concentrations in the daycare centers and kindergartens increased sooner than in the elementary schools. The daycare centers and kindergartens in Korea were typically started between 7:30 and 8:00 a.m. (Table S-11). However, the elementary schools were started between 8:30 and 9:00 a.m. High peak PM_{10} concentrations in educational facilities were observed around lunch time indoors. The indoor PM_{10}

concentration in elementary schools decreased earlier than in other educational facilities due to the early closing time approximately at 3:00 p.m.

High PM_{10} concentrations above the standard of 75 μg/m^3 were underestimated by the model in this study. Such underestimation for high concentration has often been shown in other prediction models (Park et al., 2018). Despite the underestimation, the model could determine when the indoor PM_{10} concentration exceeded a certain level. In Korea, the indoor PM_{10} concentration of 75 μg/m^3 is a standard for IAQ management. In this model, the prediction level of 50 μg/m^3 could be applied as a criterion for controlling IAQ, as the prediction level can compensate for the underestimation of model.

The monitor in this study was used to measure only PM_{10} concentrations. However, $PM_{2.5}$ has been associated with important adverse health effects such as increased respiratory and cardiovascular morbidity and mortality. In addition, the relationship between indoor and outdoor $PM_{2.5}$ concentration was higher than PM_{10} concentration (Guak and Lee., 2018). $PM_{2.5}$ is mainly caused by combustion while there are few combustion activities in the educational facilities. When children move or run in the educational facilities, suspended particle such as PM_{10} can mainly generate. In this study, we developed feasible models to predict real-time PM_{10} concentrations in educational facilities. If real-time $PM_{2.5}$ data for long measurement times could be measured, the new prediction model for $PM_{2.5}$ could be developed and applied in intervention of poor indoor air quality in the future.

3.5. Conclusions

Prediction models in the daycare centers, kindergartens, and elementary schools were developed to predict real-time PM_{10} concentration with high accuracy for a long period of one year every 10 min. The outdoor PM_{10} concentration was the most important input variable in prediction models. The best performance was shown in root-transformed model with day-time predictor. Indoor PM_{10} level was the highest in the daycare centers. Our approach could be useful methodologies for highly time-resolved to predict PM_{10} concentrations in different educational facilities using outdoor environmental parameters.

References

Argunhan, Z., Avci, A.S., 2018. Statistical evaluation of indoor air quality parameters in classrooms of a university. Advances in Meteorology 2018.

Bergmeir, C., Hyndman, R.J., Koo, B., 2018. A note on the validity of cross-validation for evaluating autoregressive time series prediction. Computational Statistics & Data Analysis 120, 70-83.de Hoogh, K., Héritier, H., Stafoggia, M., Künzli, N., Kloog, I., 2018. Modelling daily $PM_{2.5}$ concentrations at high spatio-temporal resolution across Switzerland. Environmental Pollution 233, 1147-1154.

Du, Y., Wang, Y., Du, Z., Zhang, Y., Xu, D., Li, T., 2018. Modeling of residential indoor $PM_{2.5}$ exposure in 37 counties in China. Environmental Pollution 238, 691-697.

Elbayoumi, M., Ramli, N.A., Md Yusof, N.F.F., Yahaya, A.S.B., Al Madhoun, W., Ul-Saufie, A.Z., 2014. Multivariate methods for indoor PM_{10} and $PM_{2.5}$ modelling in naturally ventilated schools buildings. Atmospheric Environment 94, 11-21.

Goyal, R., Khare, M., 2011. Indoor air quality modeling for PM_{10}, $PM_{2.5}$, and $PM_{1.0}$ in naturally ventilated classrooms of an urban Indian school building. Environmental Monitoring and Assessment 176, 501-516.

Gualtieri, G., Carotenuto, F., Finardi, S., Tartaglia, M., Toscano, P., Gioli, B., 2018. Forecasting PM_{10} hourly concentrations in northern Italy: Insights on models performance and PM_{10} drivers through self-organizing maps. Atmospheric

Pollution Research 9, 1204-1213.

Haverinen-Shaughnessy, U., Shaughnessy, R.J., 2015. Effects of classroom ventilation rate and temperature on students' test scores. Plos One 10, e0136165.

Hrust, L., Klaić, Z.B., Križan, J., Antonić, O., Hercog, P., 2009. Neural network forecasting of air pollutants hourly concentrations using optimised temporal averages of meteorological variables and pollutant concentrations. Atmospheric Environment 43, 5588-5596.

Huang, K., Xiao, Q., Meng, X., Geng, G., Wang, Y., Lyapustin, A., Gu, D., Liu, Y., 2018. Predicting monthly high-resolution $PM_{2.5}$ concentrations with random forest model in the North China Plain. Environmental Pollution 242, 675-683.

Hwang, S.H., Roh, J., Park, W.M., 2018. Evaluation of PM_{10}, CO_2, airborne bacteria, TVOCs, and formaldehyde in facilities for susceptible populations in South Korea. Environmental Pollution 242, 700-708.

Hwang, S.H., Seo, S., Yoo, Y., Kim, K.Y., Choung, J.T., Park, W.M., 2017. Indoor air quality of daycare centers in Seoul, Korea. Building and Environment 124, 186-193.

Jung, C.-C., Wu, P.-C., Tseng, C.-H., Chou, C.C., Su, H.-J., 2018. Contribution of indoor-and outdoor-generated fine and coarse particles to indoor air in Taiwanese hospitals. Aerosol and Air Quality Research 18, 3234-3242.

Kabir, E., Kim, K.-H., Sohn, J.R., Kweon, B.Y., Shin, J.H., 2012. Indoor air quality assessment in child care and medical facilities in Korea. Environmental Monitoring and Assessment 184, 6395-6409.

Kim, Y., Lee, S., Ban, H., Cha, S., Kim, G., Lee, K., 2017. Temporal Variation of

Indoor Air Quality in Daycare Centers. Journal of Environmental Health Sciences 43, 267-272.

Klepeis, N.E., Nelson, W.C., Ott, W.R., Robinson, J.P., Tsang, A.M., Switzer, P., Behar, J.V., Hern, S.C., Engelmann, W.H., 2001. The National Human Activity Pattern Survey (NHAPS): a resource for assessing exposure to environmental pollutants. Journal of Exposure Science and Environmental Epidemiology 11, 231-252.

Krauskopf, J., Caiment, F., van Veldhoven, K., Chadeau-Hyam, M., Sinharay, R., Chung, K.F., Cullinan, P., Collins, P., Barratt, B., Kelly, F.J., 2018. The human circulating miRNome reflects multiple organ disease risks in association with short-term exposure to traffic-related air pollution. Environment International 113, 26-34.

Lee, J.-Y., Jo, W.-K., Chun, H.-H., 2015. Long-term trends in visibility and its relationship with mortality, air-quality index, and meteorological factors in selected areas of Korea. Aerosol and Air Quality Research 15, 673-681.

Lee, J.Y., Ryu, S.H., Kim, C.H., Bae, G.-N., 2016a. Indoor-to-outdoor pollutant concentration ratio modeling of CO_2, NO_2, and lung-deposited nanoparticles. Atmospheric Pollution Research 7, 664-670.

Lee, J.Y., Ryu, S.H., Lee, G., Bae, G.-N., 2016b. Indoor-to-outdoor particle concentration ratio model for human exposure analysis. Atmospheric Environment 127, 100-106.

Mažeikis, A., 2013. Urbanization influence on meteorological parameters of air pollution: Vilnius case study. Baltica. 26, 51-56.

Mi, K., Zhuang, R., Zhang, Z., Gao, J., Pei, Q., 2019. Spatiotemporal characteristics of $PM_{2.5}$ and its associated gas pollutants, a case in China. Sustainable Cities and Society 45, 287-295.

Nkosi, V., Wichmann, J., Voyi, K., 2017. Indoor and outdoor PM_{10} levels at schools located near mine dumps in Gauteng and North West Provinces, South Africa. BMC Public Health. 17, 42.

Oh, H.-J., Nam, I.-S., Yun, H., Kim, J., Yang, J., Sohn, J.-R., 2014. Characterization of indoor air quality and efficiency of air purifier in childcare centers, Korea. Building and Environment 82, 203-214.

Quirós-Alcalá, L., Wilson, S., Witherspoon, N., Murray, R., Perodin, J., Trousdale, K., Raspanti, G., Sapkota, A., 2016. Volatile organic compounds and particulate matter in child care facilities in the district of Columbia: Results from a pilot study. Environmental Research 146, 116-124.

Santamouris, M., Synnefa, A., Asssimakopoulos, M., Livada, I., Pavlou, K., Papaglastra, M., Gaitani, N., Kolokotsa, D., Assimakopoulos, V., 2008. Experimental investigation of the air flow and indoor carbon dioxide concentration in classrooms with intermittent natural ventilation. Energy and Buildings 40, 1833-1843.

Shendell, D.G., Prill, R., Fisk, W.J., Apte, M.G., Blake, D., Faulkner, D., 2004. Associations between classroom CO_2 concentrations and student attendance in Washington and Idaho. Indoor Air 14, 333-341.

Sousa, S.I., Ferraz, C., Alvim-Ferraz, M.C., Vaz, L.G., Marques, A.J., Martins, F.G., 2012. Indoor air pollution on nurseries and primary schools: impact on childhood asthma–study protocol. BMC Public Health. 12, 435.

Stabile, L., Jayaratne, E., Buonanno, G., Morawska, L., 2014. Charged particles and cluster ions produced during cooking activities. Science of The Total Environment 497, 516-526.

Sørensen, M., Daneshvar, B., Hansen, M., Dragsted, L.O., Hertel, O., Knudsen, L., Loft, S., 2003. Personal $PM_{2.5}$ exposure and markers of oxidative stress in blood. Environmental Health Perspectives 111, 161-166.

Tai, A.P., Mickley, L.J., Jacob, D.J., 2010. Correlations between fine particulate matter ($PM_{2.5}$) and meteorological variables in the United States: Implications for the sensitivity of $PM_{2.5}$ to climate change. Atmospheric Environment 44, 3976-3984.

Tong, X., Ho, J.M.W., Li, Z., Lui, K.-H., Kwok, T.C.Y., Tsoi, K.K.F., Ho, K.F., 2019. Prediction model for air particulate matter levels in the households of elderly individuals in Hong Kong. Science of The Total Environment 717, 135323.

Yang, W., Lee, K., Yoon, C., Yu, S., Park, K., Choi, W., 2011. Determinants of indoor activity pattern in Korean population. Journal of Exposure Science and Environmental Epidemiology 21, 310-316.

Yu, K.-P., Lee, Y.-C., Chen, Y.-C., Gong, J.-Y., Tsai, M.-H., 2019. Evaluation of PM_1, $PM_{2.5}$, and PM_{10} exposure and the resultant health risk of preschool children and their caregivers. Journal of Environmental Science and Health, Part A 54, 961-971.

Yuchi, W., Gombojav, E., Boldbaatar, B., Galsuren, J., Enkhmaa, S., Beejin, B., Naidan, G., Ochir, C., Legtseg, B., Byambaa, T., Barn, P., Henderson, S.B., Janes, C.R., Lanphear, B.P., McCandless, L.C., Takaro, T.K., Venners, S.A., Webster, G.M., Allen, R.W., 2019. Evaluation of random forest regression and multiple linear regression for predicting indoor fine particulate matter concentrations in a highly polluted city. Environmental Pollution 245, 746-753.

Chapter IV.

Seasonal spatial variation of five air pollutants ($PM_{2.5}$, PM_{10}, NO_2, CO, and O_3) at city-scale and small-scale areas in Seoul

4.1. Introduction

Ambient air quality in Korea can be evaluated by criteria air pollutants including particulate matter (PM) with an aerodynamic diameter of ≤ 2.5 μm and ≤ 10 μm ($PM_{2.5}$ and PM_{10}, respectively), nitrogen dioxide (NO_2), carbon monoxide (CO), sulfur dioxide (SO_2), ozone (O_3), lead, and benzene. Exposure to air pollutants has been linked to be increased adverse health effects (Cohen et al., 2017; Costa et al., 2017; Mills et al., 2015; Sørhaug et al., 2006). Korean government have disclosed the hourly concentrations of criteria air pollutants on a website (AirKorea; http://www.airkorea.or.kr/web) and established Korean ambient air quality standard (KAAQS) for these pollutants. Except lead and benzene, other air pollutants have standards for 1-, 8-, or 24-h mean concentrations. KAAQSs of air pollutants ($PM_{2.5}$, PM_{10}, NO_2, CO, and O_3) were summarized in Table S-12.

Ambient air quality is monitored by local air quality monitoring station (AQMS). Epidemiological studies have often used ambient air pollutant concentrations at AQMSs as a surrogate for personal exposure to air pollutants because of the limited resources for direct measurements (Atkinson et al., 2013; Chen et al., 2018). However, application of AQMS data as a proxy of personal exposure can cause classification errors due to diverse spatial-temporal variations of air pollutants. In previous studies, the interpolation method, dispersion model, and land use regression model have been commonly used to estimate exposure of air pollutants by considering spatial resolution at un-monitored areas where AQMS did not measure (Arunachalam et al., 2014; Hoek et al., 2008). Identification of spatial-temporal variation for air pollutants can be useful to mitigate the errors in estimations of air pollution in un-monitored areas.

Identification of spatial-temporal variation for air pollutants in smaller areas has been limited. Many studies in China reported spatial-temporal variations in areas > 100,000 km^2 at a regional-scale (Hu et al., 2014; Yang and Christakos, 2015; Zhao et al., 2013). At a city-scale, spatial-temporal distributions have been reported in Beijing, China (Chen et al., 2015; Ji et al., 2019; Xu et al., 2019), in Guangzhou, China (Li et al., 2014), in Vancouver, Canada (Marshall et al., 2008), in Ankara, Turkey (Raja et al., 2018), in Toronto, Canada (Su et al., 2010), and in Kaunas, Lithuania (Dėdelė and Miškinytė, 2019). Spatial-temporal variations differed in these studies because air pollutant concentrations can be easily affected depending on climatic conditions, traffic intensity, population density, and the distance to the sources (Merbitz et al., 2012). In smaller areas, it is possible to identify high spatial-temporal variation including the effects of these factors more accurately.

Air quality in Seoul with area of 605.4 km^2 is monitored by 25 AQMSs. Seoul consists of 25 administrative districts referred to “gu”; each gu has one urban AQMS. However, data from a single AQMS in each gu may not be sufficient to estimate personal exposure in the area. The area of each gu ranges from 10–47 km^2. The population of Seoul was 9657969 in January 2021 based on Korean statistical information service (KOSIS) (https://kosis.kr/index/index.do). Each gu had a population in the range from 125038–667222 in January 2021 based on KOSIS. The population per area of each gu in Seoul ranged from 6237–26056 people per km^2. Determining spatial-temporal variations in un-monitored areas of each gu is useful to estimate air pollutant exposure. In this study, additional measurements at eight in-situ monitoring sites (IMSs) surrounding one AQMS were performed using a stationary monitoring vehicle with standard monitoring methods. Mobile monitoring methodologies using vehicles equipped with monitoring machines were applied to obtain air quality data with high spatial resolution (Tessum et al., 2018).

The aim of this study was to identify seasonal spatial variation of air pollutants ($PM_{2.5}$, PM_{10}, NO_2, CO, and O_3) at the city-scale using 25 AQMSs data and small-scale areas (1 km^2) at one of the 25 administrative districts in Seoul, Korea. Using the standard monitoring methods, air quality data at 25 AQMSs and eight IMSs surrounding the AQMS were collected to include all four seasons over one year.

4.2. Methods

Study area

Seoul has 25 AQMSs in each gu. Guro-gu with area of 20.12 km^2 is one of the 25 gu in Seoul and had a population of 403518 in January 2021 based on KOSIS. Test-bed area was assigned to approximately 5 km x 5 km from an AQMS in Guro-gu. The total of eight IMSs with each an area of 1 km^2 were selected to measure the air quality surrounding an AQMS in Guro-gu. The locations of monitoring sites in Seoul are shown in Figure 4-1. The geographical coordinates of monitoring sites in Seoul are shown in Table S-13. The characteristics of the eight IMSs differed. Location 1 was in the vicinity of the highway, and thus had high traffic intensity. Location 2 was located in the vicinity of a liquefied petroleum gas charge station. Location 3 was located near a train station (Guro station). Location 4 was a residential area nearby a barbeque restaurant and parking lot. Location 5 was located in a park (Guro Geori park). Location 6 was in a residential area in the vicinity of a restaurant that utilized charcoal. Location 7 was located in a large parking lot of the Korea University Hospital. Location 8 was located in a predominantly business area.

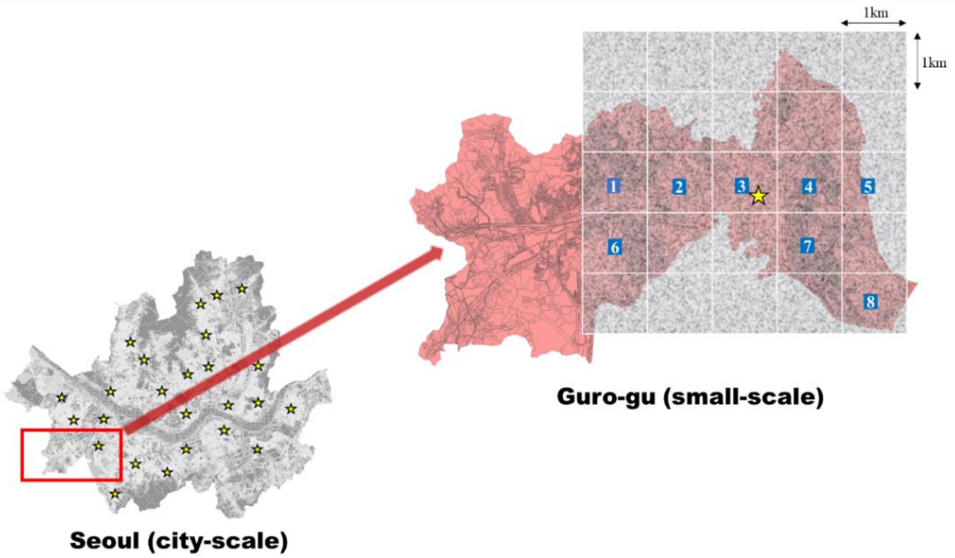

Figure 4-1. Locations of monitoring sites in Seoul. Yellow stars represent AQMSs and blue squares represent IMSs.

Concentrations of air pollutants

- **AQMS data**

Air quality data of five criteria air pollutants ($PM_{2.5}$, PM_{10}, NO_2, CO, and O_3) were monitored by 25 AQMSs in Seoul from December 2017–December 2018. Hourly air pollutant concentrations were downloaded from a website managed by the Korea Environment Corporation (http://www.airkorea.or.kr/web). AQMSs were equipped with national standard method monitors for each pollutant. Hourly air pollutant concentrations were measured by automatic PM monitors based on the beta (β) attenuation method, a NO_2 monitor based on the chemiluminescent method, a CO monitor based on the non-dispersive infrared absorption method, and an O_3 monitor based on the ultraviolet photometric method. The detection limits of monitors at AQMSs were 5 μg/m^3 for $PM_{2.5}$, 10 μg/m^3 for PM_{10}, 0.1 ppb for NO_2, 0.05 ppm for CO, and 2 ppb for O_3. Valid data were selected based on the national quality assurance/quality control (QA/QC) operation guidelines published by the Korea Ministry of Environment (https://www.airkorea.or.kr/web/board/3/267/?pMENU_NO=145).

- **IMS data**

In-situ measurements using a vehicle were performed on eight fixed monitoring sites in the test-bed area. A vehicle with standard monitoring instruments was positioned at eight IMSs to obtain air pollutant concentrations. The hourly concentrations of five criteria air pollutants were measured in each IMS for approximately 10 days in each season. The total of 12 weeks per season at the eight

IMSs was repeated in four season. The sampling periods were classified into winter (December 2017–February 2018), spring (March–June 2018), summer (June–August 2018), and autumn (September–December 2018). Detailed measurement schedules for the eight IMSs are shown in Table S-14. QA/QC for measurements was conducted once per season during 1 week based on the national QA/QC operation guidelines published by the Korea Ministry of Environment (https://www.airkorea.or.kr/web/board/3/267/?pMENU_NO=145).

Correlation analysis

Pearson correlation coefficients (*r*) between air pollutants in AQMSs and IMSs were calculated using Pearson correlation analysis, as shown in Equation (1):

$$r = \frac{\sum_{i=1}^{n}(x_i - \overline{x})(y_i - \overline{y})}{\sqrt{\sum_{i=1}^{n}(x_i - \overline{x})^2}\sqrt{\sum_{i=1}^{n}(y_i - \overline{y})^2} \qquad (1)$$

where *n* is the number of samples; x_i and y_i are the air pollutants concentration of x and y in monitoring sites, respectively; and $\overline{x}$ and $\overline{y}$ are the mean x and y values, respectively.

The correlations were classified into three categories: weak, moderate, and strong correlations. The absolute value of coefficient ($|r|$) ranged from 0–0.3 for weak correlations, from 0.3–0.6 for moderate correlations, and 0.6–1.0 for strong correlations.

Spatial autocorrelation analysis using Moran's index

Moran's index (Moran's *I*) was used as an indicator of spatial autocorrelation to identify the homogeneity and heterogeneity of air pollutants at different monitoring sites (Fang et al., 2015). Spatial autocorrelations were analyzed by the global index which represented the overall spatial patterns at all monitoring sites (Moran, 1948), and the local index which represented the local spatial autocorrelation at each specific monitoring site (Anselin, 1995).

- **Global spatial autocorrelation**

Global Moran's *I* (GMI) was used to determine the overall spatial autocorrelation of air pollutant concentrations in entire monitoring sites and ranged from -1 to 1; if GMI was > 0 (0 < GMI < 1), it represented a positive spatial autocorrelation; a larger GMI denoted that the area had the stronger spatial agglomeration with a similar concentration in the adjacent area. In contrast, if GMI was < 0 (-1 < GMI < 0), it represented a negative spatial autocorrelation which was spatially dispersed and implied that the area had less spatial agglomeration with a different concentration in the adjacent area. If GMI = 0, air pollutant concentrations were randomly distributed and there was no spatial autocorrelation. GMI was calculated using Equation (2):

$$\mathrm{GMI} = \frac{\sum_{i=1}^{n}\sum_{j=1}^{n} w_{ij}(x_i - \overline{x})(x_j - \overline{x})}{\frac{1}{n}\sum_{i=1}^{n}(x_i - \overline{x})^2 \sum_{i=1}^{n}\sum_{j=1}^{n} w_{ij}} \tag{2}$$

where *n* is the number of monitoring sites; x_i and x_j are air pollutants concentration of spatial i and j monitoring sites, respectively; $\overline{x}$ is the mean x; and

w_{ij} is the spatial weight matrix that represents the spatial relationship between spatial i and j sites. If w_{ij} is 1, the spatial unit i and j are adjacent; otherwise w_{ij} is 0.

The Z values of the standardized statistic were used to test the significance of global spatial autocorrelations and calculated according to Equation (3), (4), and (5).

$$\mathrm{Z} = \frac{I - E(I)}{\sqrt{V(I)}} \qquad (3)$$

$$\mathrm{E(I)} = -\frac{1}{\mathrm{n} - 1} \qquad (4)$$

$$\mathrm{V(I)} = E(I^2) - [E(I)]^2 \qquad (5)$$

Here, *E(I)* and *V(I)* are the expected values and variances of the Moran's I, respectively.

Among the above equations, the significance level of the global Moran's *I* can be measured by Z(I). At the 0.05 significance level, Z > 1.96 represents a positive spatial autocorrelation between spatial units, and -1.96 < Z < 1.96 indicates that the spatial autocorrelation is not obvious. If Z < -1.96, then a negative autocorrelation exists between spatial units, and the attribute value tends to be distributed.

- **Local spatial autocorrelation**

Local Moran's *I* (LMI) was used to determine the local spatial autocorrelation of air pollutant concentrations at each monitoring site. A high positive LMI implied that the concentrations were similar to those in the surrounding neighborhood; high–high clusters (i.e., high values in a high-value neighborhood) and low–low clusters (i.e., low values in a low-value neighborhood). Meanwhile, a high negative LMI implied that a spatial outlier was obviously different from the concentrations at the surrounding monitoring sites; spatial outliers included high–low (i.e., a high value in a low-value neighborhood) and low–high (i.e., a low value in a high-value neighborhood) outliers. The LMI was calculated according to Equation (6):

$$\mathrm{LMI} = \frac{(x_i - \overline{x}) \sum_{j \neq i}^{n} w_{ij}(x_j - \overline{x})}{\frac{1}{n}\sum_{i=1}^{n}(x_i - \overline{x})^2} \tag{6}$$

where n, x_i, x_j, $\overline{x}$, and w_{ij} are the same as the parameters for GMI.

The standardized statistic of LMI can be also measured by Z. At the 0.05 significance level, Z > 1.96 shows that sites with high concentrations were surrounded by sites with high concentrations (i.e., high–high) and that sites with low concentrations were surrounded by sites with low concentrations (low–low). If Z < -1.96, it shows that sites with high concentrations were surrounded by sites with low concentrations (high–low) and that sites with low concentrations were surrounded by sites with high concentrations (low–high). When Z = 0, the observations represented random distribution. When -1.96 < Z < 1.96, the spatial autocorrelation was not significant.

Statistical analysis

In the box plots, mean and median values were represented by the dotted line and plain line, respectively. Box limits represented the 25th and 75th percentiles, and the whiskers extended to the 10th and 90th percentiles. Circles above the 90th percentile represented the 95th percentile, and circles below the 10th percentile represented the 5th percentile. Box plots were drawn in SigmaPlot 10.0 (Systat Software, San Jose, CA, USA).

Spatial autocorrelations analyses using GMI and LMI were conducted using the *moran.test() and localmoran()* function in the package "spdep" (Bivand et al., 2021) of R software (version 4.0.3). All calculations and statistical analyses were conducted using R (version 4.0.3). Air pollutant concentrations in monitoring sites were compared by season to determine significant differences in means using one-way analysis of variance (ANOVA) and Tukey's *post-hoc* tests. A p-value < 0.05 was considered to indicate statistical significance for two-sided statistical tests.

4.3. Results

Seasonal characteristics of air pollutants

The hourly concentrations of five criteria air pollutants in AQMSs and IMSs in four seasons are shown in Figure 4-2. The hourly air pollutant concentrations at the 25 AQMSs were significantly different between the four seasons ($p < 0.001$). The highest $PM_{2.5}$, PM_{10}, NO_2, and CO concentrations at the 25 AQMSs were observed in winter, whereas the lowest concentrations were observed in summer. Conversely, the highest O_3 concentrations at the 25 AQMSs were observed in summer, whereas the lowest concentrations were observed in winter. Hourly air pollutant concentrations at IMSs were significantly different in the four seasons ($p < 0.001$). Seasonal characteristics of air pollutants at IMSs were similar to those at the 25 AQMSs.

The hourly mean $PM_{2.5}$ concentrations in summer and autumn at IMSs were significantly higher than those at the 25 AQMSs ($p < 0.001$), whereas the hourly mean $PM_{2.5}$ concentrations in spring at IMSs and 25 AQMSs were only slightly different ($p = 0.07$). The hourly mean PM_{10} concentrations in four seasons at IMSs were significantly higher than those at 25 AQMSs ($p < 0.001$). The hourly mean NO_2 concentrations in winter, spring, and summer at IMSs were significantly higher than those at 25 AQMSs ($p < 0.05$). The hourly mean CO concentrations in four seasons at IMSs were significantly higher than those at 25 AQMSs ($p < 0.001$). However, the hourly mean O_3 concentrations in spring and summer at IMSs were significantly lower than those at 25 AQMSs ($p < 0.001$). Descriptive statistics of hourly mean air pollutant concentrations at AQMS and IMSs in Guro-gu are shown in Tables S-15–S-20. The hourly mean air pollutant concentrations at AQMS and IMSs in Guro-gu were significantly different in all seasons ($p < 0.05$).

The noncompliance rates of the KAAQSs of air pollutants at AQMSs and IMSs are shown in Table 4-1. The noncompliance rates of the $PM_{2.5}$ KAAQS with a 24-h mean of 35 $\mu g/m^3$ were approximately 30% in winter and spring at all sites. PM_{10} concentrations did not exceed KAAQS with a 24-h mean of 100 $\mu g/m^3$ in summer at any site. The NO_2 and CO concentrations in 25 AQMSs and IMSs in all seasons did not exceed the KAAQSs. Noncompliance rates of the PM_{10} KAAQS at IMSs were higher than at 25 AQMSs in winter, spring, and autumn, whereas noncompliance rates of the O_3 KAAQS at IMSs in summer were lower than at 25 AQMSs.

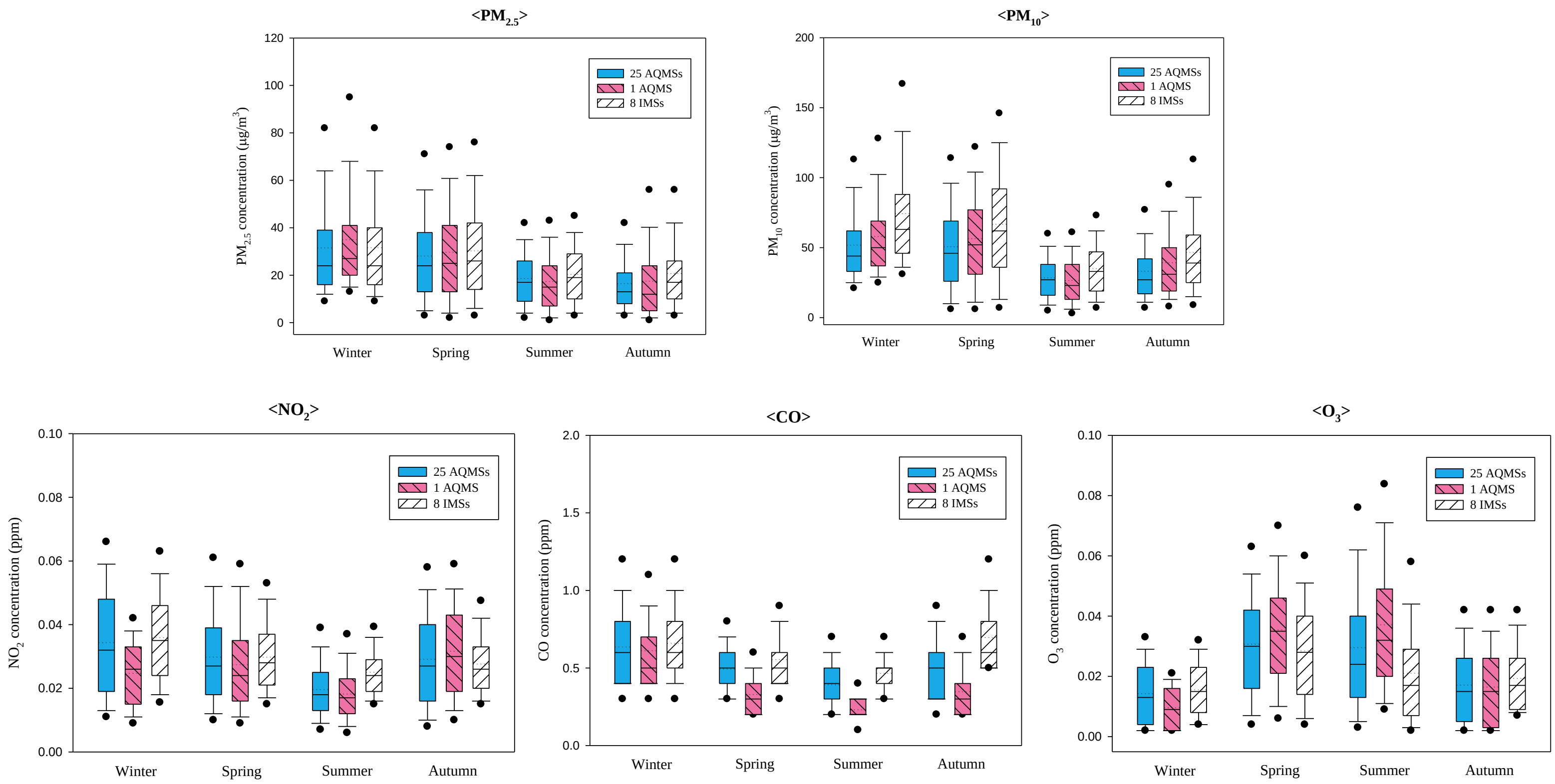

Figure 4-2. Hourly concentrations of air pollutants at 25 AQMSs (blue), 1 AQMS in Guro-gu (pink), and 8 IMSs in Guro-gu (white).

Table 4-1. The noncompliance rates (%) of the KAAQSs of air pollutants by season.

Air pollutant	Site	Winter	Spring	Summer	Autumn
$PM_{2.5}$ (24-h) (35 μg/m^3)	25 AQMSs	32.5	27.3	6.6	7.1
	Guro AQMS	35.1	33.8	5.8	12.5
	IMS	31.7	34.1	4.3	12.5
PM_{10} (24-h) (100 μg/m^3)	25 AQMSs	5.9	7.0	0	3.2
	Guro AQMS	9.3	10.4	0	4.2
	IMS	20.7	12.2	0	5.6
O_3 (8-h) (0.06 ppm)	25 AQMSs	0	3.1	6.1	0
	Guro AQMS	0	7.3	12.1	0
	IMS	0	3.4	2.0	0
O_3 (1-h) (0.1 ppm)	25 AQMSs	0	0.3	1.7	0
	Guro AQMS	0	0.6	2.5	0
	IMS	0	0.2	0.3	0

Correlations between air pollutants

Seasonal correlations between air pollutants at 25 AQMSs and the IMSs are shown in Table 4-2. The PM concentration in 25 AQMSs and the IMSs showed significant positive correlations with NO_2 and CO, especially in winter and autumn (r values > 0.5). The $PM_{2.5}$ concentrations showed significantly strong positive correlations with NO_2 and CO concentrations in autumn (r value > 0.6). However, O_3 at IMSs had significant negative weak correlations with PM in winter and autumn whereas positive correlations in summer. Strong negative correlations between O_3 and NO_2 were observed in winter whereas weak correlations were observed in summer.

Table 4-2. Pearson correlation coefficients among five air pollutants in 25 AQMSs in Seoul (gray) and IMSs in Guro-gu, Seoul (white) by season.

	$PM_{2.5}$	PM_{10}	NO_2	CO	O_3	$PM_{2.5}$	PM_{10}	NO_2	CO	O_3
	Winter					Spring				
$PM_{2.5}$	1	0.91**	0.57**	0.63**	-0.34**	1	0.78**	0.47**	0.62**	-0.003
PM_{10}	0.94**	1	0.48**	0.57**	-0.24**	0.77**	1	0.39**	0.49**	0.10*
NO_2	0.55**	0.49**	1	0.78**	-0.78**	0.16*	0.18**	1	0.66**	-0.50**
CO	0.58**	0.57**	0.63**	1	-0.57**	0.35**	0.34**	-0.43**	1	-0.32**
O_3	-0.06*	-0.03	-0.63**	-0.26**	1	0.04	0.11*	-0.55**	-0.29**	1
	Summer					Autumn				
$PM_{2.5}$	1	0.94**	0.41**	0.37**	0.35**	1	0.76**	0.64**	0.66**	-0.28**
PM_{10}	0.90**	1	0.42**	0.38**	0.36**	0.79**	1	0.48**	0.45**	-0.22**
NO_2	0.32**	0.37**	1	0.40**	-0.08*	0.61**	0.48**	1	0.71**	-0.65**
CO	0.16*	0.21**	0.33**	1	0.01	0.63**	0.50**	0.76**	1	-0.49**
O_3	0.27**	0.30**	-0.04	0.03	1	-0.22**	-0.21**	-0.50**	-0.44**	1

** : Estimates are statistically significant at $p < 0.001$. * : Estimates are statistically significant at $p < 0.05$.

The seasonal correlations between AQMS and IMS in Guro-gu are shown in Table 4-3 using Pearson correlation coefficients (*r*). The strong correlations between IMS and AQMS with above 0.8 of *r* value were observed for PM and O_3 in all seasons. However, weak correlation was especially observed for CO in summer. In autumn, strong correlations with above 0.8 of r value were observed for all air pollutants. In summer, the lowest correlations between IMS and AQMS were shown in all air pollutants.

Table 4-3. Pearson correlation coefficients of five air pollutants between IMSs and AQMS by season in Guro-gu.

	Winter	Spring	Summer	Autumn
$PM_{2.5}$	0.94	0.87	0.80	0.88
PM_{10}	0.94	0.94	0.81	0.95
NO_2	0.89	0.78	0.64	0.91
CO	0.56	0.65	0.28	0.83
O_3	0.81	0.93	0.93	0.95

All correlation coefficients had *p*-value less than 0.01.

Spatial autocorrelation

- **Global spatial autocorrelation**

Global spatial autocorrelations with city-scale at 25 AQMSs in Seoul are shown in Table 4-4 using GMI. Significant global spatial homogeneity of $PM_{2.5}$ at 25 AQMSs was observed in autumn with a positive GMI (p < 0.05). However, $PM_{2.5}$ concentrations in winter and spring were randomly distributed with a GMI of approximately 0. PM_{10} concentrations in winter and spring were spatially dispersed with a negative GMI. O_3 concentrations in winter and autumn were spatially agglomerated with a significant positive GMI (p < 0.05).

Table 4-4. Global spatial autocorrelation analysis of air pollutants at 25 AQMSs in Seoul over four seasons.

	Winter		Spring		Summer		Autumn	
	GMI	Z	GMI	Z	GMI	Z	GMI	Z
$PM_{2.5}$	0.02	0.46	0.03	0.52	0.06	0.79	0.23*	2.07
PM_{10}	-0.18	-1.01	-0.26	-1.64	0.02	0.47	0.13	1.29
NO_2	-0.17	-0.93	-0.04	0.00	0.12	1.25	0.01	0.37
CO	0.09	1.00	-0.18	-1.03	-0.16	-0.89	0.07	0.83
O_3	0.27*	2.32	0.09	0.99	0.13	1.26	0.21*	2.00

* : Estimates are statistically significant at p < 0.05.

Global spatial autocorrelations with small-scale at eight IMSs in Guro-gu are shown in Table 4-5. $PM_{2.5}$ and PM_{10} in all seasons at IMSs had negative GMI, indicating that they were spatially dispersed. $PM_{2.5}$, PM_{10}, and NO_2 concentrations in winter were randomly distributed with GMI of approximately 0. PM_{10} concentrations in winter and spring were spatially dispersed with negative GMI. O_3 concentrations in spring and autumn were spatially agglomerated with significant positive GMI ($p < 0.05$). NO_2 and CO concentrations in summer and autumn were spatially distributed with negative GMI.

Table 4-5. Global spatial autocorrelation analysis of air pollutants at 8 IMSs in Guro-gu over four seasons.

	Winter		Spring		Summer		Autumn	
	GMI	Z	GMI	Z	GMI	Z	GMI	Z
$PM_{2.5}$	-0.01	0.52	-0.30	-0.79	-0.29	-0.78	-0.33	-0.96
PM_{10}	-0.07	0.24	-0.32	-0.89	-0.29	-0.77	-0.15	-0.13
NO_2	0.01	0.64	-0.35	-1.06	-0.20	-0.33	-0.12	0.05
CO	-0.36	-1.12	0.16	1.33	-0.12	0.00	-0.35	-1.03
O_3	-0.11	0.09	0.21*	1.58	-0.19	-0.32	0.19*	1.49

* : Estimates are statistically significant at $p < 0.05$.

- **Local spatial autocorrelation**

Local spatial autocorrelations at each AQMS in Seoul are shown in Tables S-20–S-24 using LMI. The local spatial autocorrelations at eight IMSs are shown in Fig 4-3. Patterns of the local spatial autocorrelation at each monitoring site differed by season. $PM_{2.5}$ concentrations at locations 3, 5 and 8 were spatially dispersed in winter with negative GMI, whereas they were spatially agglomerated in summer and autumn with positive GMI. PM_{10} concentrations at location 3 and 8 were spatially dispersed in winter with negative GMI, while were randomly distributed in autumn with GMI of approximately 0. O_3 concentrations at location 7 were spatially agglomerated in all seasons.

The highest LMIs of $PM_{2.5}$ were 2.56 at location 3 in winter, 0.29 at location 3 in spring, 0.01 at location 7 in summer, and 0.49 at location 1 in autumn. The lowest LMI of $PM_{2.5}$ were -1.86 at location 2 in winter, -3.21 at location 6 in spring, -2.33 at location 5 in summer, and -4.43 at location 5 in autumn. The highest LMIs of PM_{10} were 0.71 at location 8 in winter, 0.11 at location 4 in spring, 0.05 at location 2 in summer, and 1.22 at location 1 in autumn. The lowest LMI of PM_{10} were -1.91 at location 2 in winter, -3.25 at location 7 in spring, -2.63 at location 5 in summer, and -1.60 at location 4 in autumn. The highest LMIs of NO_2 were 0.53 at location 3 in winter, 0.33 at location 2 in spring, 0.46 at location 4 in summer, and 1.13 at location 2 in autumn. The lowest LMI of NO_2 were -0.75 at location 4 in winter, -2.68 at location 1 in spring, -4.28 at location 5 in summer, and -3.26 at location 5 in autumn. The highest LMIs of CO were -0.11 at location 4 in winter, 1.37 at location 6 in spring, 0.65 at location 8 in summer, and 0.08 at location 3 in autumn. The lowest

LMI of CO were -2.66 at location 2 in winter, -0.72 at location 2 in spring, -1.33 at location 7 in summer, and -3.74 at location 5 in autumn. The highest LMIs of O_3 were 0.80 at location 7 in winter, 1.99 at location 5 in spring, 2.29 at location 3 in summer, and 2.01 at location 7 in autumn. The lowest LMI of O_3 were -1.20 at location 2 in winter, -1.42 at location 6 in spring, -3.81 at location 4 in summer, and -1.37 at location 6 in autumn.

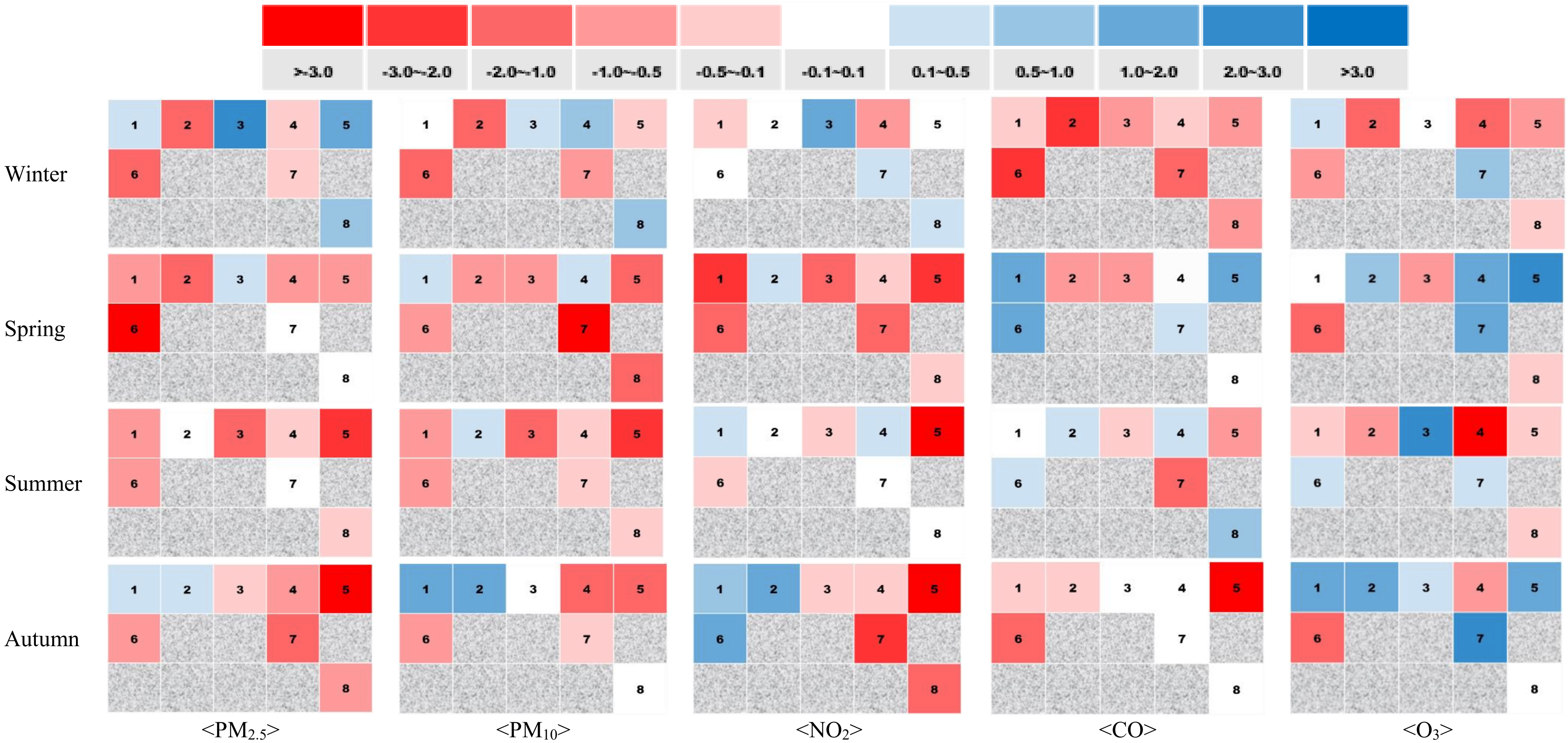

Figure 4-3. LMIs of air pollutants in eight IMSs by season. Blue represents a positive spatial autocorrelation, red represents a negative spatial autocorrelation, and white represents no spatial autocorrelation.

4.4. Discussion

In this study, air pollutant concentrations at IMSs in Guro-gu were measured by national standard monitoring instruments managed by Seoul Metropolitan Government Research Institute of Public Health and Environment. All the measurements in AQMSs and IMSs were conducted by the standard monitoring methods; therefore, the data used in this study had minimal measurement uncertainty and could be utilized for direct comparison. Korea Ministry of Environment has conducted real-time measurements using a vehicle equipped with the standard monitoring instruments to obtain high spatial variations of air pollutant concentrations at sites nearby on-road (Kim et al., 2015). These measurement can provide high spatial resolution of air pollutant concentrations in areas where AQMS does not measure. In this study, a vehicle with standard monitoring instruments was positioned at eight monitoring sites to obtain air quality with a high spatial resolution of 1km^2.

AQMS data in one administrative district in Seoul (Guro-gu) were significantly different from IMSs data surrounding the AQMS. The hourly mean PM and NO_2 concentrations at IMSs were generally higher than those at the Guro AQMS. Especially, hourly mean CO concentrations in four seasons at IMSs were approximately two-fold higher than at the AQMS. However, the O_3 concentrations at IMSs in spring and summer were significantly lower than those at the Guro AQMS. The rate of exceeding the KAAQS for O_3 at the Guro AQMS in summer was more than two-fold higher than that at IMSs, which may have been affected by the characteristics of the monitoring location; IMSs were located nearby streets and parking lots whereas the Guro AQMS was located on a building rooftop. High CO concentrations are mainly due to on-road vehicle emissions (Ghaffarpasand et al., 2020). O_3 is generated by photochemical reaction with O_3 precursors (oxides of nitrogen [NO_x] and volatile organic compounds [VOCs]) and high temperature and strong light intensity leads to increase of more photochemical reaction with O_3 precursors (Ribas and Peñuelas, 2004; Hwang and Park, 2019). A study found that the O_3 concentrations on a rooftop was higher than that on the street (Park et al., 2015; Väkevä et al., 1999).

High PM concentrations were observed in winter, followed by spring. In China, high PM concentrations in winter have previously been observed (Li et al., 2018) which is consistent with the seasonal variation observed in the present study. High PM concentrations in Korea have typically been observed in winter and spring (Kim et al., 2020). Such air quality is affected by long-range transport of air pollutants from East Asia, regional sources, and meteorological conditions in the Korean Peninsula (Kim et al., 2018). Meanwhile, low PM concentrations were observed in summer, when the PM concentrations were reduced by a washout effect during the rainy season along with rapid air dispersion (Kim and Kim, 2000).

High O_3 concentrations were observed in spring and summer whereas low O_3 concentrations occurred in winter. O_3 concentrations were affected by meteorological conditions due to higher air temperature and intense solar irradiation which trigger photochemical reactions with O_3 precursors (NO_x and VOCs) in spring and summer more so than in winter (Ribas and Peñuelas, 2004). On the other hand, during winter, the rate of photochemical reactions with O_3 was slow due to the NO_x titration effect (Jhun et al., 2015). In other studies in Korea, O_3 levels in spring and summer were significantly higher than those in winter (Vellingiri et al., 2015; Hwang and Park, 2019). These results are consistent with those in China (Chen et al., 2017) and Turkey (Kasparoglu et al., 2018).

Noncompliance rates of the KAAQS of $PM_{2.5}$ at AQMSs and IMSs were > 30% in winter and spring. A $PM_{2.5}$ advisory in Seoul, Korea was issued 10 times (winter: 7, spring: 2, and autumn: 1) during the sampling periods. In a $PM_{2.5}$ advisory, personal exposure to $PM_{2.5}$ was affected by high outdoor $PM_{2.5}$ concentration due to high $PM_{2.5}$ infiltration (Guak and Lee, 2018). $PM_{2.5}$ remained present in ambient air for a long period due to the low temperature, low wind speed, and low air circulation in winter (Li et al., 2021). Therefore, the seasonal trend of ambient $PM_{2.5}$ levels should be considered in making policies to reduce personal exposure to air pollution.

High NO_2 and CO concentrations were observed in winter and autumn, and low NO_2 concentrations occurred in summer and spring. The hourly mean NO_2 and CO concentrations in AQMSs and IMSs did not exceed the corresponding KAAQS. The highest NO_2 concentration can be explained by the weak solar irradiation for photochemical conversion to O_3, along with stagnant atmosphere conditions (Li et al., 2012). In contrast, intense light irradiation also caused low concentrations of NO_2 and other nitrogen oxides (Marković et al., 2008). NO_2 is a gaseous traffic-related pollutant with motor vehicle emissions as a main source (Costa et al., 2017). CO is a colorless, nonirritating, odorless, and tasteless gas caused by incomplete combustion of carbon compounds such as burning gasoline, wood, propane, charcoal or other fuel (Sørhaug et al., 2006).

The correlations between air pollutants differed by season. Stronger positive correlations between $PM_{2.5}$ and gaseous pollutants (e.g., NO_2 and CO) were observed in autumn than in other seasons. This result implied that increases in NO_2 and CO concentration affected $PM_{2.5}$ concentrations in autumn. High correlations between PM and gaseous pollutants in autumn were observed in China (Li et al., 2017); the results were similar to those obtained in the present study, with low PM concentration in autumn. However, O_3 had weaker correlations with PM in winter and spring compared to the correlations in summer. As mentioned above, this was mainly associated with the photochemical reactions as properties of O_3 related to climate and meteorological conditions (Ribas and Peñuelas, 2004). PM pollution was severe in winter and spring, whereas it was mild in summer. In winter and spring, there was low temperature and weak light intensity which resulted in fewer reactions between PM and O_3. In summer, high temperature and strong light intensity lead to an increase in O_3 concentrations due to increase photochemical reactions. Seasonal characteristics between PM and O_3 need to be considered on a taking preventive control policies of air pollution.

Global spatial autocorrelation can be used to identify whether the overall sampling areas have spatial autocorrelations, and, if so, to reflect the correlation intensity. In 25 AQMSs in Seoul, GMIs of $PM_{2.5}$ and O_3 were close to zero in spring and were significantly positive in autumn. The result implies a random distribution in spring and spatial agglomeration in autumn. This may be related to seasonal patterns of $PM_{2.5}$ and O_3 concentrations. Low $PM_{2.5}$ and O_3 concentrations were observed in autumn whereas high $PM_{2.5}$ and O_3 concentrations occurred in spring. Spatial autocorrelation was affected by seasonal patterns of air pollutants (Zhou et al., 2021).

Global spatial autocorrelation patterns of $PM_{2.5}$ were different at the city-scale in 25 gu of Seoul and small-scale areas of 1 km^2 in Guro-gu, Seoul. Global autocorrelations of $PM_{2.5}$ in all season were spatially homogenized with positive GMIs at 25 AQMSs. However, global spatial autocorrelations of $PM_{2.5}$ in all season were spatially dispersed with negative GMIs at IMSs. AQMS data at the city-scale were limited to represent air quality in smaller areas including un-monitored locations. Spatial autocorrelation should be considered at a smaller scale than city-scale.

LMI was used to determine the local spatial autocorrelation of air quality and the distribution patterns in each area. Seasonal local spatial patterns of homogeneity and heterogeneity of air pollutants were differently observed by each IMS. It was difficult to generalize and identify the local spatial autocorrelation patterns of air quality in each monitoring area. The characteristics of eight IMSs were different. Various spatial variations could be affected by significant complex factors depending on local emission sources, climate conditions, or meteorological occurrences such as local circulations and topographic features (Wang et al., 2014). Air pollutant concentrations were spatially heterogeneous within areas where different emission sources and characteristic of dispersion by air pollutants existed (Valari et al., 2020). Various spatial autocorrelations in different areas have been reported in other studies (Shen et al., 2019; Wang et al., 2015; Xu et al., 2019).

4.5. Conclusions

Seasonal spatial variations of five air pollutants were identified in city-scale and small-scale areas in Seoul using measurements with standard monitoring methods over 1 year. Air pollutant concentrations measured at AQMSs and IMSs were differed significantly by season. The air pollutants concentrations in IMS were generally higher than in AQMSs, while the O_3 concentrations at IMS in spring and summer were lower than at AQMSs. Seasonal spatial autocorrelations of air pollutants at the city-scale in 25 gu of Seoul were different from those in smaller scale (1 km^2) areas obtained from eight IMSs. Seasonal patterns of spatial autocorrelation for air pollutants at the city-scale did not reflect small-scale variations. Therefore, seasonal spatial variations of air pollutants at a small-scale should be considered to assess more accurate estimations of personal exposure to air pollutants with implication for human health.

References

Anselin, L., 1995. Local indicators of spatial association—LISA. Geographical Analysis 27, 93-115.

Arunachalam, S., Valencia, A., Akita, Y., Serre, M.L., Omary, M., Garcia, V., Isakov, V., 2014. A method for estimating urban background concentrations in support of hybrid air pollution modeling for environmental health studies. International Journal of Environmental Research and Public Health 11, 10518-10536.

Atkinson, R.W., Carey, I.M., Kent, A.J., van Staa, T.P., Anderson, H.R., Cook, D.G., 2013. Long-term exposure to outdoor air pollution and incidence of cardiovascular diseases. Epidemiology 24, 44-53.

Bivand, R., Altman, M., Anselin, L., Assuncao, R., Berke, O., Blanchet, G., & Yu, D., 2021. spdep: Spatial dependence, weighting schemes, statistics. R package version 1.1-7. Retrieved from https://cran.r-project.org/web/packages/spdep/spdep.pdf.

Chen, C., Cai, J., Wang, C., Shi, J., Chen, R., Yang, C., Li, H., Lin, Z., Meng, X., Zhao, A., Liu, C., Niu, Y., Xia, Y., Peng, L., Zhao, Z., Chillrud, S., Yan, B., Kan, H., 2018. Estimation of personal $PM_{2.5}$ and BC exposure by a modeling approach – Results of a panel study in Shanghai, China. Environment International 118, 194-202.

Chen, W., Tang, H., Zhao, H., 2015. Diurnal, weekly and monthly spatial variations of air pollutants and air quality of Beijing. Atmospheric Environment 119, 21-

34.

Chen, Y., Zang, L., Chen, J., Xu, D., Yao, D., Zhao, M., 2017. Characteristics of ambient ozone (O_3) pollution and health risks in Zhejiang province. Environmental Science and Pollution Research 24, 27436-27444.

Cohen, A.J., Brauer, M., Burnett, R., Anderson, H.R., Frostad, J., Estep, K., Balakrishnan, K., Brunekreef, B., Dandona, L., Dandona, R., Feigin, V., Freedman, G., Hubbell, B., Jobling, A., Kan, H., Knibbs, L., Liu, Y., Martin, R., Morawska, L., Pope, C.A., Shin, H., Straif, K., Shaddick, G., Thomas, M., van Dingenen, R., van Donkelaar, A., Vos, T., Murray, C.J.L., Forouzanfar, M.H., 2017. Estimates and 25-year trends of the global burden of disease attributable to ambient air pollution: An analysis of data from the Global Burden of Diseases Study 2015. The Lancet 389, 1907-1918.

Costa, A.F., Hoek, G., Brunekreef, B., Ponce de Leon, A.C.M., 2017. Effects of NO_2 exposure on daily mortality in São Paulo, Brazil. Environmental research 159, 539-544.

Dėdelė, A., Miškinytė, A., 2019. Seasonal and site-specific variation in particulate matter pollution in Lithuania. Atmospheric Pollution Research 10, 768-775.

Fang, C., Liu, H., Li, G., Sun, D., Miao, Z., 2015. Estimating the impact of urbanization on air quality in China using spatial regression models. Sustainability 7, 15570-15592.

Ghaffarpasand, O., Talaie, M.R., Ahmadikia, H., Khozani, A.T., Shalamzari, M.D., 2020. A high-resolution spatial and temporal on-road vehicle emission inventory in an Iranian metropolitan area, Isfahan, based on detailed hourly traffic data. Atmospheric Pollution Research 11, 1598-1609.

Guak, S., Lee, K., 2018. Different relationships between personal exposure and ambient concentration by particle size. Environmental Science and Pollution Research 25, 16945-16950.

Hoek, G., Beelen, R., de Hoogh, K., Vienneau, D., Gulliver, J., Fischer, P., Briggs, D., 2008. A review of land-use regression models to assess spatial variation of outdoor air pollution. Atmospheric Environment 42, 7561-7578.

Hu, J., Wang, Y., Ying, Q., Zhang, H., 2014. Spatial and temporal variability of $PM_{2.5}$ and PM_{10} over the North China Plain and the Yangtze River Delta, China. Atmospheric Environment 95, 598-609.

Hwang, S.H., Park, D.U., 2019. Ambient endotoxin and chemical pollutant (PM_{10}, $PM_{2.5}$, and O_3) levels in South Korea. Aerosol and Air Quality Research 19, 786-793.

Jhun, I., Coull, B.A., Zanobetti, A., Koutrakis, P., 2015. The impact of nitrogen oxides concentration decreases on ozone trends in the USA. Air Quality, Atmosphere & Health 8, 283-292.

Ji, W., Wang, Y., Zhuang, D., 2019. Spatial distribution differences in $PM_{2.5}$ concentration between heating and non-heating seasons in Beijing, China. Environmental Pollution 248, 574-583.

Kasparoglu, S., Incecik, S., Topcu, S., 2018. Spatial and temporal variation of O_3, NO and NO_2 concentrations at rural and urban sites in Marmara region of Turkey. Atmospheric Pollution Research 9, 1009-1020.

Kim, B., Kim, D., 2000. Studies on the environmental behaviors of ambient $PM_{2.5}$

and PM_{10} in Suwon area. Journal of Korean Society for Atmospheric Environment 16, 89-101.

Kim, D., Choi, H.-E., Gal, W.-M., Seo, S., 2020. Five year trends of particulate matter concentrations in Korean regions (2015–2019): When to ventilate? International Journal of Environmental Research and Public Health 17, 5764.

Kim, K.H., Woo, D., Lee, S.-B., Bae, G.-N., 2015. On-road measurements of ultrafine particles and associated air pollutants in a densely populated area of Seoul, Korea. Aerosol and Air Quality Research 15, 142-153.

Kim, Y., Seo, J., Kim, J.Y., Lee, J.Y., Kim, H., Kim, B.M., 2018. Characterization of $PM_{2.5}$ and identification of transported secondary and biomass burning contribution in Seoul, Korea. Environmental Science and Pollution Research 25, 4330-4343.

Li, C., Han, X., Kang, S., Yan, F., Chen, P., Hu, Z., Yang, J., Ciren, D., Gao, S., Sillanpää, M., 2019. Heavy near-surface $PM_{2.5}$ pollution in Lhasa, China during a relatively static winter period. Chemosphere 214, 314-318.

Li, J., Gao, W., Cao, L., He, L., Zhang, X., Yan, Y., Mao, J., Xin, J., Wang, L., Tang, G., Liu, Z., Ji, D., Hu, B., Zhao, D., Zhao, S., Jia, D., Wang, Y., 2021. Effects of different stagnant meteorological conditions on aerosol chemistry and regional transport changes in Beijing, China. Atmospheric Environment 258, 118483.

Li, K., Song, W., Liu, X., Shen, J., Luo, X., Sui, X., Liu, B., Hu, Y., Christie, P., Tian, C., 2012. Atmospheric reactive nitrogen concentrations at ten sites with contrasting land use in an arid region of central Asia. Biogeosciences 9, 4013-

4021.

Li, L., Qian, J., Ou, C.-Q., Zhou, Y.-X., Guo, C., Guo, Y., 2014. Spatial and temporal analysis of air pollution index and its timescale-dependent relationship with meteorological factors in Guangzhou, China, 2001–2011. Environmental Pollution 190, 75-81.

Li, R., Cui, L., Li, J., Zhao, A., Fu, H., Wu, Y., Zhang, L., Kong, L., Chen, J., 2017. Spatial and temporal variation of particulate matter and gaseous pollutants in China during 2014–2016. Atmospheric Environment 161, 235-246.

Marković, D.M., Marković, D.A., Jovanović, A., Lazić, L., Mijić, Z., 2008. Determination of O_3, NO_2, SO_2, CO and PM_{10} measured in Belgrade urban area. Environmental Monitoring and Assessment 145, 349-359.

Marshall, J.D., Nethery, E., Brauer, M., 2008. Within-urban variability in ambient air pollution: comparison of estimation methods. Atmospheric Environment 42, 1359-1369.

Merbitz, H., Fritz, S., Schneider, C., 2012. Mobile measurements and regression modeling of the spatial particulate matter variability in an urban area. Science of The Total Environment 438, 389-403.

Mills, I.C., Atkinson, R.W., Kang, S., Walton, H., Anderson, H., 2015. Quantitative systematic review of the associations between short-term exposure to nitrogen dioxide and mortality and hospital admissions. BMJ Open 5, e006946.

Moran, P.A.P., 1948. The interpretation of statistical maps. Journal of the Royal Statistical Society: Series B (Methodological) 10, 243-251.

Park, S.-B., Kwak, K.-H., Han, B.-S., Ganbat, G., Lee, H., Seo, J.M., Lee, S.-H., Baik, J.-J., 2015. Measurements of turbulent flow and ozone at rooftop and sidewalk sites in a high-rise building area. SOLA 11, 1-4.

Raja, N.B., Aydin, O., Türkoğlu, N., Çiçek, İ., 2018. Characterising the seasonal variations and spatial distribution of ambient PM_{10} in urban Ankara, Turkey. Environmental Processes 5, 349-362.

Ribas, À., Peñuelas, J., 2004. Temporal patterns of surface ozone levels in different habitats of the North Western Mediterranean basin. Atmospheric Environment 38, 985-992.

Shen, Y., Zhang, L., Fang, X., Ji, H., Li, X., Zhao, Z., 2019. Spatiotemporal patterns of recent $PM_{2.5}$ concentrations over typical urban agglomerations in China. Science of The Total Environment 655, 13-26.

Sørhaug, S., Steinshamn, S., Nilsen, O.G., Waldum, H.L., 2006. Chronic inhalation of carbon monoxide: effects on the respiratory and cardiovascular system at doses corresponding to tobacco smoking. Toxicology 228, 280-290.

Su, J.G., Jerrett, M., Beckerman, B., Verma, D., Arain, M.A., Kanaroglou, P., Stieb, D., Finkelstein, M., Brook, J., 2010. A land use regression model for predicting ambient volatile organic compound concentrations in Toronto, Canada. Atmospheric Environment 44, 3529-3537.

Tessum, M.W., Larson, T., Gould, T.R., Simpson, C.D., Yost, M.G., Vedal, S., 2018. Mobile and fixed-site measurements to identify spatial distributions of traffic-related pollution sources in Los Angeles. Environmental Science & Technology 52, 2844-2853.

Väkevä, M., Hämeri, K., Kulmala, M., Lahdes, R., Ruuskanen, J., Laitinen, T., 1999.

Street level versus rooftop concentrations of submicron aerosol particles and gaseous pollutants in an urban street canyon. Atmospheric Environment 33, 1385-1397.

Valari, M., Markakis, K., Powaga, E., Collignan, B., Perrussel, O., 2020. EXPLUME v1. 0: a model for personal exposure to ambient O_3 and $PM_{2.5}$. Geoscientific Model Development 13, 1075-1094.

Vellingiri, K., Kim, K.-H., Jeon, J.Y., Brown, R.J.C., Jung, M.-C., 2015. Changes in NOx and O_3 concentrations over a decade at a central urban area of Seoul, Korea. Atmospheric Environment 112, 116-125.

Wang, Y., Ying, Q., Hu, J., Zhang, H., 2014. Spatial and temporal variations of six criteria air pollutants in 31 provincial capital cities in China during 2013–2014. Environment International 73, 413-422.

Wang, Y., Zhang, X., Sun, J., Zhang, X., Che, H., Li, Y., 2015. Spatial and temporal variations of the concentrations of PM_{10}, $PM_{2.5}$ and PM_1 in China. Atmospheric Chemistry and Physics 15, 13585-13598.

Xu, J., Yang, W., Han, B., Wang, M., Wang, Z., Zhao, Z., Bai, Z., Vedal, S., 2019. An advanced spatio-temporal model for particulate matter and gaseous pollutants in Beijing, China. Atmospheric Environment 211, 120-127.

Yang, Y., Christakos, G., 2015. Spatiotemporal characterization of ambient $PM_{2.5}$ concentrations in Shandong province (China). Environmental Science & Technology 49, 13431-13438.

Zhao, P., Dong, F., He, D., Zhao, X., Zhang, X., Zhang, W., Yao, Q., Liu, H., 2013. Characteristics of concentrations and chemical compositions for $PM_{2.5}$ in the region of Beijing, Tianjin, and Hebei, China. Atmospheric Chemistry and Physics 13, 4631-4644.

Zhou, D., Lin, Z., Liu, L., Qi, J., 2021. Spatial-temporal characteristics of urban air pollution in 337 Chinese cities and their influencing factors. Environmental Science and Pollution Research.

Chapter V.

Summary and Conclusions

The outdoor $PM_{2.5}$ concentrations at AQMSs often used as a surrogate for population exposure to $PM_{2.5}$ in numerous epidemiological studies. However, indoor air pollution as well as ambient air pollution could be considered to reflect the actual $PM_{2.5}$ exposure. Modeling population exposure to $PM_{2.5}$ is useful for assessing the exposure level for groups of people. Population exposure to $PM_{2.5}$ could be estimated as the sum of microenvironmental exposure based on a combination of the $PM_{2.5}$ concentration and the time spent in microenvironments. Therefore, the outdoor $PM_{2.5}$ concentration for a surrogate of $PM_{2.5}$ exposure should be applied by additional consideration of the relationship between the microenvironment and the outdoor $PM_{2.5}$ concentrations. This study developed a population exposure model to predict population exposure to $PM_{2.5}$. The population exposure model for $PM_{2.5}$ could be used to implement effective interventions and evaluate the effectiveness of control policies to reduce exposure. In addition, Study 2 and study 3 will provide useful insights into refining KoSEM in further study for estimation of population exposure.

In the first study, a population exposure model found significant seasonal difference in distribution of population exposure to $PM_{2.5}$ in Seoul, Korea. Population exposure to high $PM_{2.5}$ levels mainly occurred in winter. Significant determinants of high population exposure to $PM_{2.5}$ were identified in the model, including gender, age, working hours, and health condition. Population in the high $PM_{2.5}$ exposure was relatively characterized as having a higher proportion of males, being of a lower age, having fewer working hours, and having fewer ‘unhealthy’ health condition. Identification of determinants for population exposure to $PM_{2.5}$ could be used to evaluate the effectiveness of control policies to reduce personal exposure to $PM_{2.5}$ and implement effective interventions.

In the second study, prediction models in education facilities were developed outdoor PM concentration and meteorological parameters as inputs to predict real-time PM_{10} concentration with high accuracy for one year every 10 min. Much of the outdoor data are already being continuously generated by local monitoring stations and can be easy to access for indoor predictions with time-saving and cost-effective. The outdoor PM_{10} concentration was the most important input variable in prediction models. The best performance was shown in root-transformed model with day-time predictor. Indoor PM_{10} level was the highest in the daycare centers. Our approach could be useful methodologies for highly time-resolved to predict PM_{10} concentrations in different educational facilities using outdoor environmental parameters.

In the third study, spatial-temporal variation at small-area with relatively high resolution of $1km^2$ was identified based on real-time in-situ measurements over one year. Differences of five criteria air pollutants concentrations between AQMS and IMS were significantly different by season. Due to meteorological conditions, seasonal variations of all PM were observed with the highest concentrations in winter, but high O_3 levels were shown in spring and summer. Seasonal patterns of spatial autocorrelation for air pollutants at city-scale area did not reflect variation at small-scale area. The results provided a basis understanding of seasonal spatial variations by air pollutants. Spatial-temporal variation by air pollutants and monitoring sites should be considered on more accurate estimation of air pollution.

Through these studies, a model for population exposure to $PM_{2.5}$ could be useful to assess population exposure without direct measurement. The identification of exposure determinants could be used to evaluate the effectiveness of control policies to reduce personal exposure to $PM_{2.5}$, and to implement effective interventions. The population exposure model could be expanded to apply different air pollutants and cities in future study. Seasonal spatial variation of air pollutants at small-scale area should be considered on more accurate estimation of personal exposure to air pollutants.

Supplements

Indoor multi-use facilities in Table 1-1 and Table S-1 were classified into as below.

1: Underground station, underground shopping mall, waiting room in railway station, waiting room in bus terminal, waiting room among port facilities, passenger terminal in airport, library・museum and art gallery, bureau store, funeral hall, movie theater, academy, exhibition facility, internet computer game room, public bathhouse

2: Medical institutions, postpartum care centers, nursing homes for the elderly, day care center, children play facilities

3: Indoor parking lot

4: Indoor sports facility, indoor performance hall, business facility, buildings used for more than one purpose

Table S-1. IAQ standards and guidelines in indoor multi-use facilities.

Facility	Standard		Guideline		
	Formaldehyde (μg/m^3)	Total airborne bacteria (CFU/m^3)	Radon (Bq/m^3)	TVOCs (μg/m^3)	Mold (CFU/m^3)
1	100	-	148	500	-
2	80	800		400	500
3	100	-		1000	-

* TVOCs: Total Volatile Organic Compounds

Table S-2. IAQ guidelines in public transportations managed by the Korea Ministry of Environment.

	$PM_{2.5}$ ($\mu g/m^3$)	CO_2 (ppm)
Rush hours[a]	50	2500
Non rush hours		2000

a: Rush hours

- subway : 7:30-9:30 a.m. and 6:00-8:00 p.m. in weekdays
- train and bus : Saturday, Sunday and public holidays.

Table S-3. IAQ standards and guidelines in kindergartens, schools, and university managed by the Korea Ministry of Education.

	$PM_{2.5}$ (μg/m^3)	PM_{10} (μg/m^3)	CO_2 (ppm)	CO (ppm)	NO_2 (ppm)	O_3 (ppm)
Classroom, school cafeteria	35	75	1000	10[a]	0.05[a]	0.06[b]
Gym, auditorium	-	150	-	-	-	-

It was based on partial amendment by Ministry of Education Decree No. 194, Oct. 24, 2019.

a: Classroom which has individual heating system and is located nearby on-road

b: Teacher's room which has copying machine as emission source of O_3

Table S-4. IAQ standards in workplace managed by Korea Ministry of Employment and Labor.

	$PM_{2.5}$ (μg/m^3)	PM_{10} (μg/m^3)	CO_2 (ppm)	CO (ppm)	NO_2 (ppm)
Office	50	100	1000	10	0.05

It was based on partial amendment by Ministry of Employment and Labor No. 2020-45, Jan. 14, 2020
*Average time is 8-h time-weighted value.

Table S-5. Descriptive statistics of socio-demographic characteristics of population by seasons.

	Summer (N=960)	Autumn (N=1898)	Winter (N=1126)
Age, av±sd (range)	41.8 ± 18.9 (10–90)	43.2 ± 18.8 (10–94)	41.7 ± 18.9 (10–93)
<20	127 (13.2%)	234 (13.2%)	180 (16.0%)
20-39	317 (33.3%)	595 (31.3%)	349 (31.0%)
40-59	338 (35.2%)	664 (35.0%)	376 (33.4%)
≥60	178 (18.5%)	405 (21.3%)	221 (19.6%)
Gender			
Male	408 (42.5%)	896 (47.2%)	557 (49.5%)
Female	552 (57.5%)	1002 (52.8%)	569 (50.5%)
Educational level			
Elementary school and below	123 (12.8%)	110 (5.8%)	111 (9.9%)
Middle/high school	350 (36.5%)	750 (39.5%)	391 (34.7%)
College/University	409 (42.6%)	802 (42.3%)	550 (48.8%)
Graduate school	78 (8.1%)	126 (6.6%)	74 (6.6%)
Monthly income (USD, $)			
<1500	565 (58.9%)	1118 (58.9%)	665 (59.1%)
1500-3000	253 (26.4%)	435 (22.9%)	248 (22.0%)
>3000	142 (14.8%)	345 (18.2%)	213 (18.9%)
Marriage status			
Married	588 (61.3%)	1184 (62.4%)	712 (63.2%)
Unmarried	372 (38.8%)	714 (37.6%)	414 (36.8%)
Health condition			
Healthy	414 (43.1%)	746 (39.3%)	465 (41.3%)
Normal	426 (44.4%)	890 (46.9%)	491 (43.6%)
Unhealthy	120 (12.5%)	262 (13.8%)	170 (15.1%)
Housing type			
Detached house	316 (32.9%)	599 (31.6%)	304 (27.0%)
Apartment	381 (39.7%)	851 (44.8%)	524 (46.5%)
Others	263 (27.4%)	448 (23.6%)	298 (6.5%)
Housing ownership			
Owner	396 (41.3%)	804 (42.4%)	616 (54.7%)
Tenant	564 (58.8%)	1094 (57.6%)	510 (45.3%)

MicroPEM quality assurance

The $PM_{2.5}$ concentrations were measured at the near breathing zone using personal environmental monitor (MicroPEM, Model 3.2A, RTI International, Research Triangle Park, NC, USA). Prior to the measurements, $PM_{2.5}$ inlet were zero-calibrated with a high-efficiency particulate air (HEPA) filter and cleaned once a day. The air flow rate was adjusted to 0.5 L/min using a flow meter (TSI 4100 series, TSI, Inc., Shoreview, MN, USA). Pre-weighed polytetrafluoroethylene (PTFE) filters (25 mm diameter and, 3.0 µm pore size, PALL, Mexico) were placed in the MicroPEM filter cassette during sampling. Due to the low flow rate, $PM_{2.5}$ mass on the filter was collected for 2 days. $PM_{2.5}$ filters were dried before and after sampling for 24 h in a controlled chamber (temperature : 20-23 °C, relative humidity : 30-40%) and were pre- and post-weighed at three times with a Mettler Toledo microbalance (XP6 ; Metteler Toledo International Inc., Switzerland). Field blank filter was used to validate weighing condition. The 2-day average of difference between pre- and post-weighed for three values was used to calculate gravimetric $PM_{2.5}$ concentration. The real-time mass $PM_{2.5}$ data were downloaded by MicroPEM Docking Station software (RTI International, Research Triangle Park, NC, USA). The real-time $PM_{2.5}$ mass concentrations of MicroPEM were calibrated by the gravimetric mass concentration from MicroPEM $PM_{2.5}$ samples on filter.

$$C_{calibrated} = C_{non-calibrated} \times \frac{C_{filter}}{C_{real-time}}$$

where $C_{calibrated}$ is the calibrated real-time $PM_{2.5}$ concentration, $C_{non-calibrated}$ is the raw real-time $PM_{2.5}$ concentration from MicroPEM, C_{filter} is the 2-day weighted $PM_{2.5}$ mass concentrations from the gravimetric method, and the $C_{real-time}$ is the concurrent two-day mean $PM_{2.5}$ concentrations calculated using the raw real-time concentrations. Microenvironmental $PM_{2.5}$ concentrations were calculated using the calibrated real-time data.

Table S-6. Specification of MicroPEM.

	Specification
Principle of measurement	Light-scattering (continuous nephelometer) and gravimetric measurement
Minimum size response	Response down to 90 nm
Inlet D_{50} cut point	<10% for $PM_{2.5}$
Operating range	3–15000 μg/m^3
Operating resolution	3 μg/m^3
Flow rate	0.5 L/min
Precision	<10% variability
Accuracy	< 15% for any given unit using default settings

Table S-7. Sample size of microenvironmental measurement.

Microenvironment	Summer	Autumn	Winter
Home	39614	31791	42774
Workplace/school	15818	12104	14431
Other indoor locations	7811	6022	6579
Restaurant	2070	1857	2257
Walking	2085	1903	1774
Car	1614	1656	1667
Public transportation	2830	2236	2512

Table S-8. Means of $PM_{2.5}$ concentrations in the seven microenvironments by season.

Microenvironment	$PM_{2.5}$ concentration ($\mu g/m^3$)		
	Summer	Autumn	Winter
Home	18.2±19.3	8.1±10.6	15.0±12.0
Workplace/school	16.5±14.4	9.7±10.4	22.7±25.1
Other indoor locations	28.0±48.1	12.3±11.2	39.3±60.2
Restaurant	53.9±88.9	31.6±41.5	75.1±122.9
Walking	45.8±65.4	11.6±13.5	33.5±27.5
Car	10.5±10.7	11.4±12.9	18.6±14.3
Public transportation	26.3±21.5	21.7±16.0	44.1±34.4

Table S-9. Specifications of the AirGuard K.

	Specification
PM_{10} monitor model	AirGuard K IAQ Station (K weather Inc., Korea)
Measurement principle	Light scattering
Measurement range	0–500 μg/m^3
Reproducibility	± 10%
Weight	450 g
Width x Height	81.07 mm x 190.83 mm
Power consumed	2.5 (W)
Power supply	220 VAC

Table S-10. Outdoor environmental parameters as input variable for multiple linear regression models.

Facility	Predictors	Coefficients(β) (95% CI)	Standard Error	P-value
Daycare center	Intercept	-1.92×10^{0} $(-2.52 \times 10^{0}, -1.33 \times 10^{0})$	3.04×10^{-1}	<0.001
	PM_{10} concentration	5.17×10^{-1} $(5.15 \times 10^{-1}, 5.18 \times 10^{-1})$	6.87×10^{-4}	<0.001
	Temperature	4.46×10^{-3} $(3.79 \times 10^{-3}, 5.13 \times 10^{-3})$	3.42×10^{-4}	<0.001
	Precipitation	-3.33×10^{-3} $(-4.03 \times 10^{-3}, -2.62 \times 10^{-3})$	3.59×10^{-4}	<0.001
	Wind direction	1.29×10^{-4} $(1.02 \times 10^{-4}, 1.55 \times 10^{-4})$	1.36×10^{-5}	<0.001
	Wind speed	5.79×10^{-2} $(5.56 \times 10^{-2}, 6.02 \times 10^{-2})$	1.19×10^{-3}	<0.001
	Atmospheric pressure	8.25×10^{-3} $(7.67 \times 10^{-3}, 8.83 \times 10^{-3})$	2.98×10^{-4}	<0.001
	Relative humidity	1.28×10^{-2} $(1.26 \times 10^{-2}, 1.29 \times 10^{-2})$	9.29×10^{-5}	<0.001
	Solar radiation	-2.32×10^{-3} $(-3.62 \times 10^{-3}, -1.02 \times 10^{-3})$	6.62×10^{-4}	<0.001
	Sunshine	-2.91×10^{-6} $(-3.48 \times 10^{-6}, -2.34 \times 10^{-6})$	2.92×10^{-7}	<0.001
Kindergarten	Intercept	6.21×10^{0} $(5.21 \times 10^{0}, 7.22 \times 10^{0})$	5.14×10^{-1}	<0.001
	PM_{10} concentration	4.07×10^{-1} $(4.04 \times 10^{-1}, 4.10 \times 10^{-1})$	1.35×10^{-3}	<0.001
	Temperature	-1.89×10^{-2} $(-2.01 \times 10^{-2}, -1.76 \times 10^{-2})$	6.31×10^{-4}	<0.001
	Precipitation	9.73×10^{-4} $(2.74 \times 10^{-4}, 1.67 \times 10^{-3})$	3.57×10^{-4}	<0.01
	Wind direction	-1.53×10^{-4} $(-1.96 \times 10^{-4}, -1.10 \times 10^{-4})$	2.20×10^{-5}	<0.001
	Wind speed	9.61×10^{-2} $(9.20 \times 10^{-2}, 1.00 \times 10^{-1})$	2.09×10^{-3}	<0.001
	Atmospheric pressure	-4.39×10^{-3} $(-5.37 \times 10^{-3}, -3.40 \times 10^{-3})$	5.02×10^{-4}	<0.001
	Relative humidity	5.78×10^{-3} $(5.43 \times 10^{-3}, 6.12 \times 10^{-3})$	1.75×10^{-4}	<0.001
	Solar radiation	-3.82×10^{-3} $(-6.02 \times 10^{-3}, -1.62 \times 10^{-3})$	1.12×10^{-3}	<0.001
	Sunshine	-1.20×10^{-6} $(-2.15 \times 10^{-6}, -2.53 \times 10^{-7})$	4.83×10^{-7}	<0.05

Elementary school	Intercept	9.02×10^{0} (8.15×10^{0}, 9.88×10^{0})	4.40×10^{-1}	<0.001
	PM_{10} concentration	4.12×10^{-1} (4.10×10^{-1}, 4.15×10^{-1})	1.14×10^{-3}	<0.001
	Temperature	-6.61×10^{-3} (-7.63×10^{-3}, -5.58×10^{-3})	5.22×10^{-4}	<0.001
	Precipitation	4.34×10^{-3} (3.70×10^{-3}, 4.97×10^{-3})	3.25×10^{-4}	<0.001
	Wind direction	-6.55×10^{-5} (-1.04×10^{-4}, -2.71×10^{-5})	1.96×10^{-5}	<0.001
	Wind speed	7.76×10^{-2} (7.42×10^{-2}, 8.11×10^{-2})	1.78×10^{-3}	<0.001
	Atmospheric pressure	-7.29×10^{-3} (-8.13×10^{-3}, -6.45×10^{-3})	4.30×10^{-4}	<0.001
	Relative humidity	4.63×10^{-3} (4.34×10^{-3}, 4.93×10^{-3})	1.50×10^{-4}	<0.001
	Solar radiation	-6.49×10^{-3} (-8.43×10^{-3}, -4.55×10^{-3})	9.89×10^{-4}	<0.001
	Sunshine	-2.53×10^{-6} (-3.35×10^{-6}, -1.71×10^{-6})	4.16×10^{-7}	<0.001

Table S-11. Time tables at educational facilities.

Facility	Start time	End time
D1-D54	7:30	19:30
K1	8:30	19:30
K2-K12	9:00	20:00
E1-E21	9:00	15:00–16:00

D: Daycare center
K: Kindergarten
E : Elementary school

Table S-12. KAAQSs of air pollutants.

Air pollutant		KAAQS
$PM_{2.5}$ ($\mu g/m^3$)	Annual mean	15
	24-h mean	35
PM_{10} ($\mu g/m^3$)	Annual mean	50
	24-h mean	100
NO_2 (ppm)	Annual mean	0.03
	24-h mean	0.06
	1-h mean	0.1
CO (ppm)	8-h mean	9
	1-h mean	25
O_3 (ppm)	8-h mean	0.06
	1-h mean	0.1

Table S-13. Latitude and longitude of monitoring sites in Seoul.

	Location	Latitude	Longitude
AQMS (gu)	Gangnam	37.5175282	127.04746990000001
	Gangdong	37.5449625	127.1367917
	Gangbuk	37.6479299	127.01195180000002
	Gangseo	37.5446400	126.83515060000002
	Gwanak	37.4873546	126.92710199999999
	Gwangjin	37.5471803	127.09249290000002
	Geumcheon	37.4523569	126.90829559999997
	Nowon	37.6574151	127.06787629999996
	Dobong	37.6541919	127.02908789999992
	Dongdaemun	37.5757428	127.02888480000001
	Dongjak	37.4809167	126.97148070000003
	Mapo	37.5555803	126.9055975
	Seodaemun	37.5937421	126.94967870000005
	Seocho	37.5045471	126.99445779999996
	Seongdong	37.5418642	127.04965889999994
	Seongbuk	37.6067189	127.0272794
	Songpa	37.5026857	127.0925092
	Yangcheon	37.5259388	126.85660289999998
	Yeongdeungpo	37.5250065	126.89737049999996
	Yongsan	37.5400327	127.00485000000003
	Eunpyeong	37.6098232	126.93484760000001
	Jongno	37.5720164	127.00500750000003
	Jung	37.5642629	126.97467570000003
	Jungnang	37.5848485	127.09402290000003
	Guro	**37.4984981**	**126.88969240000006**
IMS in Guro-gu	1	37.49706490000001	126.84877540000002
	2	37.4964388	126.8590964
	3	37.5032025	126.87815460000001
	4	37.500809	126.8860211
	5	37.5030878	126.88938359999997
	6	37.4873205	126.8554934
	7	37.4922173	126.88494779999996
	8	37.4815733	126.8934683

Table S-14. Measurement schedules in eight IMSs over one year.

Season	Location No.	Start date	End date
Winter	2	2017-12-05	2017-12-15
	1	2017-12-15	2017-12-26
	7	2017-12-26	2018-01-08
	6	2018-01-08	2018-01-18
	3	2018-01-18	2018-01-26
	4	2018-01-26	2018-02-06
	5	2018-02-06	2018-02-14
	8	2018-02-19	2018-02-28
Spring	1	2018-02-28	2018-03-12
	6	2018-03-22	2018-04-03
	2	2018-04-03	2018-04-11
	3	2018-04-11	2018-04-20
	4	2018-04-20	2018-05-02
	5	2018-05-02	2018-05-10
	8	2018-05-10	2018-05-21
	7	2018-05-21	2018-05-30
Summer	6	2018-06-07	2018-06-15
	1	2018-06-15	2018-06-25
	2	2018-06-25	2018-07-03
	3	2018-07-03	2018-07-11
	4	2018-07-11	2018-07-19
	5	2018-07-19	2018-07-27
	7	2018-07-27	2018-08-06
	8	2018-08-06	2018-08-14
Autumn	1	2019-09-13	2019-09-21
	2	2019-09-27	2019-10-08
	3	2019-10-08	2019-10-17
	4	2019-10-17	2019-11-01
	5	2019-11-01	2019-11-07
	8	2019-11-20	2019-11-29
	6	2019-11-29	2019-12-04
	7	2019-12-04	2019-12-10

Table S-15. Means of $PM_{2.5}$ concentrations (μg/m^3) both IMSs and AQMS in Guro-gu.

Season	IMS		AQMS
	L	AM±SD	AM±SD
Winter	1	33.5±24.8	38.3±27.0
	2	24.6±11.9	26.6±12.6
	3	25.2±21.9	30.5±28.2
	4	19.8±7.3	24.2±7.9
	5	26.5±17.3	29.0±16.5
	6	46.5±32.5	49.5±33.5
	7	35.5±23.2	42.5±26.2
	8	39.8±18.1	37.3±18.9
	T	31.7±22.8	35.1±24.8
Spring	1	25.1±15.7	37.9±20.7
	2	20.3±14.1	21.6±16.1
	3	27.4±14.0	28.4±12.2
	4	36.3±24.7	30.4±18.7
	5	16.7±10.5	11.2±7.5
	6	51.9±24.0	56.4±29.7
	7	29.3±14.7	25.0±10.7
	8	26.3±25.0	19.4±21.1
	T	30.4±22.0	29.8±23.4
Summer	1	28.5±13.0	29.8±14.3
	2	19.8±15.0	19.7±16.4
	3	10.9±8.8	7.2±7.4
	4	19.1±9.3	14.2±6.3
	5	25.5±12.9	20.1±9.4
	6	17.7±14.1	15.3±12.7
	7	22.4±11.9	17.9±10.0
	8	17.6±9.9	12.0±7.8
	T	20.5±13.1	17.5±12.9
Autumn	1	14.9±9.4	13.2±9.7
	2	12.1±6.8	7.0±5.0
	3	19.2±13.2	18.0±15.3
	4	17.8±12.4	15.7±14.2
	5	44.7±25.1	49.2±25.7
	6	24.7±8.8	19.8±6.7
	7	14.1±9.9	5.8±4.6
	8	31.1±21.2	23.4±19.5
	T	20.9±16.9	17.6±18.0

Table S-16. Means of PM_{10} concentrations (μg/m^3) both IMSs and AQMS in Guro-gu.

Season	IMS		AQMS
	L	AM±SD	AM±SD
Winter	1	74.4±43.5	57.9±33.2
	2	56.4±22.0	45.3±16.7
	3	72.0±48.1	54.5±40.7
	4	52.8±16.8	46.8±17.4
	5	74.0±28.7	65.8±25.2
	6	95.4±57.2	69.8±41.5
	7	80.2±43.3	63.1±32.8
	8	93.2±39.6	61.3±25.7
	T	74.6±42.1	58.3±32.4
Spring	1	65.6±36.5	56.0±26.5
	2	57.1±64.3	53.1±63.9
	3	72.1±32.7	61.5±29.2
	4	62.0±38,9	54.0±30.7
	5	38.9±23.6	32.7±18.2
	6	101.9±38.1	85.1±29.1
	7	83.8±37.8	69.3±32.5
	8	43.6±36.3	33.5±30.9
	T	67.0±44.0	56.7±38.3
Summer	1	48.8±20.9	46.6±17.2
	2	34.0±25.0	27.2±24.3
	3	23.3±16.7	13.3±10.0
	4	30.8±12.9	20.8±8.6
	5	42.6±17.7	31.5±13.4
	6	31.4±22.1	25.4±17.9
	7	37.3±17.6	26.1±13.1
	8	29.2±15.1	17.8±10.0
	T	35.3±20.4	26.8±18.1
Autumn	1	32.1±18.3	27.4±17.3
	2	26.1±13.3	20.6±11.0
	3	45.4±24.1	39.0±22.9
	4	39.2±21.9	35.2±20.1
	5	87.0±41.9	76.8±33.8
	6	61.6±24.5	50.1±19.6
	7	33.5±15.0	25.1±12.0
	8	74.4±63.8	61.7±59.6
	T	46.8±37.1	39.5±33.0

Table S-17. Means of NO_2 concentrations (ppm) both IMSs and AQMS in Guro-gu.

	IMS		AQMS
Season	L	AM±SD	AM±SD
Winter	1	0.034±0.011	0.027±0.010
	2	0.039±0.016	0.023±0.009
	3	0.029±0.013	0.021±0.011
	4	0.030±0.012	0.021±0.010
	5	0.037±0.016	0.026±0.012
	6	0.039±0.019	0.027±0.012
	7	0.038±0.013	0.026±0.009
	8	0.041±0.014	0.025±0.011
	T	0.036±0.015	0.025±0.011
Spring	1	0.035±0.012	0.031±0.014
	2	0.027±0.011	0.023±0.014
	3	0.036±0.013	0.034±0.016
	4	0.032±0.013	0.031±0.018
	5	0.026±0.007	0.018±0.010
	6	0.021±0.009	0.031±0.015
	7	0.034±0.010	0.028±0.015
	8	0.028±0.010	0.023±0.014
	T	0.030±0.012	0.028±0.016
Summer	1	0.026±0.008	0.022±0.011
	2	0.027±0.010	0.023±0.013
	3	0.022±0.006	0.015±0.008
	4	0.020±0.004	0.015±0.005
	5	0.029±0.011	0.020±0.007
	6	0.023±0.005	0.018±0.009
	7	0.025±0.007	0.017±0.009
	8	0.030±0.013	0.015±0.006
	T	0.025±0.009	0.018±0.009
Autumn	1	0.027±0.006	0.025±0.011
	2	0.023±0.006	0.023±0.012
	3	0.028±0.009	0.032±0.015
	4	0.029±0.011	0.033±0.016
	5	0.044±0.011	0.051±0.015
	6	0.029±0.006	0.041±0.009
	7	0.018±0.004	0.021±0.009
	8	0.027±0.007	0.035±0.012
	T	0.028±0.010	0.032±0.016

Table S-18. Means of CO concentrations (ppm) both IMSs and AQMS in Guro-gu.

Season	IMS		AQMS
	L	AM±SD	AM±SD
Winter	1	0.68±0.35	0.65±0.25
	2	0.48±0.23	0.59±0.26
	3	0.71±0.20	0.64±0.24
	4	0.68±0.16	0.60±0.16
	5	0.75±0.26	0.65±0.26
	6	0.75±0.50	0.48±0.19
	7	0.56±0.16	0.68±0.25
	8	0.72±0.21	0.61±0.19
	T	0.66±0.29	0.61±0.24
Spring	1	0.73±0.39	0.36±0.13
	2	0.50±0.14	0.29±0.10
	3	0.58±0.13	0.33±0.09
	4	0.53±0.13	0.33±0.11
	5	0.44±0.07	0.26±0.06
	6	0.61±0.21	0.42±0.15
	7	0.52±0.11	0.32±0.09
	8	0.48±0.16	0.31±0.13
	T	0.56±0.22	0.33±0.12
Summer	1	0.44±0.08	0.27±0.07
	2	0.41±0.14	0.30±0.10
	3	0.56±0.17	0.20±0.08
	4	0.36±0.07	0.18±0.06
	5	0.52±0.07	0.22±0.05
	6	0.41±0.12	0.24±0.05
	7	0.53±0.10	0.24±0.07
	8	0.51±0.09	0.22±0.05
	T	0.47±0.13	0.23±0.08
Autumn	1	0.59±0.17	0.26±0.08
	2	0.57±0.13	0.25±0.11
	3	0.71±0.20	0.33±0.14
	4	0.67±0.20	0.34±0.16
	5	1.03±0.26	0.64±0.21
	6	0.83±0.26	0.44±0.14
	7	0.55±0.11	0.26±0.07
	8	0.78±0.27	0.41±0.23
	T	0.70±0.24	0.35±0.19

Table S-19. Means of O_3 concentrations (ppm) both IMSs and AQMS in Guro-gu.

Season	IMS		AQMS
	L	AM±SD	AM±SD
Winter	1	0.016±0.007	0.008±0.006
	2	0.014±0.007	0.008±0.006
	3	0.016±0.009	0.013±0.007
	4	0.017±0.010	0.012±0.007
	5	0.016±0.010	0.012±0.008
	6	0.021±0.010	0.009±0.006
	7	0.012±0.008	0.007±0.005
	8	0.016±0.011	0.014±0.009
	T	0.016±0.009	0.010±0.007
Spring	1	0.019±0.012	0.026±0.012
	2	0.026±0.013	0.028±0.014
	3	0.026±0.015	0.031±0.017
	4	0.033±0.020	0.040±0.022
	5	0.037±0.014	0.046±0.016
	6	0.033±0.019	0.031±0.015
	7	0.032±0.021	0.046±0.025
	8	0.024±0.016	0.035±0.019
	T	0.029±0.018	0.036±0.020
Summer	1	0.030±0.018	0.046±0.022
	2	0.018±0.014	0.038±0.020
	3	0.013±0.011	0.026±0.014
	4	0.010±0.010	0.022±0.016
	5	0.025±0.026	0.041±0.034
	6	0.024±0.014	0.036±0.018
	7	0.025±0.021	0.047±0.030
	8	0.021±0.014	0.037±0.021
	T	0.021±0.018	0.037±0.024
Autumn	1	0.029±0.012	0.025±0.014
	2	0.023±0.012	0.022±0.015
	3	0.020±0.014	0.018±0.015
	4	0.020±0.012	0.016±0.013
	5	0.015±0.010	0.010±0.012
	6	0.010±0.004	0.006±0.006
	7	0.018±0.006	0.018±0.008
	8	0.014±0.008	0.011±0.009
	T	0.019±0.012	0.017±0.014

Table S-20. LMIs of $PM_{2.5}$ at 25 AQMSs in Seoul by season.

Gu (district)	Winter	Spring	Summer	Autumn
Gangnam	-0.74	-0.03	1.09	0.94
Gangdong	-0.72	-0.11	1.05	0.95
Gangbuk	2.34	2.86	0.07	-0.89
Gangseo	-1.65	-1.45	-1.05	1.34
Gwanak	1.47	-0.30	-3.61	1.52
Gwangjin	0.19	0.02	1.25	2.15
Guro	1.05	0.16	-1.17	2.92
Geumcheon	1.55	-0.25	0.57	2.52
Nowon	-2.59	2.53	0.62	-1.76
Dobong	1.02	1.48	0.34	-0.07
Dongdaemun	-0.35	0.70	0.98	0.15
Dongjak	1.83	-1.57	-0.30	-0.91
Mapo	-3.97	0.52	2.92	1.74
Seodaemun	0.85	0.50	1.04	1.03
Seocho	-3.71	0.36	-2.57	-0.25
Seongdong	0.04	-4.57	0.57	0.92
Seongbuk	1.97	0.00	-2.36	0.19
Songpa	-0.92	-0.02	1.42	1.59
Yangcheon	0.08	0.47	1.85	3.05
Yeongdeungpo	0.41	0.12	1.53	2.00
Yongsan	0.07	0.23	0.64	-0.88
Eunpyeong	0.80	0.91	1.50	1.86
Jongno	2.05	-0.66	-1.09	-0.31
Jung	0.74	-0.82	-0.19	-0.03
Jungnang	-0.01	1.33	0.46	0.88

Table S-21. LMIs of PM_{10} at 25 AQMSs in Seoul by season.

Gu (district)	Winter	Spring	Summer	Autumn
Gangnam	-1.86	-1.22	0.19	-0.34
Gangdong	1.87	1.37	-0.14	-0.37
Gangbuk	-1.23	-0.37	-1.86	-2.16
Gangseo	0.13	0.13	0.62	2.26
Gwanak	-0.85	0.39	1.24	1.31
Gwangjin	-0.01	-0.10	0.87	0.51
Guro	-1.66	-0.55	-1.00	3.41
Geumcheon	-0.10	-0.84	0.62	-0.81
Nowon	0.00	0.60	0.07	-0.67
Dobong	-0.66	-0.69	0.13	0.32
Dongdaemun	-0.29	0.07	0.86	0.42
Dongjak	-0.73	-3.95	3.28	2.30
Mapo	0.05	-0.45	0.20	-0.66
Seodaemun	-3.12	-1.23	-1.01	0.37
Seocho	-2.74	-1.49	-0.49	0.43
Seongdong	-1.72	-4.70	-1.33	-1.32
Seongbuk	-0.84	-3.83	-7.17	-4.37
Songpa	1.03	0.90	-0.06	-0.15
Yangcheon	-1.56	-3.38	0.00	2.43
Yeongdeungpo	0.30	-1.80	2.38	6.90
Yongsan	-0.54	-1.35	0.15	0.31
Eunpyeong	0.08	-0.13	-0.09	0.21
Jongno	-2.26	-1.72	1.00	0.09
Jung	1.21	1.12	2.56	1.67
Jungnang	-0.04	0.28	0.89	-0.60

Table S-22. LMIs of NO_2 at 25 AQMS in Seoul by season.

Gu (district)	Winter	Spring	Summer	Autumn
Gangnam	-0.12	-0.53	0.00	-0.21
Gangdong	0.07	-0.09	-0.01	-0.17
Gangbuk	-0.12	1.35	4.54	2.70
Gangseo	-0.46	1.21	1.26	1.33
Gwanak	-1.62	-1.58	-0.97	0.69
Gwangjin	0.17	-0.06	0.19	0.05
Guro	-6.69	-6.44	-3.38	-2.46
Geumcheon	-0.45	-0.75	-0.06	0.10
Nowon	-0.35	0.18	3.41	1.11
Dobong	1.35	3.63	5.53	4.13
Dongdaemun	0.92	1.50	0.60	0.38
Dongjak	-0.80	-0.08	-0.44	0.17
Mapo	-0.57	0.16	-0.60	0.53
Seodaemun	-0.95	-0.80	0.10	-1.80
Seocho	-2.77	-0.53	0.11	-0.02
Seongdong	-0.53	-0.36	-1.09	-1.03
Seongbuk	0.36	-0.66	-1.18	-0.86
Songpa	0.08	-0.38	-0.07	-0.38
Yangcheon	-1.95	-0.61	0.49	-0.21
Yeongdeungpo	0.26	-0.16	-0.03	-1.69
Yongsan	0.19	-0.01	0.43	0.15
Eunpyeong	0.33	-0.01	-1.55	0.80
Jongno	-0.62	1.63	2.24	-0.11
Jung	-0.85	0.65	1.46	-1.19
Jungnang	0.55	-0.89	0.01	-1.29

Table S-23. LMIs of CO at 25 AQMS in Seoul by season.

Gu (district)	Winter	Spring	Summer	Autumn
Gangnam	0.53	-1.04	-1.04	0.72
Gangdong	0.23	0.11	-0.60	-0.07
Gangbuk	-1.55	-1.92	-2.70	-2.50
Gangseo	-0.79	-2.12	-1.07	0.16
Gwanak	2.61	0.49	3.04	2.77
Gwangjin	-1.48	-0.68	-0.29	-0.74
Guro	-0.25	-2.24	1.53	-0.43
Geumcheon	0.03	0.28	1.16	0.87
Nowon	0.88	0.42	-0.65	0.07
Dobong	0.51	-0.02	-2.82	-0.69
Dongdaemun	-0.51	-1.25	0.57	0.36
Dongjak	0.45	-1.15	0.05	-0.07
Mapo	-0.79	0.33	0.07	-0.05
Seodaemun	-1.32	0.40	-0.99	-0.57
Seocho	2.62	1.42	1.18	2.81
Seongdong	1.47	0.58	0.30	0.35
Seongbuk	1.99	-0.81	-1.85	0.18
Songpa	-0.36	-1.83	-1.95	-0.57
Yangcheon	-0.52	0.11	0.25	0.11
Yeongdeungpo	-1.20	-6.58	-4.74	-3.52
Yongsan	3.67	0.04	-1.07	1.52
Eunpyeong	2.60	-0.63	-1.52	2.35
Jongno	1.11	1.70	0.69	4.09
Jung	0.23	-0.01	-0.01	0.19
Jungnang	-2.09	-1.45	-1.63	-1.26

Table S-24. LMIs of O_3 at 25 AQMS in Seoul by season.

Gu (district)	Winter	Spring	Summer	Autumn
Gangnam	-0.39	-1.59	-1.50	1.80
Gangdong	-0.10	-0.09	0.06	0.23
Gangbuk	5.45	1.68	-0.54	0.69
Gangseo	-1.86	-1.66	-0.20	-0.10
Gwanak	0.39	0.94	0.77	0.43
Gwangjin	-0.35	-2.57	3.11	-0.03
Guro	3.37	-0.03	1.25	-0.23
Geumcheon	0.24	0.13	0.21	-0.16
Nowon	2.76	0.97	0.20	0.71
Dobong	4.91	2.55	1.61	2.62
Dongdaemun	0.74	3.16	4.15	2.05
Dongjak	-0.53	0.49	0.99	-0.12
Mapo	-0.20	0.03	0.36	1.29
Seodaemun	2.59	0.84	-1.42	3.62
Seocho	-0.18	-0.35	-0.85	1.65
Seongdong	1.13	4.34	3.32	2.13
Seongbuk	-0.46	-0.84	-1.46	-2.06
Songpa	-0.33	-0.41	0.19	0.69
Yangcheon	2.32	-0.64	-1.44	-0.10
Yeongdeungpo	1.74	-0.53	0.67	-0.27
Yongsan	-0.40	1.63	0.79	-0.14
Eunpyeong	2.30	1.48	0.54	3.89
Jongno	0.45	-1.35	-1.19	-0.02
Jung	0.17	-0.47	-0.92	0.04
Jungnang	-0.08	0.32	2.47	0.18

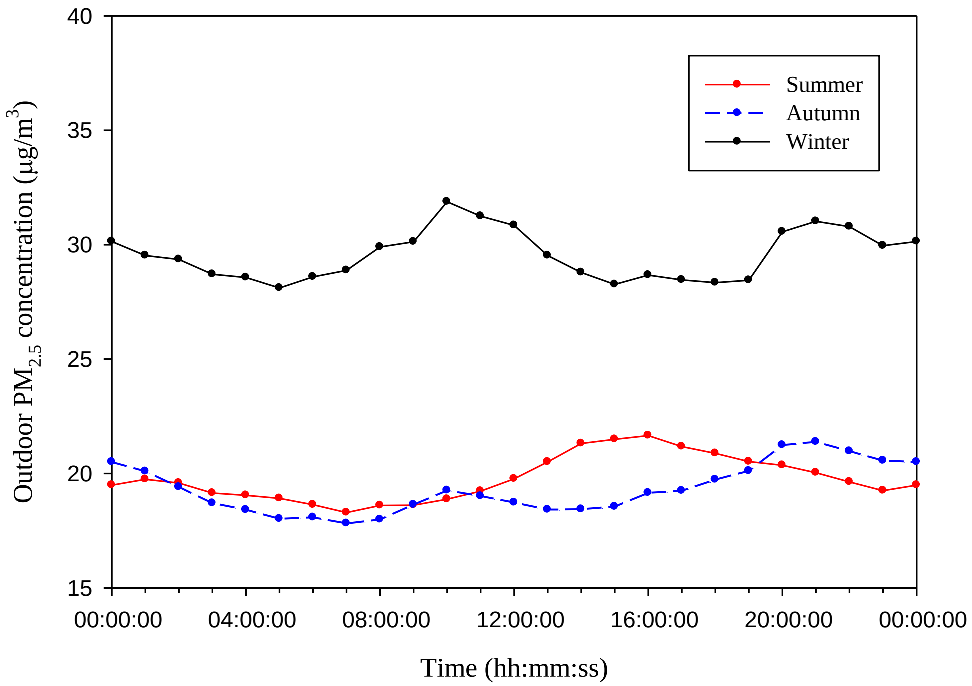

Figure S-1. 24-h profiles of hourly average of outdoor $PM_{2.5}$ concentrations over 5 year.

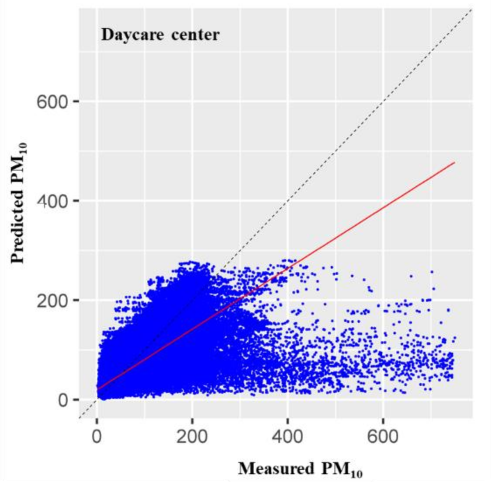

(a) Daycare center

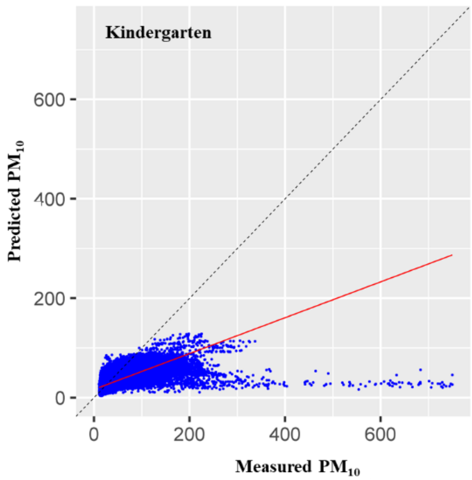

(b) Kindergarten

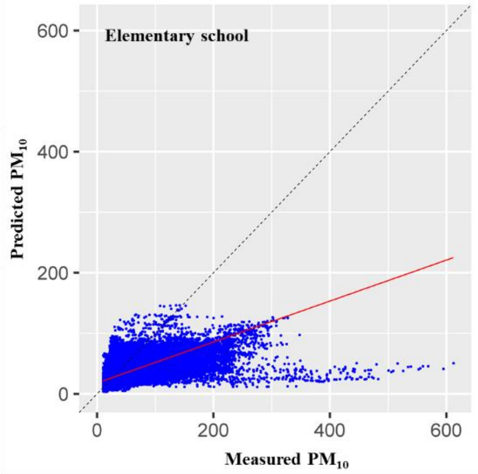

(c) Elementary school

Figure S-2. Scatter plots in educational facilities.

AirGuard K monitor quality assurance : field experiments

Prior to the field measurement, performance test for AirGuard K was conducted in 40 indoors including 25 non-smoking home and 15 restaurants in Seoul, Korea. The field evaluation could provide monitor performance in indoors where people stayed with natural emission source of PM_{10}, not artificial source. Therefore, AirGuard K was evaluated by 40 co-location tests with a gravimetric measurement of PM_{10} to ensure accuracy. The gravimetric PM_{10} monitor, MicroPEM v3.2 (RTI incorporated, Research Triangle Park, NC, USA), provided reference values of the PM_{10} concentration. The conditions of co-location tests were a temperature of 25-28 °C and a relative humidity of 48-52%.

The MicroPEM was operated at 0.5 liters per minute, and the flow rate was maintained before and after the sampling with a flowmeter (TSI 4100 series, TSI Inc., MN, USA). Teflon filter (Zefon International, Ocala, FL, USA) was placed in MicroPEM for collecting PM_{10} sample. Filters were dried before and after sampling and were pre- and post-weighed at three times with a microbalance (Mettler XP6 Microbalance, Mettler Toledo International Inc., Switzerland). Field blank filter was used to validate weighing condition. The 2-day average of difference between pre- and post-weighed for three values was used to calculate gravimetric PM_{10} concentration.

The calibration dataset between MicroPEM filter and AirGuard K was used to generate the regression equation. The linear regression results are shown equation (1) and Figure S-3. The results showed a good linear relationship (R^2 = 0.83). The intercept was not included in the linear regression analysis. The linear regression slop of PM_{10} was 1.50 and the 95% confidence intervals (CI) ranged from 1.38 to 1.62 ($p < 0.001$). Standard error was 0.06.

Gravimetric PM_{10} = 1.50 * AirGuard K (R^2=0.831) (1)
where PM_{10} is the mass concentration in μg/m³

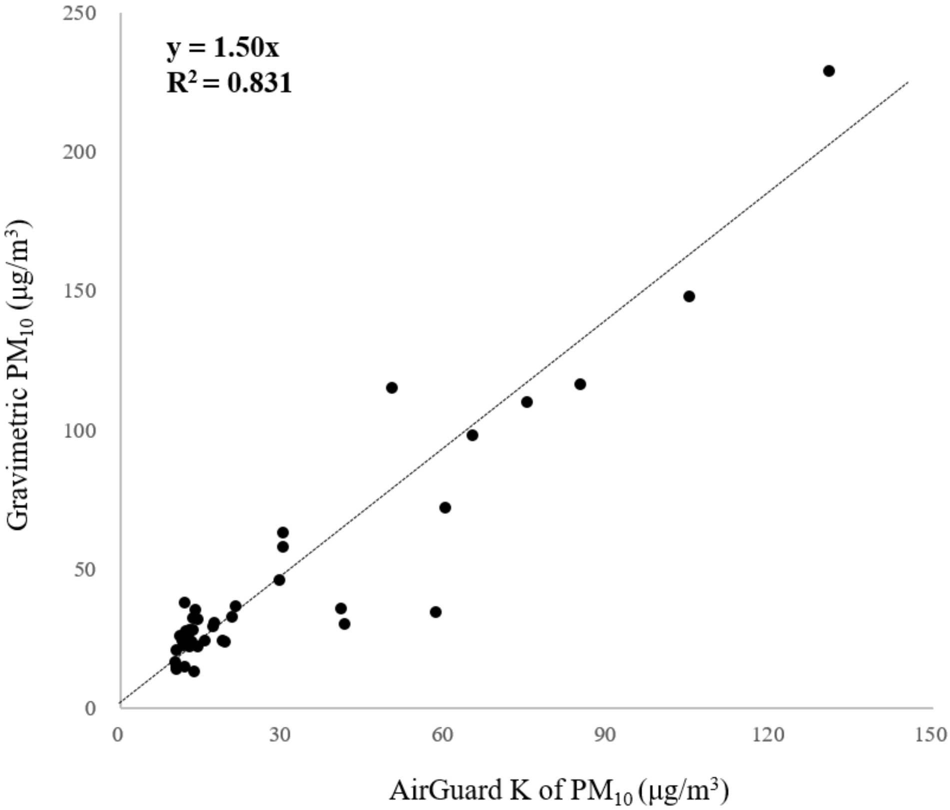

Figure S-3. Relationship between gravimetric measurement and AirGuard K concentration using 2-day average of PM_{10}.

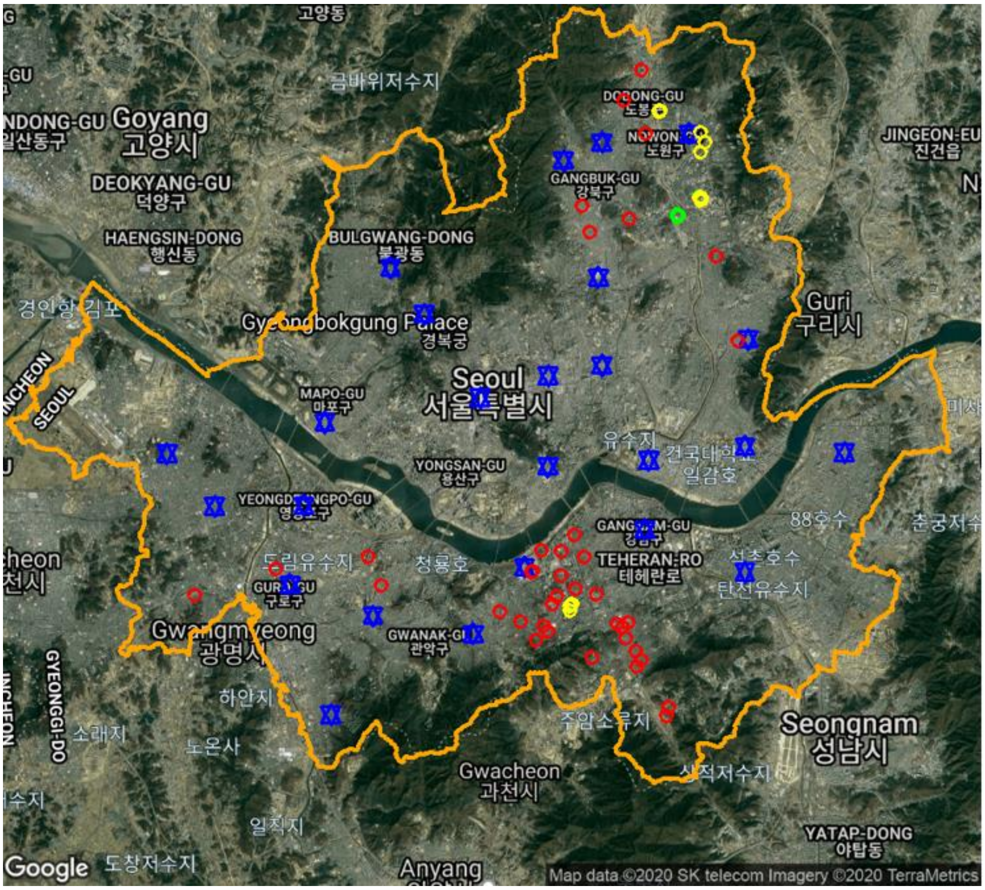

Figure S-4. Location of AQMSs and educational facilities in Seoul.

*Blue point : AQMS (n=25)
*Red point : Daycare center (n=54)
*Green point : Kindergarten (n=12)
*Yellow point : Elementary school (n=21)
*Orange line : Border of Seoul

국문초록

서울 인구의 미세먼지 노출 예측에 관한 연구

서울대학교 보건대학원
환경보건학과 환경보건학 전공
곽 수 영

미세먼지 (Particulate matter, PM)의 노출은 여러 역학 연구에서 호흡기계 및 심혈관계 질병의 유병률과 조기사망률을 증가시킨다고 밝혀진 바 있다. 특히 초미세먼지 ($PM_{2.5}$) 는 공기역학적 직경이 2.5 µm 인 입자상 물질로 입자 크기가 미세하여 흡입시 코 점막에서 걸러지지 않고 폐포까지 도달하여 많은 건강영향을 유발한다. 초미세먼지 노출 관리에 대한 중요성과 필요성은 커지고 있으며 국민의 건강을 보호하기 위해서는 국민이 미세먼지에 얼마나, 어디서, 어떻게 노출되고 있는지를 파악할 수 있는 개인노출 연구가 필수적이다. 미세먼지에 대한 개인이 노출되는 정도를 정확히 파악하기 위해서는 개인의 시간활동패턴에 따라 언제 (time), 어디서 (microenvironment), 어떤 활동 (activity)을 했는지에 따라 실제 활동공간에서의 노출 농도와 머무른 시간활동 양상을

파악하여야 한다. 하지만 이는 여러 시간적, 경제적 제약이 따른다는 한계점이 있다. 많은 역학연구에서는 국가 대기측정망에서 측정된 실외 대기오염물질 농도를 개인노출 농도와 같다고 간주하여 개인노출을 간접적으로 추정하려는 시도들이 있었다. 하지만 많은 선행연구에서 실외 미세먼지 농도만으로 개인노출 농도를 추정하는 것은 그 오차가 크다고 규명 하였으며, 정확한 미세먼지 개인노출 평가를 하기 위해서는 실내와 실외 모두에서의 노출 수준을 고려하여야 한다. 본 연구의 목표는 초미세먼지 실외농도와 실내외 농도비를 활용한 인구집단 초미세먼지 노출모델을 개발하여 서울 시민의 계절별 초미세먼지 노출 분포를 예측하고 고노출 인구집단의 특성을 파악하는 것이며, 개발한 모델에서 나아가 추후 연구에서 인구집단 노출 예측을 고도화 시킬 수 있는 방법에 대해 고찰하였다.

첫번째 연구(chapter 2)는 인구집단 초미세먼지 노출모델을 개발하여 서울 시민의 계절별 초미세먼지 노출분포를 도출하여 고노출 인구집단의 특성을 파악하였다. 모델의 입력값은 통계청 2014년 생활시간조사의 계절별 평일의 서울 시민 시간활동패턴 3984개 (여름: 960, 가을: 1898, 겨울: 1126)와 7개의 미세환경 (집, 직장/학교, 기타장소, 식당, 도보, 자동차, 대중교통)에서의 계절별 초미세먼지 농도이다. 미세환경에서의 초미세먼지 농도는 서울시 25개구 도시대기측정망에서의 5개년 (2015-2019년) 실외 초미세먼지 농도 dataset과 미세환경 실측을 통해 산출한 미세환경 및 실외 농도비 (M/O ratio) 각 분포를 곱하여 산출하였다.

산출한 미세환경별 초미세먼지 농도는 10분 단위의 계절별 시간활동 패턴에 각각 적용하여 확률론적 예측 방법 (몬테카를로 시뮬레이션)을 통해 서울시민의 계절별 초미세먼지 개인노출 분포를 도출하였다. $PM_{2.5}$ 개인노출 평균은 여름철에 21.3 ± 4.0 μg/m^3 이었고, 가을철에 9.8 ± 2.7 μg/m^3 이었고, 겨울철에 29.9 ± 10.6 μg/m^3 이었다. 노출군은 도출한 노출 분포에서 상위 20%에 해당하는 사람들을 고노출군, 하위 20%를 저노출군, 나머지 60%를 기준 노출군으로 정의하였다. 고노출군의 $PM_{2.5}$ 개인노출 평균은 45.4 ± 13.1 μg/m^3 이었고, 저노출군 평균은 20.4 ± 2.1 μg/m^3, 기준 노출군 평균은 27.9 ± 3.4 μg/m^3 이었다. 고노출에 영향을 준 인자는 성별, 나이, 일한시간, 건강상태였으며, 고노출군은 남자일수록, 나이가 어릴수록, 월수입이 높고 일한 시간이 긴 사람으로 특성되었다.

두번째 연구(chapter 3)는 여러 실외변수들을 이용하여 교육 기관에서의 실시간 실내 미세먼지 농도를 예측하는 모델을 개발하였다. 예측 모델 개발에는 데이터 특성을 반영한 4가지 모델 형태 (Original, I/O ratio, Root, Log)를 고려하였고, 9가지 실외변수를 활용하여 다중회귀모델을 개발하였다. 실외변수는 실외공기질 자료, 실외 기후관측 자료 (온도, 습도, 강수량, 풍향, 풍속, 기압, 일사량, 일조량) 이었고, 반응변수는 서울이 87곳에서의 교육기관 (어린이집 54곳, 유치원 12곳, 초등학교 21곳) 교실에서의 1년 동안 10분 단위의 실시간 실내 미세먼지 농도를 활용하였다. 최종 개발된 예측 모델은 변수를 루트변형하고 요일-시간 상호작용 변수를 포함하였고 가장 주요한 설명변수는 실외

미세먼지 농도였다. 예측 모델의 R^2는 어린이집은 0.64, 유치원은 0.45, 초등학교는 0.43이었으며 실측된 실내 미세먼지 농도의 시간대별 추이를 잘 예측하여 좋은 예측력을 나타냈다. 본 실내 예측 모델은 직접 측정을 하지 않더라도 공개된 국가자료를 활용하여 실내 미세먼지 농도 예측 가능성을 보여줬으며 본 모델을 활용하여 노출에 대한 중재 (Intervention)를 할 수 있다.

세번째 연구(chapter 4)는 서울시 내 공간 크기에 따라 city-scale과 보다 더 작은 1 km^2의 작은 공간 단위 (small-scale)로 나누어 5가지 대기오염물질 (PM_{10}, $PM_{2.5}$, NO_2, CO, O_3) 농도의 계절별 공간적 패턴에 대해 파악하였다. 대기오염물질의 시공간적 농도 변이의 이해와 고찰을 바탕으로 실외농도를 개인노출 평가에 적용한다면 보다 더 정확한 개인노출 평가가 가능하다. 2017년 12월부터 2018년 12월까지의 서울시 25개구 도시대기측정망에서의 대기오염물질 시간 농도는 에어코리아 홈페이지 (http://www.airkorea.or.kr)에서 다운로드 받았다. 구로구 내 작은 공간 단위 (1 km^2)에서 대기오염물질 시간 농도는 도시대기측정망의 측정법과 동일한 공정시험기준에 따라 차량을 이용하여 측정하였다. 측정 지점은 서울시 구로구 도시대기측정망 1곳을 기준으로 5 km x 5 km test-bed를 설정하여 1 km^2 크기의 공간 단위로 8곳을 선정하고, 한 계절당 각 지점에서 약 10일 동안 농도를 4계절 반복 측정하였다. 분석 방법은 Moran's 지수를 이용하여 대기오염물질 농도의 전역적, 국지적 공간 자기상관성을 파악하였다. 25개구 도시 대기측정망에서의 대기

오염물질 농도와 보다 더 8곳의 작은 공간단위에서의 오염물질 농도는 계절별로 유의한 차이를 나타냈다. 일반적으로 도시대기측정망에서의 오염물질 농도가 높았지만 오존의 경우 봄과 여름에 더 작은 공간 단위에서의 농도가 더 높았다. 25개구 도시 대기측정망의 농도를 활용한 공간 자기상관성은 구로구 내 8곳의 작은 공간 단위의 공간 자기상관성과 다른 패턴을 나타내어 작은 공간까지 대변할 수 없었다. 보다 더 정확한 대기오염물질에 대한 개인노출을 예측하기 위해서는 city-scale보다 더 작은 공간 단위의 대기오염물질 농도 변이가 고려되어야 하겠다.

본 연구는 인구집단 노출 모델을 개발하여 서울 시민의 초미세먼지 노출 분포를 도출하였고 고노출의 특성을 파악하여 노출 중재에 대한 과학적인 근거를 마련하였다. 본 연구에서 개발한 초미세먼지 인구집단 노출 모델을 통해 개인노출을 직접 측정을 하지 않아도 개인의 노출 수준을 예측할 수 있어 경제적인 노출평가를 할 수 있으며 궁극적으로 초미세먼지 고노출 인구집단에 대한 국가 정책 수립의 기초자료로 활용될 수 있다. 또한 보다 더 실제 노출을 반영할 수 있는 노출평가 모델을 보완, 발전시킬 수 있는 방향에 대한 연구를 통해 추후 인구집단 노출평가에 대한 정확도와 활용도를 높일 수 있는 통찰력을 제공할 수 있다. 실내 미세환경의 미세먼지 농도를 실외 변수만으로도 예측할 수 있는 가능성을 확인하였고 실외 미세먼지 농도를 인구집단 노출모델에 적용시 예측 공간의 단위에 대한 신중한 접근 관점을 제공하였다. 향후

추가 연구를 통해 초미세먼지 인구집단 노출모델을 국내 다른지역, 다른 대기오염물질에 대해 확대, 적용하여 개발한 노출평가 모델의 범용성을 확인할 수 있다.

주요어: 개인노출, 공간자기상관성, 노출평가, 노출모델, 대기오염물질, 미세환경, 초미세먼지, 확률론적 모델

학 번: 2017-35801